Università degli Studi della Tuscia di Viterbo
in convenzione con il Consiglio Nazionale della Ricerca (CNR) e l'Istituto Superiore di Sanità (ISS)

Corso di Dottorato di Ricerca in

Scienze delle Produzioni Vegetali e Animali - XXX Ciclo

Endocrine disrupting chemicals in the agro-zootechnical environment: transgenic or untransformed cell-based sensoristic technology for early detection.

(**s.s.d. CHIM/05**)

Tesi di dottorato di:

Dott. Giulia Cocco

Coordinatore del corso

Prof. Stefania Masci

Tutore

Dott. Roberto Dragone

Co-tutore

Dott. Chiara Frazzoli

Co-tutore

Prof. Renato D'Ovidio

DECEDUTO

A.A. 2016/17

To Lorenzo

Abstract

Endocrine Disrupting Chemicals (EDCs) are involved in the etiology of metabolic disorders anticipating metabolic syndromes and chronic diseases. The prevention of environmental and dietary exposure to EDCs is therefore crucial in public health. The aim of this PhD study has been to develop different whole cell-based biosensoristic devices for early detection of EDCs in the agro-zootechnical environment, i.e. one of the main interface between humans, animals and environment.

To this end, the following sensoristic systems have been designed and developed:

i) A **fluorimetric sensor based on a transgenic yeast strain** for the assessment of the total estrogenic level (linked to the total amount of estrogenic-like Endocrine Active Substances presents in the sample).

METHOD: A construct derived from the insertion of the human sequence for an estrogen receptor (GPER) linked to the sequence for a fluorophore (TurboGFP) in a yeast vector (pIB3), with the sequence for a constitutive promoter, was engineered in *Pichia pastoris* GS115 cells.

RESULTS: Molecular analyses on the outcome of the electroporation gave positive results, however fluorescence measurements did not show Turbo-GFP-related spectra. Assuming that a misfolding of chimeric protein has been occurred, Turbo-GFP was substitute with mCherry (an easier-to-fold protein that turns the medium red). The recombination reaction was successfully used and the obtained plasmid was engineered in *P. pastoris* cells. Red positive colonies were cultured to analyze cell pellet and cellular extracts fluorescence: mCherry-related spectra were observed and samples extracted with a detergent had fluorescence values 6.7X higher than samples extracted without detergent. The next step will be biomediator testing by fluorescent spectral analyses using 17β-estradiol as a model chemical.

ii) An **amperometric sensor based on an untransformed yeast strain** to detect herbicide simazine (with known endocrine disrupting properties). This sensor was then applied to spiked agricultural water and raw cow's milk samples.

METHOD: Percentage interference (%ρ) caused to aerobic cellular respiration of *Saccharomyces cerevisiae* suspensions was assessed by measurements of oxygen consumption of cell suspensions exposed to the herbicide compared with controls (not exposed suspensions). Considering the European residue limits in drinking water (0.1ppb) and cow's milk (10ppb), various concentrations were tested.

RESULTS: The results obtained from short-term (3h) tests showed that the biosensoristic device is able to detect the presence of simazine, without any sample pretreatments, up to concentrations 5 times below the EU legal concentration limit for both the matrices. Cellular respiratory inhibition (%ρ>0) was found at 2ppb in milk samples and at 0.02 and 0.2ppb in agricultural water samples; cellular respiratory hyperstimulation over the maximum physiological rate (%ρ<0) was found at 200ppb in milk samples and at 0.1ppb in water samples. From these results we hypothesized a dose-dependent combination effect between three different cellular mechanisms triggered by the presence of simazine.

iii) Two **fluorimetric sensors based on an untransformed algal strain** to detect the herbicide diuron (with known endocrine disrupting properties).

a) METHOD: The sensor exploited the variation of selected parameters in Kautsky curves measured from dark-adapted *Chlamydomonas reinhardtii* cells as toxicological endpoint. In particular inhibition of photosynthesis by diuron leads to an increase in the fluorescence yield at the J transient in the Kautsky curve. In our experimental conditions, fluorescence at 8ms were considered, as they are less variable than data at 2ms. Relative variable fluorescence at 8ms (V8ms), and a normalized effect index (ε%) which compares V_{8ms} in blank samples (V8msblk) and in exposed samples (V8msexp) values were analyzed.

RESULTS: At 2ppb of diuron V8msexp values were significantly higher than V8msblk; at 0.02ppb V8msblk values were significantly higher than V8msexp; at 0.2ppb significant differences were not found. ε% shows an inhibition effect at 2ppb; a null effect at 0.2ppb; a presumptive hormetic-like effect at 0.02ppb.

b) METHOD: The sensor exploited the two chlorophyll fluorescence maxima (684 and 735nm) as toxicological endpoint.

RESULTS: In presence of diuron fluorescence values incremented similarly in both maxima thus it was considered only the fluorescence at 684nm. The normalized parameter analyzed was the percentage increase (%ι) in F684nm. The assay proved to be able to detect herbicide diuron till 0.2ppb.

In conclusion, all the tested whole cells biosensoristic devices proved to be suitable for the prefixed aims. Through further improvement such devices and relating bioassays could represent a new technological opportunity for future applications in monitoring at critical control points including agro-zootechnical environment.

Key words: Xenoestrogens, biosensoristic devices, GPER receptor, One Health, dairy chain.

General introduction

According to World Health Organization (WHO), unsafe food, spoiled by contamination with harmful bacteria, viruses, parasites or chemical substances, are cause of more than 200 foodborne illness or foodborne diseases – ranging from diarrhoea to cancers (WHO, 2014). Foods are produced by living organisms, plants and animals, and so the environment where the food-producing organisms grow, including what is eaten by the food-producing animals, are essential determinants of the wholesomeness and quality of our diet (Mantovani et al., 2009).

Food contaminations can occur at different steps of agro-zootechnical environment and food supply chain ("from farm to fork") and the primary productions (the first step of this chain) is the most critical step for contamination risks. This criticality stems from the fact that interactions between the agro-zootechnical environment and food supply chain occur mainly at this level (Dragone et al, 2017). In the example of raw milk contaminations can obviously derive from animal ingestion of contaminated feed or drinking water (“feed to-food carry-over”) but even from milk handling practices, chemicals release from milking system and use of veterinary products.

Although this criticality anyway the primary production step is not supported nowadays by an adequate technology that can detect the presence of chemical contaminants in raw products through rapid and continuous monitoring. Such monitoring process thus would be a useful tool for primary producers self-control and for reducing the possibility of progression to post-primary production of a non-compliant product containing pesticide residues.

1. Endocrine disruption

Contaminations leading to foods spoilage can cause serious both short- and long-term detrimental effects on human and animal health even through bioaccumulation and biomagnification processes (Dragone et al, 2017).

Nowadays some major concern effects are the ones deriving from the endocrine disruption, linked to diseases really serious or even fatal like male infertility, adverse pregnancy outcomes, neurobehavioral disorders, endocrine-related cancers (breast, endometrial, ovarian, prostate, testicular and thyroid) and metabolic disorders linked to obesity and type 2 diabetes (Bergman et al., 2012).

Endocrine disruption is caused by endocrine disruptors (EDs), chemicals belonging to the group of the endocrine active substances (EASs). EASs are defined as "substances which can interact or interfere with normal hormonal activity in the endocrine system". When an EAS has adverse effects on human and animal health is called EDC.

(http://www.efsa.europa.eu/en/topics/topic/endocrine-active-substances). Examples of EDCs are several pesticides (e.g. triazines, organochlorines and phenylureas), environmental pollutants, as dioxins and PCBs, the food contact material bisphenol A, or birth control pills and thyroid hormone substitutes.

The main, but not exclusive, targets of ED effects are endocrine homeostasis of sex steroids and thyroid (Mantovani A., 2006). These are complex systems with a high degree of interactions and interdependency mechanisms. Moreover, normal endocrine function is not steady state, but depends on cyclical patterns, age, and developmental stage (Mantovani A., 1999). EDCs can interfere with the function of the endocrine system through diverse mechanisms, such as agonism/antagonism with nuclear receptors, inhibition of hormone biosynthesis, and interference with the hypothalamus–hypophysis axis (Mantovani A., 2006).

The concern about EDCs derives also from their being hazardous even for next generation's health, since hormones are crucial for development, from embryo through to puberty (Mantovani A., 2017). Moreover early life exposures to EDCs may alter gene expression via non-genomic, epigenetic mechanisms, thus interfering with the germ-line (Latini et al., 2010).

Nowadays data show that a variety of EDCs can act also as "obesogens" promoting obesity with various mechanisms (reviewed in Heindel J.J. et al., 2015). Some of these "obesogens" effects might be also epigenetically transmitted to future generations (Janesick & Blumberg, 2016).
Moreover, even if the increased susceptibility to obesity/diabetes/metabolic syndrome may require a second "hit" (e.g. increased fat or sugar in the diet and/or stress for the functional change) to be expressed as a phenotype, it may also result directly from exposure to the metabolic disruptors (Heindel J.J. et al., 2015).

For all these reasons further studies on EDCs are necessary in order to make more steps in the prevention of environmental exposure to these chemicals road.

Thus, as mentioned, EASs are currently recognized to have three main targets and modes of action, namely, the disruption of thyroid-, estrogen- or androgen-regulated pathways. In this study we worked with EASs disrupting the estrogen and androgen pathways.

1.1. Estrogens and estrogenic-like endocrine active substances

Estrogens are ubiquitous and small steroidal hormones, principally produced by the ovary or, in pregnant women, by the placenta. In men and in women after menopause, they derive principally from the aromatization of steroidal precursors. Estrogens main function is to regulate physiological changes associated with reproduction in both sexes but they also regulate many other important physiological processes, including immune function and mineral homeostasis (Pinto et al., 2014). The major, most abundant and most potent natural estrogen sex hormone in humans and animals is 17-β-estradiol or E2 (figure 1).

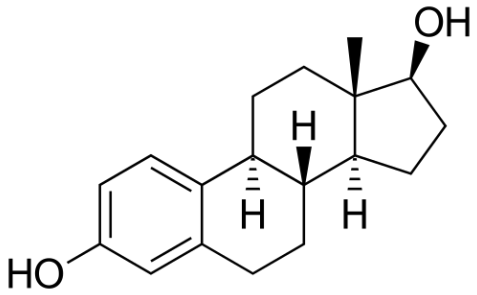

Figure 1: 17-β-estradiol (E2) molecule

In plants there are peculiar estrogens, called phytoestrogens, natural-occurring but considered xenoestrogens as they are not produced by endocrine system of humans and animals. Phytoestrogens are non-steroidal compounds but their structural similarity with the 17-β-estradiol enables them to have estrogenic or antiestrogenic activity. An example is genistein (figure 2) which is an isoflavone highly present in food because is found in a number of plants including lupin, fava beans and soybeans.

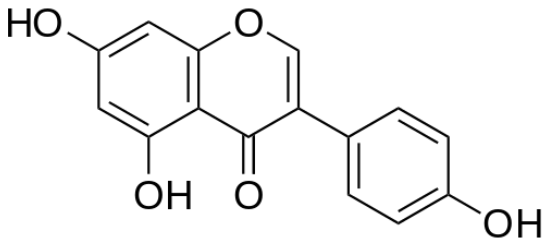

Figure 2: example of phytoestrogen (genistein)

A good dietary intake of phytoestrogens might be a protective factor toward several cancers and postmenopausal diseases but possible concerns exist regarding the exposure to

high doses during pregnancy or early infancy, for example, through the use of dietary integrators or soy-based milk (Mantovani A., 2006).

Estrogenic-like endocrine disruptors are structurally diverse compounds deriving from multiple sources, even natural, that have estrogenic and/or anti-estrogenic activities with negative effects, and can also affect other endocrine systems (Pinto et al., 2014). Nowadays humans are widely exposed to these compounds through food contaminations that can occur by: residues of persistent, omnipresent industrial chemicals such as PCBs (or polychlorinated biphenyls) and estrogens deriving from the intentional use in agriculture production (e.g. various pesticides, like DDT); unintentional side effects of leaching from food packaging (e.g. phthalates, plastic monomers, bisphenol A) (Ibarreta et al., 2001).
In figure 3 just some example of xenoestrogens classified as EDCs: the PCB deca-chlorinated biphenyls (A), DDT (B) and bisphenol A (C).

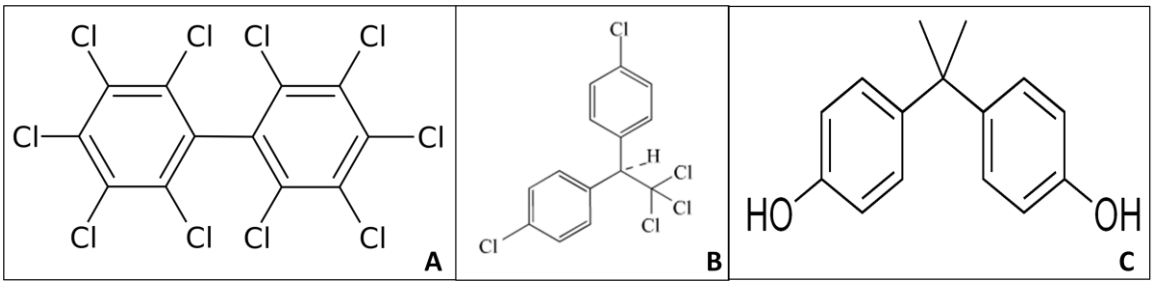

Figure 3: examples of endocrine disruptors with estrogenic activity

In the estrogenic-like endocrine active substances list there are also some drugs which interact with estrogen receptors with either an agonist or antagonist effect depending on the specific tissue and the percentage of them intrinsic activity (IA). They are called selective estrogen receptor modulators, SERMs, and are used for the treatment of various estrogen-related diseases. The two more classical examples are:

- tamoxifen (A in figure 4), a failed contraceptive currently used to treat all stages of breast cancer and for chemo-prevention in women at high breast cancer risk;
- raloxifene (B in figure 4), a failed breast cancer drug, is the only SERM approved internationally for the prevention and treatment of osteoporosis and vertebral fractures occurring in postmenopausal.

Although SERMs have many benefits, they also have some potentially serious adverse effects, such as thromboembolic disorders and, in the case of tamoxifen, uterine cancer. These adverse effects represent a major concern given that long-term therapy is required to prevent osteoporosis or prevent and treat breast cancer (Maximov et al., 2013).

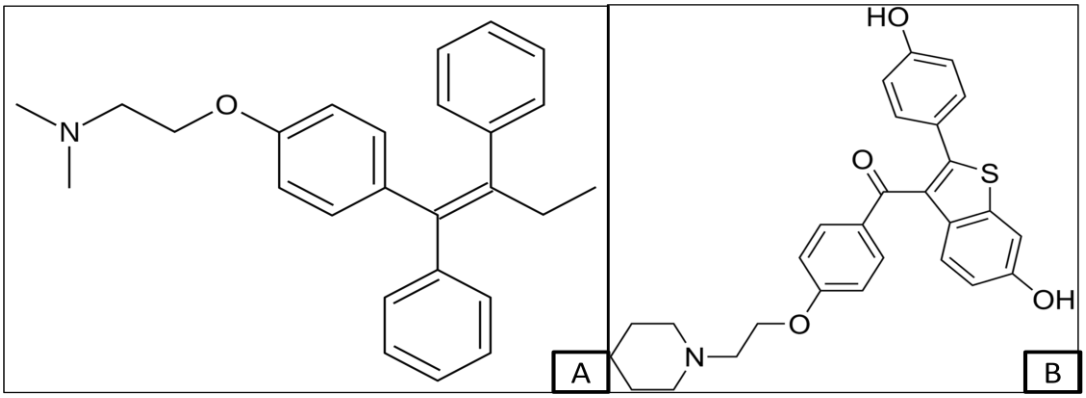

Figure 4: examples of SERMS

Estrogenic-like endocrine active substances have recently drawn the attentions of the scientific community because is recognized that the estrogenic-like endocrine disrupting chemicals are potentially hazardous factors for human health (Roy J.R. et al, 2009). They influence negatively our endogenous hormone's balance and cause various defects on health of both male and female reproductive tracts, particularly during puberty (Roy J.R. et al, 2009), but also cancers to testis, prostate and breast.

1.2.Androgens and androgenic-like endocrine active substances

Androgens are steroidal hormones acting principally on virilization of the male accessory glands and external genitalia during fetal life but also in childhood and adulthood (Hiort O., 2002). They are also precursors of estrogens through the action of the enzyme aromatase. It converts androstenedione to estrone and testosterone to estradiol (figure 5).

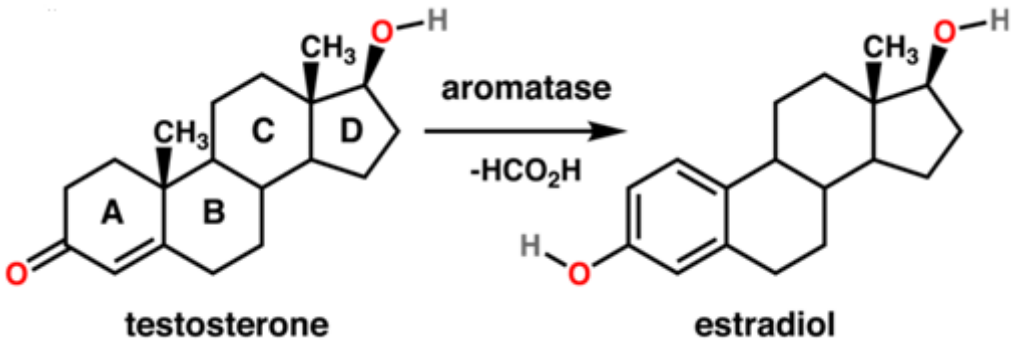

Figure 5: Conversion reaction of testosterone to estradiol through the action of aromatase enzyme

The major androgen hormone in humans is testosterone (figure 5) mainly produced in Leydig cells and secreted by testicles of male and, to a lesser extent, by the ovaries of female. The biosynthesis of androgens in the testis and ovaries is regulated by the hypothalamic-pituitary gonadal (HPG) axis. The weaker androgens are synthesized in both sexes in the adrenal cortex. This synthesis is regulated by the adrenocorticotropic hormone (ACTH) and by adrenal glands. Testosterone is even the substrate for further irreversible conversions via either the cited aromatization to estradiol or reduction to dihydrotestosterone (Hiort et al, 2002), another of the four major androgenic steroids.

In plants there are peculiar androgens, called phytoandrogens, and, as for phytoestrogens, they are considered xenoandrogens. An example is drupanol (figure 6) which is a phenol isolated from the fruit of *Psoralea drupacea*.

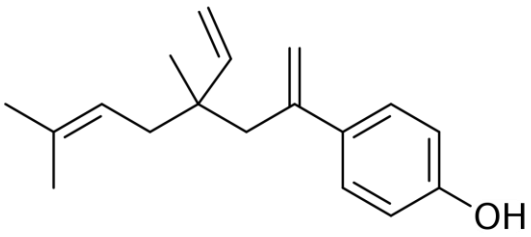

Figure 6: example of phytoandrogen (drupanol)

Like the estrogen receptors even the androgen receptor (AR) is activated by a range of exogenous molecules (xenoandrogens). The xenoandrogens of major concern are synthetic anabolic-androgenic steroid (AAS), compounds used illegally (prohibited by the World Anti-Doping Agency) from some athletes, like body builders, for their anabolic properties

(Joseph and Parr, 2015). Examples are testosterone esters (A in fig. 7: testosterone undecanoate), nandrolone esters (B in fig. 7: nandrolone decanoate), stanozolol (C in fig. 7) and metandienone (D in fig. 7). They can be classified as EDCs due to their side effects like cardiovascular diseases, psychiatric symptoms and dependence.

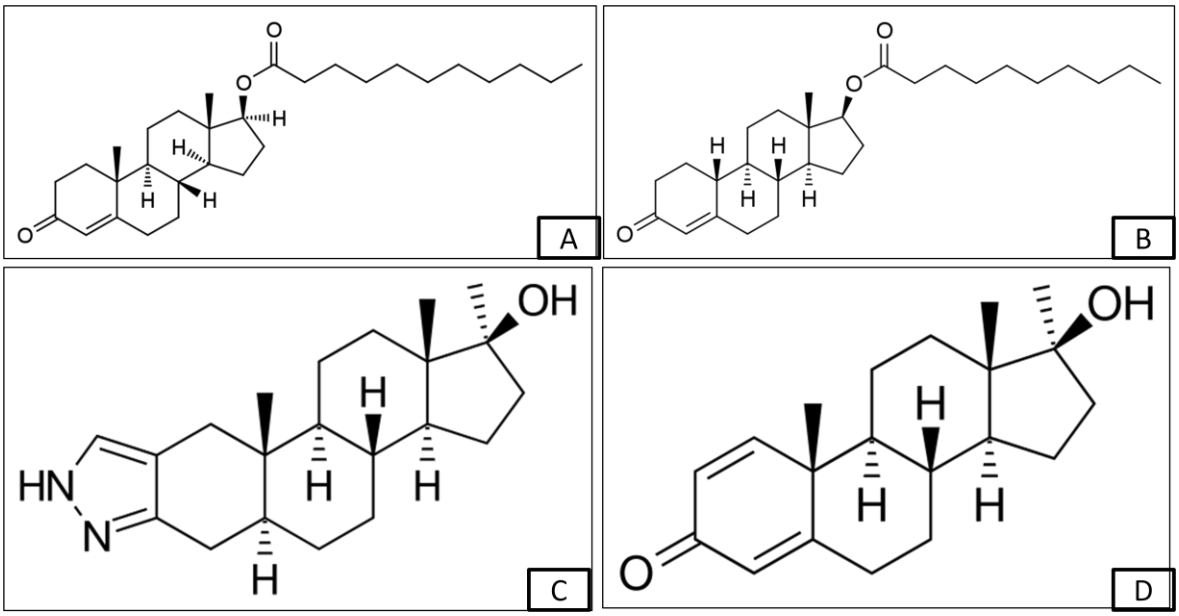

Figure 7: examples of xenoandrogens

In the androgenic-like endocrine active substances list, as in the estrogenic-like EASs, there are also some drugs, called selective androgen receptor modulators (SARMs), that bind androgen receptor and display an androgenic signaling activation specific in each tissue. Structurally, SARM compounds can be categorized into steroidal and nonsteroidal. Steroidal SARMs are modifies of the chemical structure of testosterone molecule. An example of steroidal SARM is 19-nortestosterone (figure 8). Examples of non steroidal SARMs are aryl propionamide analogs and bicyclic hydantoin analogs (Bhasin and Jasuja, 2009).

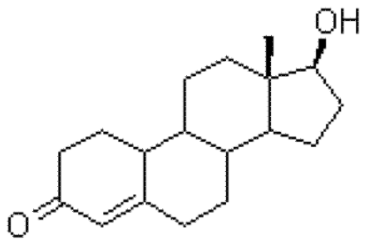

Figure 8: example of steroidal SARM (19-nortestosterone)

1.3.Pesticides

An example of EDC contamination source which is important in agro-zootechnical environment (e.g. in soils and ground waters) and food (e.g. residues in raw milk) is the class of pesticides because of their excessive use. In 2014 (latest available data), the total quantity of pesticide sales in the EU-28 amounted to close to 400.000 tonnes. Spain (19.9 %), France (19.0 %), Italy (16.2 %), Germany (11.6 %) and Poland (5.9 %) were the Member States in which the highest quantities of pesticides were sold, and together they made up 72.7 % of the EU-28's pesticide sales (table 1).

Table 1: pesticides sales in EU-28 (Eurostat, 2014)

	Total pesticides sales	Fungicides and bactericides	Herbicides, haulm destructors and moss killers	Insecticides and acaricides	Molluscicides	Plant growth regulators	Other plant protection products	Share in the total EU-28 pesticide sales
	(Tonnes)							(%)
EU-28 (*)	395 944.4	173 250.8	131 263.5	20 706.3	1 684.4	12 843.7	56 195.7	100.0
Belgium	7 001.1	3 095.0	2 519.7	555.8	47.7	261.2	521.6	1.8
Bulgaria	1 002.0	186.1	652.4	163.4	:	:	:	0.3
Czech Republic	5 663.4	1 788.3	2 755.3	337.7	15.5	350.3	416.2	1.4
Denmark	1 974.6	530.2	1 242.5	38.3	15.4	114.2	33.9	0.5
Germany	46 078.5	12 739.9	17 876.7	977.2	255.5	2 171.3	12 058.0	11.6
Estonia	596.0	88.2	425.8	25.3	:	56.6	:	0.2
Ireland	2 736.0	635.5	2 039.2	51.4	9.9	:	0.0	0.7
Greece	3 907.1	1 866.4	1 194.6	588.8	1.2	148.5	107.7	1.0
Spain	78 818.3	38 379.7	14 908.0	7 515.1	66.2	156.4	17 793.0	19.9
France	75 287.5	34 430.6	30 965.5	2 610.9	870.2	2 802.9	3 607.5	19.0
Croatia	2 119.1	1 004.8	889.1	143.1	5.4	72.2	4.5	0.5
Italy	64 071.1	37 907.1	7 864.4	2 251.9	75.0	367.4	15 605.2	16.2
Cyprus	1 046.7	698.1	153.4	180.6	1.0	1.2	12.5	0.3
Latvia	1 417.4	224.7	847.5	64.0	0.0	274.5	6.6	0.4
Lithuania	2 545.6	604.8	1 394.2	43.6	0.0	502.9	:	0.6
Luxembourg (²)	176.1	91.0	82.8	:	2.3	:	:	0.0
Hungary	8 959.5	3 634.1	4 011.1	916.5	3.5	203.3	190.9	2.3
Malta	108.4	97.4	7.6	2.9	0.5	0.0	:	0.0
Netherlands	10 665.6	4 869.1	3 266.4	252.0	45.1	452.0	1 780.8	2.7
Austria	3 373.2	1 641.1	1 375.8	240.2	16.2	53.5	46.4	0.9
Poland	23 550.6	7 442.5	12 073.4	1 479.2	35.3	2 128.0	392.3	5.9
Portugal	12 889.2	8 244.4	2 410.8	732.9	35.7	1.4	1 464.0	3.3
Romania	10 021.2	4 131.9	5 025.4	569.0	1.2	270.6	23.1	2.5
Slovenia	1 009.0	723.7	238.5	33.5	2.2	0.6	10.5	0.3
Slovakia	2 198.0	567.2	1 215.1	106.5	:	179.8	129.4	0.6
Finland	3 579.9	198.5	1 305.4	12.8	:	88.6	1 974.5	0.9
Sweden	2 486.7	302.3	2 103.8	34.2	:	29.3	17.1	0.6
United Kingdom	22 662.7	7 128.1	12 418.9	779.4	179.4	2 156.8	:	5.7
Norway	859.8	121.8	692.0	4.8	1.3	39.1	0.7	:
Switzerland	2 240.9	1 002.2	745.4	83.1	55.9	30.7	323.6	:

(*) Confidential data have been removed from the sums of pesticides sales. They represent 0,003% of Total pesticides sales in the EU.
(²) 'Fungicides and bactericides': 2012 data , other data: 2013.

In spite of the beneficial effects on agricultural production, all pesticides have impacts less positive on the environment and habitats in where they are used, even due to the persistence of some of them. Their toxic effects can influence non-target organisms, as microorganisms (Estève K. et al., 2009), and humans (Eddleston M. et al, 2002; Sass J.B. & Needleman H.L., 2004), as clear evidences demonstrate. In some cases, it has been

suggested that some diseases (e.g. cancers, allergies, neurological and reproductive disorders), may be connected to pesticide exposure (Mnif W. et al, 2011).
Moreover the fate of pesticides after application on crops or soil may be affected by numerous biophysicochemical degradation processes resulting in a change of the chemical entity of the pesticide and occurrence of a mixture of compounds in harvestable commodities and the environment – the active substance, metabolites and degradates. Thus simultaneous dietary exposure to multiple metabolites should be taken account of and the possibility that all or part of the metabolites will cause the same adverse outcome has to be considered (EFSA PPR Panel, 2016) because, in such case, dose addition concept should be used in cumulative risk assessment (EFSA PPR Panel, 2013).

For these reasons, and because pesticides that shown ED properties are going to be phased out in the European Union (see http://eur-lex.europa.eu/LexUriServ/LexUriServ.do?uri=OJ:L:2009:309:0001:0050:EN:PDF), the monitoring of these chemical's presence in environmental and food samples is of big importance.

In this PhD project two biosensoristic devices were designed to detect the presence of two herbicides (simazine and diuron) in water and in cow's milk, with known endocrine disrupting properties as well as interfering effects on both chloroplastic and mitochondrial functions.
The latter effects have been exploited for biosensoristic detection. Regarding the chloroplastic function, those compounds inhibit the photosynthesis by blocking the thylakoid electron transfer chain in the passage from the primary electron acceptor QA and the secondary electron acceptor QB in photosystem II (PSII) (figure 9) by binding QB pocket of D1 protein of PS II and causing the displacing of the plastoquinone QB (Lazár, 1999). Thus, interruption of the photosynthetic electron transport chain reduces the ability of the photosynthetic organisms to turn light energy into chemical energy (ATP and reduction potential). This condition causes a series of detrimental effect ,including starvation, photooxidative stress, chlorosis and lipid peroxidation mediated membrane damages (Hess, 2000).

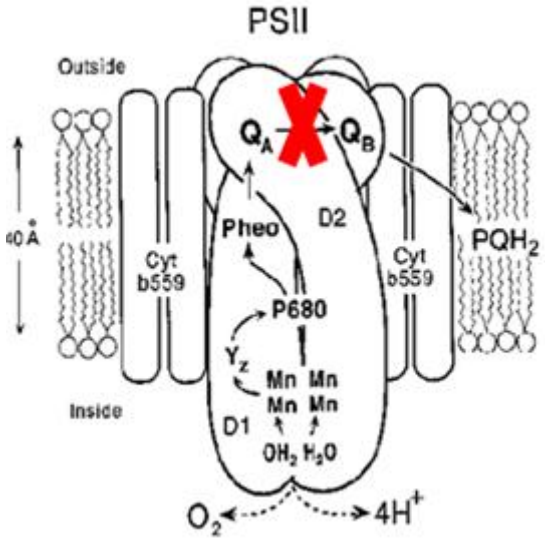

Figure 9: PSII inhibitors block the electron transfer chain from QA to QB

Regarding the mitochondrial function, these herbicides inhibit the coupling between the electron transport and phosphorylation reactions and thus ATP synthesis (Terada H., 1990) (scheme in figure 10).

In particular it was found that atrazine, a triazinic herbicide with a scaffold similar to simazine, has the potential to inhibit mitochondrial function by binding to mitochondrial F1F0-ATP synthase (Hase Y. et al., 2008). Williams et al., 2004 shown also that a set of triazine compounds directly bind to F1F0-ATP synthase, so Hase Y. et al., 2008 supposed the possible generalization of the finding that certain triazine compounds affect F1F0-ATP synthase function.

Diuron, instead, is able of acting as uncoupler of oxidative phosphorylation (Abo-Khatwa and Hollingworth, 1974) by blocking the electron flow at the cytochrome bc1 segment (Convent and Briquet, 1978), also called Complex III (from da Silva et al., 2017).

In figure 10 the mitochondria effects of simazine (green symbol) and diuron (red symbol).

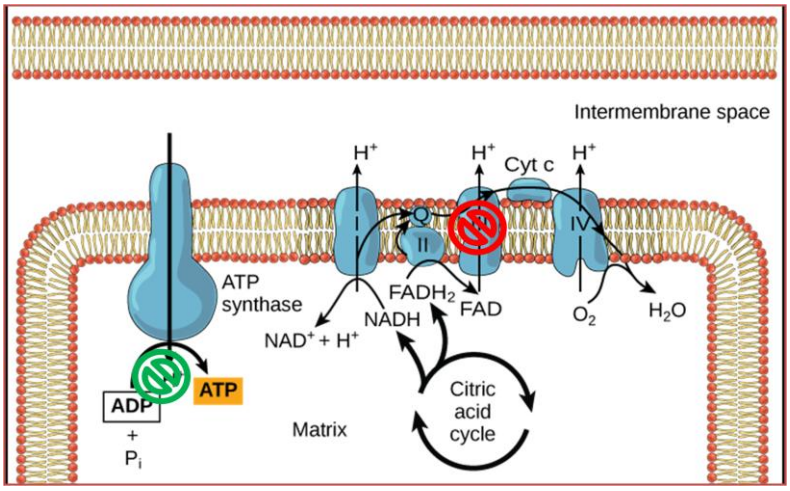

Figure 10: uncoupler activity of simazine (green symbol) and diuron (red symbol)

1.3.1. Simazine

The herbicide simazine (figure 11) is part of the triazinic herbicides. This chemical is used to destroy unwanted vegetation especially various types of weeds, grasses (Poaceae) and woody plants

The primary modes of action are the photosynthesis inhibition and the thylakoid grains damage, but in literature some endocrine disruptor effects on rats (Park H. & Bae J., 2012) and toxic effects synergic with the organophosphate pesticide clorpirifos (Trimble, A.J. & Lydy, M. J. 2006) are also reported.

Simazine has been classified as "very toxic to aquatic life" both in acute and chronic way, as "suspected to cause cancer" (https://pubchem.ncbi.nlm.nih.gov/compound/simazine#section=Safety-and-Hazards) and, although it is does not bind significantly to the estrogen nuclear receptors ERα or ERβ, is a substance that disrupts the estrogen-regulated pathways *in vivo*.

These disrupting effects may be partly explained by simazine ability to induce the aromatase enzyme activity *in vitro* (as said, the rate-limiting enzyme in the conversion of androgens to estrogens) because ultimately this can cause an increase in the conversion of testosterone to estrogen (Sanderson et al., 2001). However other studies suggest that the mechanism of action of simazine could be, similarly to the other chlorotriazinic pesticides, the alteration of hypothalamic regulation of pituitary hormone secretion. For example it has been shown that atrazine, as said, structurally really similar to simazine, alters the hypothalamic regulation of LH hormone (Zorrilla et al., 2010).

Out of European Union Countries simazine is a chemical of great agronomical importance worldwide: indeed it's widely used in U.S., Canada, Brazil and China (Silva M. & Iyer P. 2014). In European Countries simazine was banned in 2004 (Directive 04/247/EC). The highest residue levels (Maximum Residue Levels, MRLs) that are legally tolerated in or on food or feed in Europe for simazine are: in water 0.1 µg/L (or ppb) [Council Directive 98/83/EC]; in cow's milk 10µg/Kg (or ppb) [Annexes II and III to Regulation (EC) No 396/2005].

Although the clear decrease in its application frequency, simazine residues concentrations in groundwater are still above the standards of environmental quality in Italy (ISPRA, 2016). Moreover simazine is a highly persistent pesticide: not relevantly degraded after 100 days in water solution, standard conditions and a pH range typical of groundwater (Comber et al., 1999).

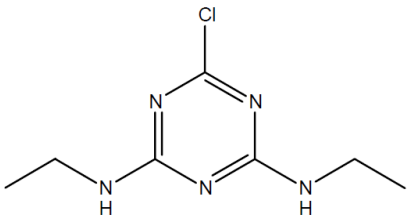

Figure 11: simazine molecule

1.3.2. Diuron

The phenylurea herbicide diuron (3-(3,4-dichlorophenyl)-1,1-dimethylurea or DCMU) (figure 12) is effective against both mono- and di-cotyledonous weeds as well as against mosses and is used as a soil sterilizing (European Food Safety Authority, 2011). The primary mode of action is photosynthesis inhibition by blocking the thylakoid electron transfer chain (Estève K. et al., 2009) but respiration inhibition in the yeast *S. cerevisiae* was also reported (Convent B. & Briquet, M., 1978).

As the simazine, diuron is classified as "suspected to cause cancer" and "very toxic to aquatic life" both in acute and chronic way (https://pubchem.ncbi.nlm.nih.gov/compound/diuron#section=Safety-and-Hazards) and is an anti-androgenic EDC because inhibits the actions of androgens (McKinlay et al. 2008).In Italy diuron's use is limited to people having an authorization of the Italian Health Ministry and to amounts of 0.5 kg/ha (Italian Ministry of Health, 2014). According to

Directive 89/778/EEC (Council Directive 98/83/EC), the MLR in potable water is 0.1ppb and in cow's milk is 50μg/Kg (or ppb). In Italy is still one of the most frequently detected pesticide in surface water (detected also in groundwater) (ISPRA, 2016). Moreover data have shown that diuron is generally persistent in soil, water and groundwater (Giacomazzi & Cochet, 2004). In laboratory, diuron showed no biodegradation over 42 days in seawater at 15°C, while the degradation products of diuron were less persistent (Thomas K.V. et al., 2002). However it must be kept in mind that diuron after undergoing biotic or abiotic partial degradation could lead to accumulation of 3,4-dichloroaniline, a by-product which exhibits higher toxicity compared to parent compound. (Giacomazzi & Cochet, 2004).

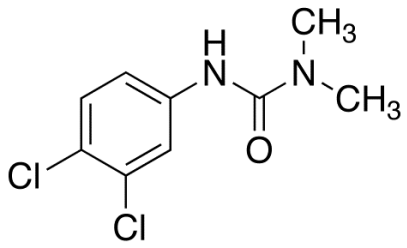

Figure 12**:** Diuron molecule

2. Monitoring of residual contaminants in agro-zootechnical environment

The implementation of safety programs calls for environmental analysis comprising two parts:

- screening methods for a continuous field monitoring. They are easy to use (even by unskilled personnel) systems able to provide qualitatively or semi-quantitatively responses;
- confirmation methods based on laboratory analytical techniques and instruments , whose use require qualified personnel, long running times of analysis but are reliable even quantitatively (Barcelo D. & Hansen P.D., 2008).

In environmental monitoring biological indicators (or bioindicators i.e. living organisms such as plants, planktons, animals, and microbes, utilized as indicators of chemical changes, environmental and food pollutions) plays an important role. In particular, for some peculiar biological responses when exposed to contaminants they can be exploited as biomediators (or biological recognition elements), in ad hoc developed biosensoristic devices.

A biosensoristic device is an integrated device constituted of a biological recognition element (called also biomediator or bioreceptor) and a transducer (fig. 13) and can be classified either according to one or the other element.

- Biomediators can be antibodies, oligonucleotides (aptamers) , enzymes and whole cells (Dragone et al., 2017).
- Transducers are mainly optical (fluorescent, bioluminescent or chemiluminescent) or electrochemical (amperometric, impedimetric, potentiometric or voltammetric).

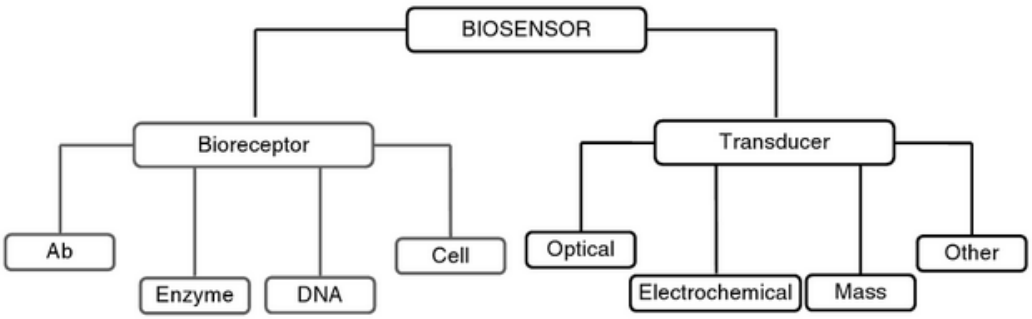

Figure 13: General scheme of a biosensor (Barcelo D. & Hansen P. D., 2008).

A biosensoristic device is based on the signal produced by the interaction of the biomediator with the analyte of interest. This signal is detected and transformed by the transducer (or detector element) into a measurable and quantifiable signal (Campanella L., 2009). A good biosensoristic device should be cheap, easy to use (also directly *in situ*) fast and suitable for a monitoring process (continuous, automatic, non destructive and cheap analyses).

Whole cell-based biosensoristic devices described in this PhD thesis also possess the following advantages: high stability, biomediators are easily stored, growth and cultured; cells can be genetically manipulated to obtain biological systems with specific characteristics.

AIM OF THE STUDY:

In this PhD study the use of a set of whole cell-based biosensoristic devices has been studied and tested for the early detection of substances able to act as EDs (also in real environmental and food samples).

The dissertation has been divided in three main chapters and in each of them a different whole-cell biosensoristic device is described.

Transgenic strain cell-based fluorimetric sensor for total estrogenic level

The first biosensoristic device was designed using the cells of a transgenic yeast, *Pichia pastoris*, as biomediator; the transduction is fluorimetric; the aim is the determination of the total estrogenic level in contaminated environmental (e.g. zootechnical wastewaters) and food (e.g. raw cow's milk) samples. *Pichia pastoris* cells were engineered with the gene encoding for a membrane estrogen receptor tagged by a fluorophore.

Untransformed strain: cell-based amperometric sensor for simazine detection

The second biosensoristic device exploits an untransformed *Saccaromyces cerevisiae* strain as biomediator, the transduction is amperometric and the aim is the detection of herbicide simazine, which may act as an ED, in spiked samples of agricultural water and raw cow's milk. The toxicological endpoint is the interference effects on cellular aerobic respiration. Analyses were done in real samples spiked with simazine at different concentrations, even below European legal limit sets for tested matrices

Untransformed strain: cell-based fluorimetric sensor for diuron detection

The third biosensoristic device uses an untransformed *Chlamydomonas reinhardtii* strain as biomediator, the transduction is fluorimetric and the aim is the detection of very low concentrations of herbicide diuron (below European legal limit for drinking water), another pesticide that possess endocrine-disrupting properties. The toxicological endpoint is the interference effects of this herbicide on chlorophyll a fluorescence.

In this chapter the toxicological endpoint was analyzed with two different approaches:

- analyzing changes in the chlorophyll fluorescence spectrum (peaks at 684nm and at 735nm) at a fixed point in non dark-adapted samples.
- analyzing changes in a kinetic curve obtained after dark-adaptation of photosynthetic material, the Kautsky effect (also called induction of fluorescence of chlorophyll a).

Chapter I

Transgenic strain cell-based fluorimetric sensor for total estrogenic level

1. Introduction

A biosensoristic device for total estrogenic level was designed. The biomediator is constituted of cells of the eukaryotic unicellular yeast *Pichia pastoris* transformed with a plasmid containing the gene for the membrane G-coupled estrogenic-receptor GPER-1 tagged at the 3' end by a fluorophore (figure 14). The transduction is fluorimetric and the aim is to detect variations in fluorophore fluorescence signals, e.g. by receptor conformational changes, deriving from the interactions between the estrogenic-like ligands and GPER receptor (scheme in figure 15).

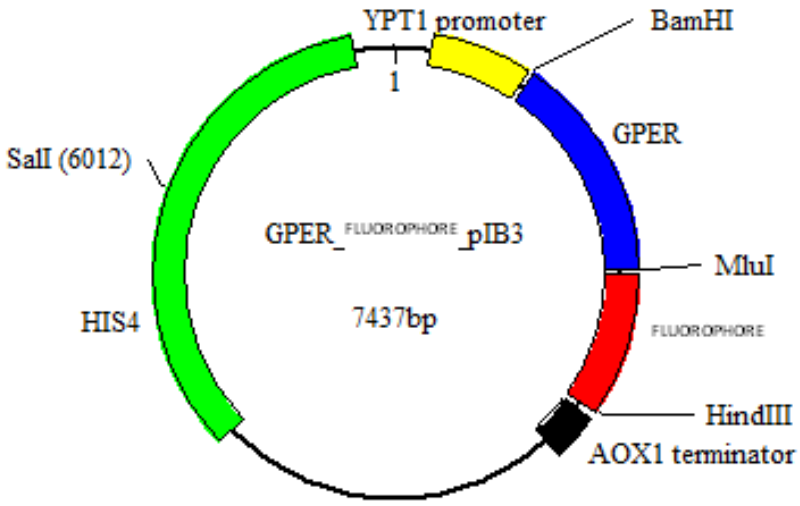

Figure 14: Scheme of the plasmid designed to be transformed in *Pichia pastoris*

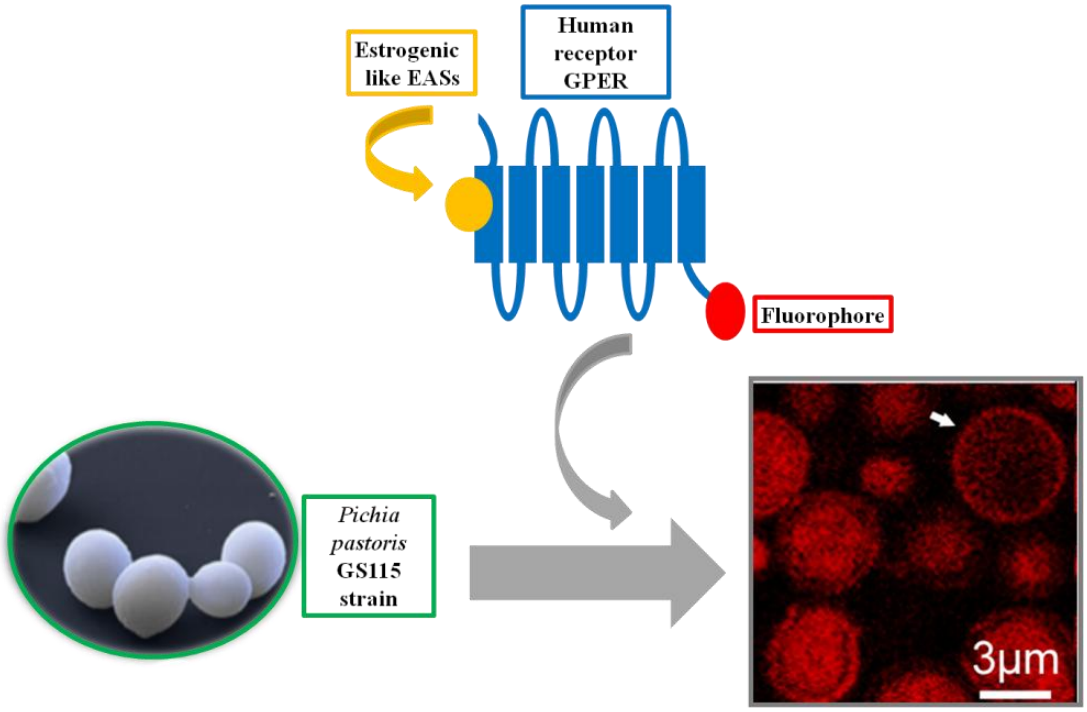

Figure 15: Scheme of the whole-cell based biosensor for the determination of endocrine active substances

The biotechnological whole cell based sensor designed in this study could led to the developing of a monitoring index for all the endocrine active substances with an estrogenic-like activity and able to interact with the receptor selected.

This biosensoristic device will be also evaluated to look at the modifications in the animal metabolism through the time (analyses on raw milk and zootechnical sewages) in order to establish the conditions of health, treatments, diet and life's environment in the farm in an holistic optic ("One Health"), following the EFSA call to such approach in risk assessment for organisms living in exposed environments (EFSA PPR Panel, 2014).

2. Differences from the state of the art

The system we designed in this study, unlike the most of the literature found, uses a single plasmid and a membrane receptor. Both of these modifications were done in this study to try to have a short response time.

2.1. Literature: two plasmids

The biosensoristic device designed falls into the recombinant receptor/reporter gene assay category. The first, widely used, yeast-based estrogen assay falling in this category is the Yeast Estrogen Screen (YES) (Routledge & Sumpter, 1996, figure 16). This biosensor is

based on a colorimetric lacZ-based estrogen-sensing *S. cerevisiae* strain. The host strain for YES assay comes from the transformation of the wild-type cells of the *Saccharomyces cerevisiae* yeast with two plasmids, one containing the human estrogen receptor alpha (hER-α) and the other the human estrogen response elements (EREs) fused to the lacZ gene. After the interaction between the estrogenic ligands and the estrogen receptor, the estrogen responsive elements are activated and the lacZ gene with them. The lacZ product, β-galactosidase, transforms the chromogenic substrate CPRG, added to the reaction, to a red product measured by absorbance at 540 nm, thus converting the biological signal in a measurable response.

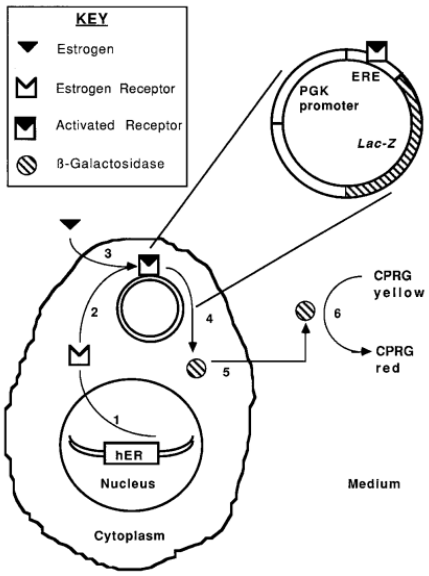

Figure 16: YES assay scheme (Routledge & Sumpter, 1996)

Also other yeast-based biosensoristic devices have been developed using a colorimetric detection, the green fluorescent protein or the firefly luciferase (as for the examples Bovee et al. 2004, Gaido et al., 1997 and Leskinen et al., 2005 from Eldridge et al., 2011).

Anyway, while the YES assay is a useful tool for its high specificity for target compounds, its colorimetric transducing system has some disadvantages: the need of the chromophore addition for color development and, most of all, a 3-5 day reaction time.

Newer colorimetric assays have dramatically shortened the time required for color development (4-6 h) through the use of alternative substrates but have the disadvantage of requiring cell lysis steps (Jaio et al., 2008).

A good effort to overcome the YES limitations was done in the bioluminescent version of the assay, called BLYES (figure 17). In this host strain the lacZ gene was substituted with the expression cassette of the bacterial luciferase (lux), a luminescent, instead of colorimetric, reporter system. The interaction of estrogens with the receptor and the subsequent activation of EREs lead to the production of luxA and luxB, detectable in the visible spectrum. The reaction time is reduced to 6 hours and there's no need of adding substrates (Sanseverino et al., 2005).

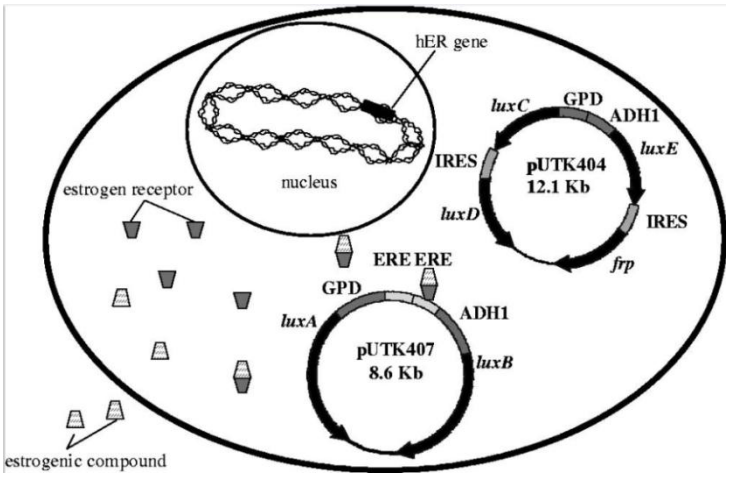

Figure 17: BLYES assay scheme (Sanseverino et al., 2005)

However, one concern with the standard systems, used for example in both YES and BLYES, is that the receptor and the reporter are on different plasmids, or the receptor is integrated into the genome and the reporter is not. Apart from making cloning tedious, particularly for high throughput applications, this approach opens up the possibility of copy number imbalances between the receptor and the reporter, which can in turn affect signal strength. This problem was recently addressed by creating a set of single copy plasmids containing both the receptor and the reporter for all the six human type I steroid receptors (Miller et al., 2010). Anyway in Miller study the activation of the reporter element is still linked to response elements (5-RE) positioned upstream of a minimal cytochrome C (CYC) promoter that controls the LacZ gene.

2.2.Our project: one plasmid

Unlike Miller et al (2010), in the approach used to design the biosensor of this study the sequence of the reporter element, a fluorophore, is directly linked at the 3' end of the receptor gene. The 3' end was selected in order to express the fluorophore in the carboxy-

terminus of the GPER-1 protein because, as in all the GPCRs receptors, the C-term is localized in the cytoplasm (Prossnitz & Arterburn, 2015).

We tried this strategy, instead of the one from Miller et al. (2010), because we wanted to try to have a very short response time (ligand-receptor interaction → transducing of the signal). The idea was to avoid the transcription dependence for the activation of the signal.

Moreover in our strategy the fluorescence of the fluorophore linked to the receptor is constitutive and the idea is that the fluorescence signal can be modified in the intensity itself or coupled to the wavelength of emission by the interaction of the receptor with the ligands (e.g. by the conformational changes occurring in the receptor).

The use of a single fluorophore linked to a receptor to measure conformational changes induced by ligand binding it was already approached and is mentioned in the review of Sridharan et al. 2014. Anyway this approach is different from the one tried in our study because they attached the fluorophore in a precise position of the transmembrane domains of the purified protein (the cytoplasmic end of the sixth transmembrane helix, as in figure 18). However, as our aim was to have an intracellular expression of the chimeric protein to screen the biological, either than the chemical, effect, we couldn't use this strategy and so we tagged the receptor sequence at its 3'end.

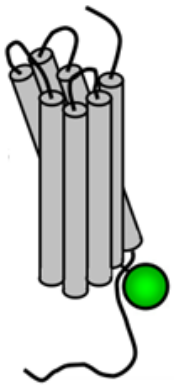

Figure 18: scheme of the use of a single fluorophore attached to a purified receptor to measure conformational changes induced by ligand binding (modified from Sridharan et al. 2014)

2.3.Literature: nuclear receptors

In the classical pathway of estrogen action the estrogen receptors binding estrogens or estrogenic-like molecules are localized in the nucleus, ER-α and ER-β. Ligand interactions

with these receptors activate transcription factors that bind to estrogen response element (ERE) regulatory sequences in target genes, thus regulating their transcription (i in figure 19) (Deroo & Korach, 2006).

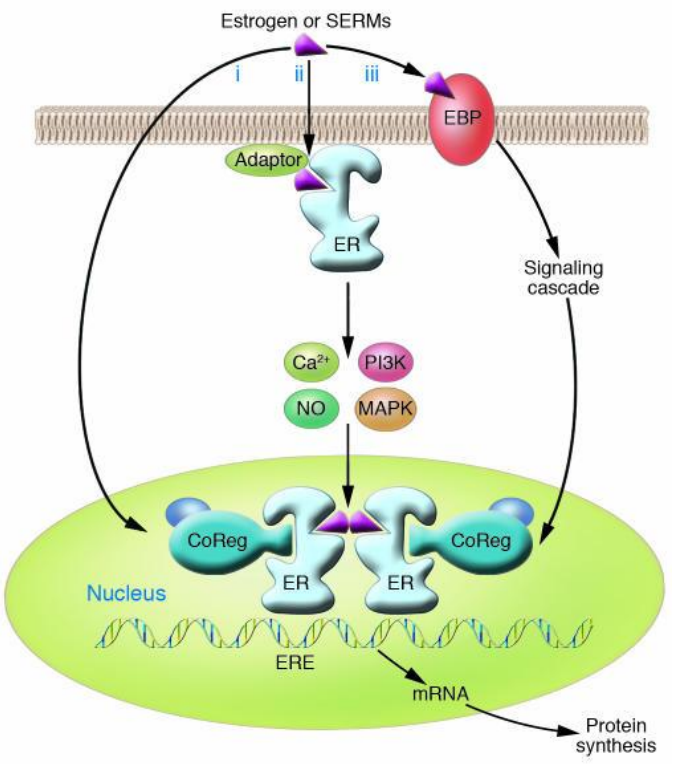

Figure 19: Models of estrogen action: "classical" for genomic responses and membrane for non-genomic pathways (Deroo & Korach, 2006).

These nuclear estrogenic receptors are nowadays the most studied and widely used ones for the development of bioassays with the aim of detecting estrogenic levels. They bind physiological estrogenic hormones and also numerous other ligands as xenobiotic estrogens. Anyway the majority of these other ligands show a weak binding affinity with the nuclear receptors and this results in a slow initiation of downstream events compared with the most potent physiological estrogen 17β-estradiol. Moreover for xenobiotic estrogens have been demonstrated rapid-onset actions (in the order of minutes) and these timing can't be explained by the pathway of nuclear receptors. This because all the process of ligand transport into cells and then in the nucleus, binding of them to nuclear receptors, ligand derived activation of transcription factors and modulation of gene expression takes periods of hours. It was demonstrated that rapid actions are non-genomic pathways mediated via membrane estrogen receptors (European Food Safety Authority, 2010).

Even if also nuclear ERs can be located or adjacent to plasma membrane with the help of adaptor proteins (ii in figure 19) and in this situation they can regulate rapid effects of estrogens, other membrane-associated estrogen-binding proteins (EBPs) were discovered which may also trigger an intracellular response (iii in figure 19).

Membrane estrogen receptors activation, both speaking of translocated ERs or other EBPs, leads to a rapid change in cellular signaling molecules which in turn may affect transcription (Deroo & Korach, 2006).

2.4. Our project: membrane receptor

In this study we decided to focus on a membrane-associated estrogen-binding protein, the membrane estrogen receptor GPER-1 (or G protein-coupled estrogen receptor 1). This receptor is part of the GPCR family and was historically called GPR30 (Prossnitz & Barton, 2014) because it was identified, between 1996 and 1998, as an orphan receptor with the seven transmembrane domain coupled to G protein. The GPER-1 cDNA was identified in various studies, but the first functional works were from Filardo and colleagues starting from 2000 (Filardo et al., 2000-2002; Revankar et al., 2005; Thomas et al., 2005; Bologa et al., 2006; Dennis et al., 2011). GPR30 was then officially designated as an estrogen receptor coupled with protein G in 2007 by the International Union of Basic and Clinical Pharmacology (Alexander et al., 2013).

The issue regarding the localization of GPER-1 inside the cell is controversy. Recent observations anyway found that GPER undergoes constitutive clathrin-mediated internalization from the cell surface to intracellular membranes, ultimately the trans-Golgi network, and that the GPER trafficking to the cell surface is regulated by coexpression of the receptor activity-modifying protein 3 (Prossnitz & Arterburn, 2015). Thus the major localization in the membranes of the endoplasmic reticulum, and the low percentages of protein found on plasmatic membranes in many cell types (Wang C. et al, 2014) can derive from an ineffective trafficking to the cell surface and a constitutive internalization of GPER. However, regulation of these trafficking mechanisms in different cell types could lead to significant levels of GPER at the cell surface (Prossnitz & Arterburn, 2015).

GPER activates various pathways thus regulating diverse cellular functions, like proliferation, metabolism, migration and secretion (Prossnitz & Arterburn, 2015). Anyway at the cellular level the effects deriving from GPER-1 and nuclear ERs cannot completely be distinguished because they are combined in different ways. Most of the compounds that interact with one receptor interact also with the other but with different affinities or also

opposite activities depending on each EAS (figure 20 -for a small overview see Prossnitz & Barton, 2014).

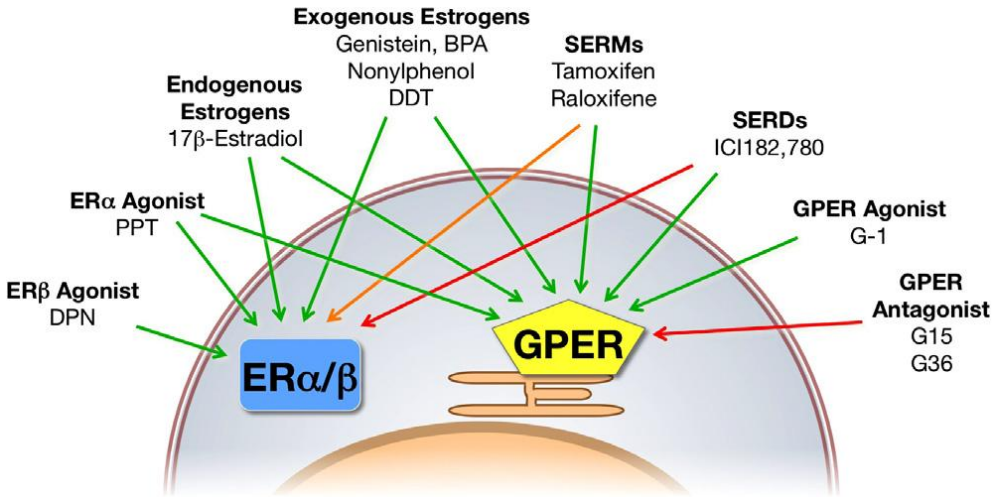

Figure 20: GPER and ERs ligands (Prossnitz & Barton, 2014): agonists (green arrows), partial agonists (SERMS, orange arrows) and antagonists (red arrows).

GPER-1 is recognized as the major mediator of rapid cellular effects linked to estrogens (Prossnitz E.R. & Barton M., 2014) and, although rapid estrogen disruption is still a concept that needs further investigation, the important consequences that it may have in wildlife and humans requires immediate action to design new estrogenic bioassays that include it (Ropero et al., 2006). Moreover it was demonstrated in studies with GPER-1-positive and ER-negative cells that GPER-1 can work like a "stand alone" receptor (Filardo et al., 2006; Revankar et al., 2005), thus it could be feasible and interesting evaluating the biological effects of estrogenic-like EASs with GPER-1 in the designed biosensor.

3. Materials and methods

3.1. The selected vector

The *Pichia pastoris* vector more useful for our aims should have two features: a constitutive promoter and the absence of a secretion signal. The first to avoid induction processes and the second to have an intracellular expression of the chimeric protein.

The selection started from Sears I.B. et al. (1998), which designed three *Pichia pastoris* vectors without a secretion signal, two with a constitutive promoter and one with an inducible promoter (table 2). Between the two having a constitutive promoter, pIB2 was excluded because this vector has the GAP promoter which reaches very strong expression levels. High levels of expression could overwhelm the protein rearrangement system of the cell and so could be toxic in some cases (Balamurugan V. et al., 2007). As the chimeric protein should be intracellular, the moderate expression which can be reached with the YPT1 promoter of pIB3 was preferred.

Table 2: vectors designed by Sears et al. (1998)

Plasmid name	Size (bp)	GenBank accession no.	Promoter	Promoter characteristics
pIB1	5270	AF027958	(None)	
pIB2	5546	AF027959	*GAP*	Strong constitutive
pIB3	5565	AF027960	*YPT1*	Moderate constitutive
pIB4	5796	AF027961	*AOX1*	Very strong on methanol; strong on mannitol; weak on glycerol; off on glucose

The pIB3 vector, apart from the promoter characteristics, and as pIB2 and pIB4, has two other important features: the AOX1 terminator, which ensures a good processing of the 3' end, and the HIS4 gene, important for the site-specific integration into the *Pichia pastoris* genome in the his4 locus.

The use of this vector imposes for transformant selection the use of a histidine-auxotrofic strain of *Pichia pastoris*, like GS115. Selecting the transformation on a medium lacking histidine, like RDB medium, only the positively transformed colonies will have the possibility to produce this amino acid and then to grow (Balamurugan V. et al., 2007).

3.2.The first attempt

E.Coli DH5α cells containing the vector pIB3 were cultured on LB supplemented with ampicillin. The extracted plasmidic DNA corresponding to the pIB3 vector (figure 21) was then checked by double-digestion with SalI/NcoI restriction enzymes (Promega). The linearization was done with BamHI and HindIII (Promega), enzymes selected because in this vector the insertion between them enables the expression of the gene (Sears et al. 1998).

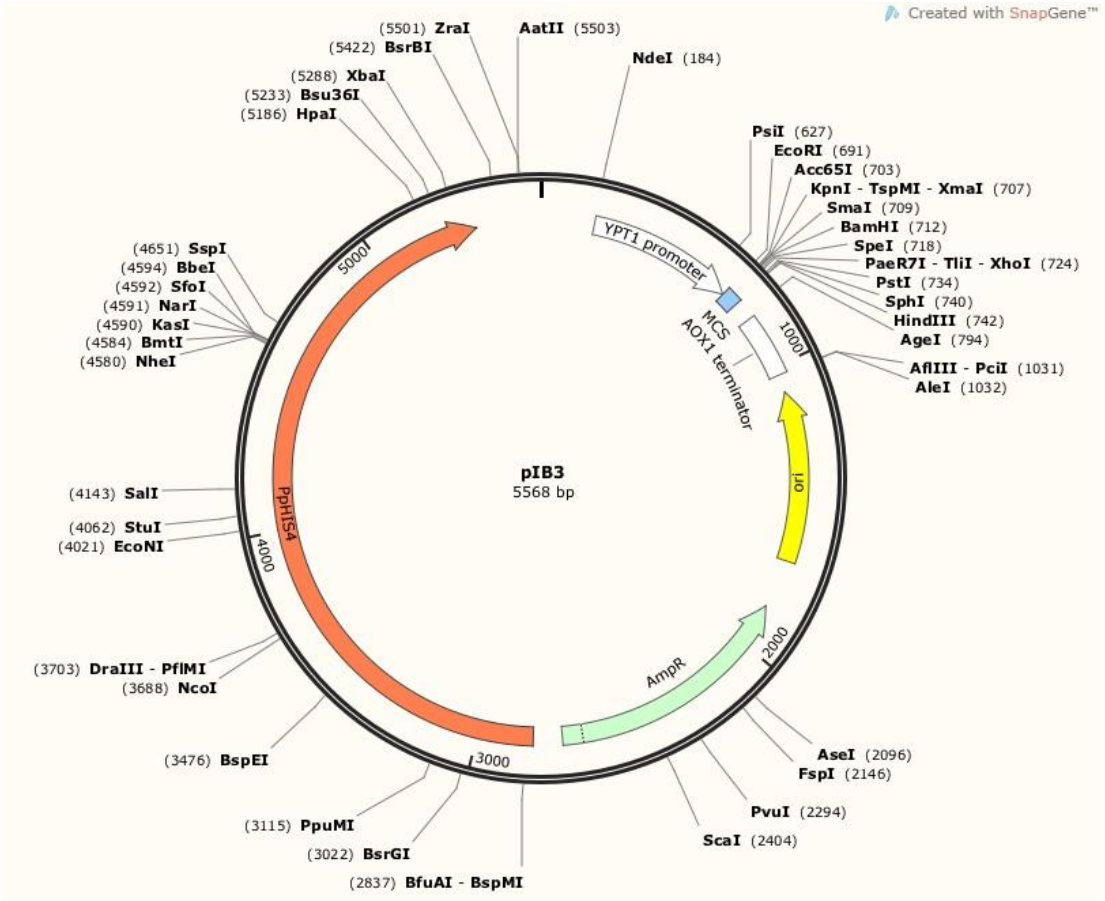

Figure 21: pIB3 vector Addgene plasmid #25452

The first attempt was done using the sequence for a human estrogen receptor (GPER-1) tagged at 3' end to a fluorophore (TurboGFP). This fluorophore is a bright green fluorescent protein (which can help in sensitivity), with a really useful fast maturation step (which can help in reducing times) and is defined suitable to generate stably transfected cell lines (which can help in the maintaining of the biosensor) so, as we find a commercial human plasmid (Origene) in which this fluorophore was tagged at the 3' end of GPER1, it was our first choice (fig. 22).

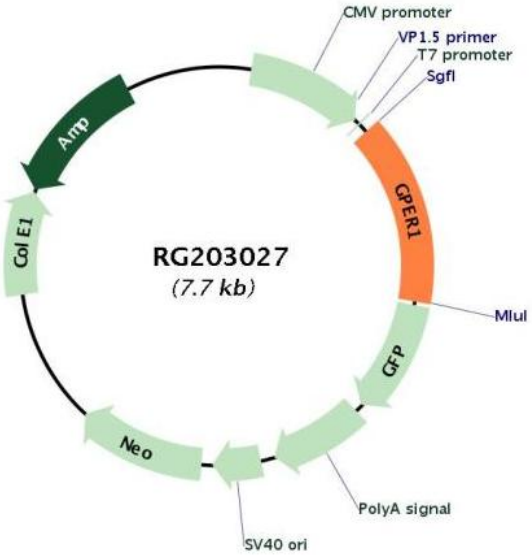

Figure 22: commercial human plasmid (Origene RG203027)

The sequence encoding for the GPER-TurboGFP insert was PCR amplified from the commercial plasmid, after optimizing parameters, with two primers (table 3) designed for the insertion of the restriction sites for BamHI and HindIII respectively at 5' of GPER and 3' of Turbo-GFP. The Platinum SuperFi DNA Polymerase (Invitrogen) was used. The purified PCR product was then double-digested with BamHI/HindIII (Promega).

Table 3: primers for the insertion of the restriction sites for BamHI and HindIII and PCR parameter

Name	**Sequence**	**PCR parameters**
BamHI_ORF_F	AATAGGATCCATGGATGTGACTTCCCAAGCC	Ta=60°C 34 cycles
HindIII_GFP_R	AATAAAGCTTTTAAACTCTTTCTTCACCGGCATC	

A ligation reaction between the double-digested insert and vector was done using the T4 DNA ligase (Promega). The product was then transformed in competent *E.Coli* DH5α competent cells and selected in LB medium supplemented with ampicillin. The grown colonies were used to extract the plasmidic DNA using the Gene Elute HP Plasmid Miniprep Kit (Sigma-Aldrich). The plasmidic DNA obtained was checked by double-

digestion with BamHI/HindIII and by sequencing (Macrogen EZ7 www.ezseq.com) with the forward primer in the promoter region (table 4).

Table 4: primers used to check the insertion in the plasmidic DNA extracted with miniprep

Name	**Sequence**
PromYPT1 -139F	CCAGCCAAAACCCCTAAACC
HindIII_GFP_R	AATAAAGCTTTTAAACTCTTTCTTCACCG GCATC

The plasmidic DNA was then extracted in bigger quantities, with the Qiagen "Plasmid Maxi Kit", from the colonies in which both the controls were positive and checked by digestion and sequencing (SmartSeq/Value Read of Eurofins genomics https://eurofinsgenomics.com) again. The primers used in this step were five and the sequence was fully aligned (fig. S1 in Annexes) with the theoric (table 5).

Table 5: Primers used for the sequences analysis of the plasmidic DNA extracted at high concentrations

Name	**Sequence**	**Sequenced zone**
PromYPT1 -139F	CCAGCCAAAACCCCTAAACC	Promoter-ATG
GPER_941_R	CCAGCAGACGAAGAAGACCA	GPER
GPER1_GFP_F	CCTGTGCTACTCCCTCATTG	GPER-GFP
GFP_1612_F	GATCTGGATGGCAGCTTCAC	GFP-Terminator
HindIII_GFP_R	TTAAACTCTTTCTTCACCGGCATC	GFP-TAA

The plasmidic DNA was prepared for the transformation in *Pichia pastoris* by linearization with SalI enzyme (Promega), having a unique restriction site in the HIS4 gene. The linearization reaction was done at 37°C for 7.30 hours and the DNA was purified with a precipitation protocol (95% ethanol and sodium acetate 3M pH 5.2). *Pichia pastoris* cells of the histidine-auxotrofic strain GS115 (Thermofisher) were grown till an OD_{600nm} = 1.3-1.5 was reached, with a first overnight at 30°C/200rpm and a subsequent monitored growth. At that point the protocol for the preparation of competent cells was followed. The *Pichia pastoris* cells were then immediately electroporated (Voltage=1500V;

Resistor=0400Ω; Capacitor=0025μF; Time 9.6ms) in presence of the linearized plasmid. Positive colonies were selected on RDB Agar, a medium lacking of histidine.

The transformed colonies grown on RDB were checked with two molecular techniques:

- a colony-PCR with two primers (table 6) amplifying a product (~500bp) between the end of the GPER and the beginning of the Turbo-GFP genes;

Table 6: primers used for colony PCR

Name	**Sequence**	**PCR parameter**
1100_ORF_F	cggatgtgaggttcagcagt	Ta=55°C
1576_GFP_R	Cgttgctgcggatgatcttg	35 cycle

- an RT-PCR with the same primers (retro-transcription done with Qiagen "Quantitect Reverse Transcription" kit) on two colonies having positive results from colony PCR. We also done, as controls, a PCR on extracted DNA before the retrotranscription (same primers) and a PCR on retrotranscripted samples using a forward primer located on promoter (Prom_YPT1-139F) and a reverse primer (GPER_941_R) at an appropriate distance on the retrotranscripted samples (to check the retrotranscription reaction).

Then the fluorescence signals of positive *Pichia pastoris* colonies were tested with the spectrofluorometer Varian Cary Eclipse. The emission spectra between 490 and 750nm were measured at various excitation λ = 400, 440, 470 e 480nm. Excitation slit = 10nm; Emission slit = 5nm; Scan rate = 600nm/min. All the treatments tried on the samples before to analyze the fluorescence are listed in table 7.

Table 7: treatments done on sample to try to observe fluorescence signals

No.	***Samples treatment***
1	O/n growth of colonies: transformed ones in selective (RDB) and wild-type ones in non selective (YPD) medium;
2	Pelleting of o/n colonies → **resuspension in 0.7% NaCl**;
3	Pelleting of o/n colonies → **washing** and resuspension in 0.7% NaCl;
4	Pelleting of o/n colonies → washing and resuspension in 0.7% NaCl → **dilution in sterile water**;

5	Pelleting of o/n colonies → washing and resuspension in 0.7% NaCl → **supplementing with 1% glucose**;
6	Pelleting of o/n colonies → washing and resuspension in 0.7% NaCl → supplementing with 1% glucose → **exposition to 0.25mM of 17β-estradiol**.

3.3. The second attempt

As unfortunately we didn't observe any Turbo-GFP related fluorescence signal, not constitutively and neither under exposition to 0.25mM of 17-β estradiol (Sigma), we thought to have folding problems and we decided to change the fluorophore with mCherry. This is an easier to fold fluorophore, compared to Turbo-GFP, and has the peculiarity of turning red the media, thus avoiding the necessity of molecular analyses on positive colonies.

The restriction sites for MluI (Gibco) and HindIII (Promega) were added by PCR respectively to 5' and 3' ends (primers in table 8) of the mCherry sequence (from a plasmid previously present in the laboratory of professor D'Ovidio). Then the amplificate product was digested with these two enzymes.

Table 8: primers for the insertion of the restriction sytes of MluI and HindIII

Name	**Sequence**	**PCR parameter**
MluI_mCherryF	AATAACGCGTATGGTGAGCAAGGGCGAG	Ta=62°C
HindIII_mCherryR:	AATAAAGCTTCTAGGAACCACCTCCCTTGTA	30 cycle

The plasmid from the first attempt, containing the GPER-TurboGFP sequence, was similarly digested to excide out the Turbo-GFP. The ligation reaction was tried with various vector/insert ratios but unfortunately we couldn't have *E.Coli* colonies positively grown on LB supplemented with ampicillin. Supposing the problem was in the incorrect production of the MluI/HindIII tails, it was decided to polyadenylate mCherry sequence, using the GoTaq G2 Flexi DNA Polymerase (Promega), ligate it in pGEM Easy vector (Promega), extract the plasmidic DNA from colonies positively grown on selective medium and then digest the mCherry gene to obtain correct tails.

However, as a restriction site for MluI is already present in pGEM Easy vector, the possible outcomes to check were two:

- Insertion of mCherry in pGEM Easy oriented MluI/HindIII:

The single digestion with MluI produces a 792bp band and a bigger band (pGEM). The double digestion with MluI and HindIII produce a 792bp band (HindIII in 794 position and MluI in 65 position), a 63bp band (MluI in 857 position and HindIII in 794 position) and a bigger band (pGEM).

- Insertion of mCherry in pGEM Easy oriented HindIII/MluI

The single digestion with MluI produces a 63bp band and a bigger one (pGEM). The double digestion with MluI and HindIII produce a 63bp band (MluI in 857 position e MluI in 794 position), a 729bp band (MluI in 794 position and HindIII in 65 position) and a bigger band (pGEM).

The obtained mCherry sequence digested from pGEM and selected with an electrophoretic run as explained, was then ligated in the similarly double digested plasmid (the first attempt plasmid without Turbo-GFP gene) and transformed in *E.Coli* DH5α competent cells. Unfortunately we didn't obtain positive colonies again.

Supposing the problem was due to the high quantity of GC residues at the MluI end, it was decided to use the recombination approach with In-Fusion® HD Cloning Kit (Clontech® Laboratories). First of all the mCherry sequence was excised from the original plasmid. Then two primers *ad hoc* (table 9) for the recombination were designed. They contain:

- 18 and 20bp of mCherry sequence respectively for forward and reverse primer;
- The reconstruction of the desired restriction sites;
- 15 bp before and after the position where mCherry will be in the final GPER-mCherry plasmid.

Table 9: primers for the recombination of mCherry inside the plasmid containing GPER-1 gene

Primer forward
GPER_MluI_mCherry_F:
CAGTGCCGTGACGCGTATGGTGAGCAAGGGCGAG

Primer reverse pIB3_HindIII_mCherry_R: CATGTCTAAGAAGCTTCTAGGAACCACCTCCCTTGT

A PCR on the mCherry gene was then done with these primers and checked on agarose gel to obtain a product useful for the recombination, constructed as follows:

15bp GPER – MluI – mCherry – 15bp pIB3

At this point the pIB3 vector containing GPER and the obtained PCR product were recombinated as in the protocol of the kit. The recombination product was checked by digestion with NcoI enzyme (Promega), which produces three cuts, and then transformed in *E.Coli DH5α* competent cells. Finally positive colonies were obtained and the plasmidic DNA was extracted from them and checked by digestion and sequencing (SmartSeq/Value Read of Eurofins genomics https://eurofinsgenomics.com). Starting from the colonies in which these controls were positive, the DNA was extracted in higher quantities and checked by digestion and sequencing again (SmartSeq/Value Read of Eurofins genomics https://eurofinsgenomics.com). The primers used are in table 10 and the plasmid resulted completely aligned.

Table 10: primers used to sequence the plasmid obtained from recombination

Name	**Sequence**
GPER_GFP_F	CTGTGCTACTCCCTCATTG
MluI_mCherryF	AATAACGCGTATGGTGAGCAAGGGCGAG
HindIII_mCherryR:	AATAAAGCTTCTAGGAACCACCTCCCTTGTA

The plasmid obtained, containing GPER-mCherry gene in the pIB3 vector, was prepared for transformation in *Pichia pastoris* linearizing with SalI-HF (Biolabs®) in a reaction at 37°C/2h blocked at the end with a 20 minutes step at 65°C. The digested product was checked in an agarose run and precipitated with sodium acetate 3M pH 5.2 and EtOH 100% cold.

In the meantime, *Pichia pastoris* cells of the GS115 strain were grown in YPD at 30°C/200rpm in a preinoculum of 5mL for 7h. An aliquot of 250µL of the preinoculum was inoculated in 250mL of YPD and grown overnight. The day after the OD_{600nm} of the

culture was monitored till reaching a value between 1.3 and 1.5. At that point the cells were harvested by centrifugation at 2000g/4°C for 5 minutes and the protocol to obtain competent cells was followed.

The transformation with linearized and purified plasmid was then directly done without freezing the cells. The transformation was done by electroporation (1500V/5msec) and the positive colonies were selected on RDB agar. Some colonies positively grown on the selective plates and a little of them were clearly red.

We decided to culture a red transformed colony and an untransformed GS115 colony. They were inoculated in 5mL of RDB and RDB supplemented with histidine respectively (growth at 30°C/200rpm/7h). After 7h growth, 4mL aliquots of the preinocula were inoculated in 500mL of RDB and RDB supplemented with histidine (growth at 30°C/200rpm/40h) respectively.
The obtained cultures were pelleted at 2000rpm/4°C/10min and the supernatant was discarded. Pellets were used to extract the chimeric protein.
A first extraction reaction was done with the breaking buffer (50mM sodium phosphate monobasic pH 7.4, 1mM PMSF, 1mM EDTA, 5% glycerol) of the EasySelect™ *Pichia* Expression Kit (Invitrogen) protocol and breaking the cells by vortexing (30 sec/8 times) with acid-washed glass beads (0.5mm) directly inside the 50mL Falcons.

As we observed that, after centrifuging at 2000rpm/10min/4°C and transferring the supernatant to new tubes, the pellet of the transformed colony was still red, we decided to do a second extraction step from the same pellets. A lysis buffer containing a detergent (1% Triton X-100, 50mM Tris-Cl [pH 7.4], 300mM NaCl, 5mM edetic acid [EDTA], 0.02%, sodium azide, and 1mM PMSF) (Liu et al., 2009) was added to the pellets to help the extraction, as the chimeric protein should be in a membrane. The reaction was maintained 30 min in agitation in ice then, as for the first step, the extraction with detergent was centrifuged at 2000rpm/10min/4°C and the supernatant was transferred to new tubes.

The supernatant samples obtained from the extractions were analyzed for the mCherry fluorescence signals (Synergy™ Mx Monochromator-Based Multi-Mode Microplate Reader, BioTek, Aix-Marseille University):

- A fluorescence spectrum was done with the following parameters: Fixed Excitation length: 580/9.0 nm - Emission Start length: 600/9.0 nm and emission stop length:

700 nm with a 5nm step – Optics on top - Read Speed: Normal - Delay: 100 ms - Measurements/Data Point: 10 - Read Height: 8 mm;

- A fluorescence endpoint analysis was done with excitation length: 580/13.5nm and emission length: 635/13.5nm - Read Speed: Normal - Delay: 100msec - Measurements/Data Point: 10 - Read Height: 8 mm. This fluorescence analysis was done also on aliquots of cellular pellet resuspended in MilliQ water.

To confirm membrane localization of the chimeric protein cells were observed under a Zeiss LSM 700 confocal microscope (CP2M Platform, Aix-Marseille University). Cell membranes were labeled with WGA-FITC. WGA is a dimeric protein which interact with N-acetyl glucosamine (GlcNAc), a structure present in many bacterial cell wall peptidoglycans and FITC is a green fluorescent marker.
The protocol for labeling was as follows (Vector Laboratories - Fluoresceine lectine kit: ref:FLK-2100): Cells fixing in PFA 4% - 1H – RT; Saturation, 1H, in PBS/5% BSA (non permealibized condition) or in PBS/5%BSA/0,1% saponine (permeabilized condition); one wash in PBS; labeling with WGA-FITC lectin at 1/200 in PBS/0,5% BSA; 3 wash in PBS; mounting between blade and lamella in Mowiol

We also overlaid the signals obtained with and without WGA-FITC. Parameters used for confocal microscopy analyses were: laser excitation light at 580nm and emission light at 630nm.

4. Results

4.1. The first attempt

To obtain the linearized vector was firstly screened the pIB3 vector by double-digestion with SalI and NcoI (produces two fragments of 455 and 5113bp). This screen was positive for only one colony, as shown in the electrophoretic run in figure 23. The BamHI/HindIII linearized gel band corresponding to this positive colony was purified.

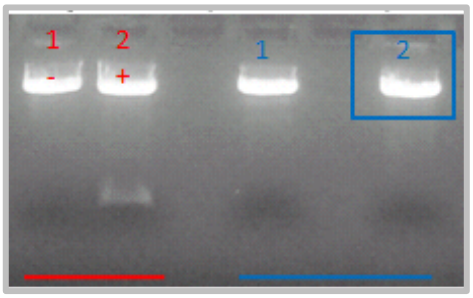

Figure 23: screening (red) and linearization (blue) digestion of two different colonies containing the vector pIB3

Obtained also the PCR product containing the sequence for GPER-1 tagged by Turbo-GFP and flanked by BamHI (5') and HindIII (3') restriction sites and digested it with them, an electrophoretic run of the linearized vector and insert was done (figure 24). The vector was estimated around 50ng/µl and the insert around 25ng/µl.

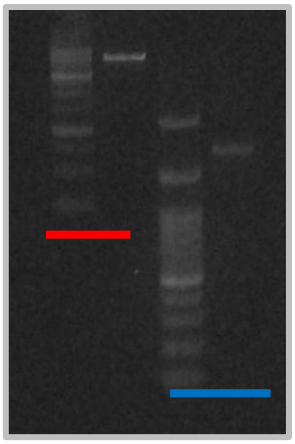

Figure 24: vector (red) and insert (blue) double-digested with BamHI/HindIII (100bp marker)

Vector and insert were then ligated and transformed in *E.Coli DH5α* competent cells. The plasmidic DNA was then extracted from the colonies positively grown on selective medium and digested again with BamHI/HindIII (Promega) to check the good insertion. As we can observe from figure 25 two of the colonies are positive as they show two bands: insert (around 1800bp) and vector (higher).

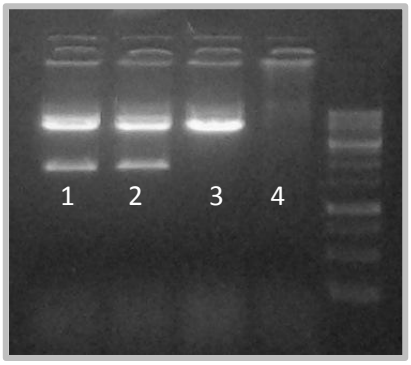

Figure 25: BamHI/HindIII double-digestion done to check the good insertion of GPER-TurboGFP in pIB3 vector (marker 1Kb)

The colonies corresponding to the positive double-digestion results were inoculated again in LB medium supplemented with ampicillin to extract the plasmidic DNA in higher quantities. The obtained plasmids were checked again with BamHI and HindIII double digestion showing an excised fragment of around 1800bp, as expected, in both colonies. The two plasmids were then sent to sequencing and only one of them was completely aligned with the desired sequence.

Positive plasmidic DNA was extracted again in bigger quantities from this positive colony (figure 26). Basing on the 1Kb marker an estimate of the quantity of the plasmidic DNA in each dilution was done: not diluted is not estimable; 1:10 dilution seems around 46ng/μL band → 460ng/μL; 1:20 dilution seems around 15ng/μL band → 300ng/μL; 1:50 dilution seems around 8ng/μL band → 400ng/μL. The different dilutions were also quantified with a spectrophotometer reading their absorbance at 260-280 and 240nm and the estimated concentration was 500ng/μL. Doing an average of all the values, we estimated a concentration of around 440ng/μL so we had around 0.22 mg of plasmidic DNA.

Figure 26: Electrophoretic check and quantification of plasmidic DNA

The plasmidic DNA quantified was then checked by BamHI/HindIII double digestion and sequencing and was found positive as expected.

The obtained plasmid was linearized with SalI (New England Biolabs®$_{Inc.}$), which has a unique restriction site inside the His4 gene. The goodness of the digestion was checked by an electrophoretic run of the linearized product on 1% agarose gel (figure 27 with marker 1Kb).

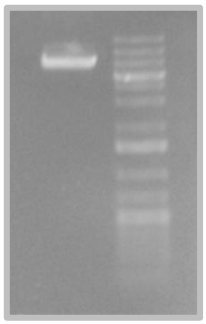

Figure 27: plasmidic DNA linearized with SalI

After the transformation by electroporation in *Pichia pastoris* GS115, some colonies were positively grown on selective medium lacking histidine (RDB). These colonies were checked by two molecular techniques (fig. 28):

- colony PCR (panel A);
- RT-PCR (panel B: samples RT1 and RT2 the second). As controls of the RT-PCR we did also a PCR on extracted DNA before the retrotranscription reaction (panel B: samples 1 and 2) and a PCR on retrotranscripted samples with the forward primer in the promoter to check the goodness of the retrotranscription (panel C).

As we can observe, all except one of the transformed colonies were positive to the colony-PCR; RT-PCR, done on two positive colonies, shows positive results and both their controls are positive (panel C doesn't show any amplificate, as expected).

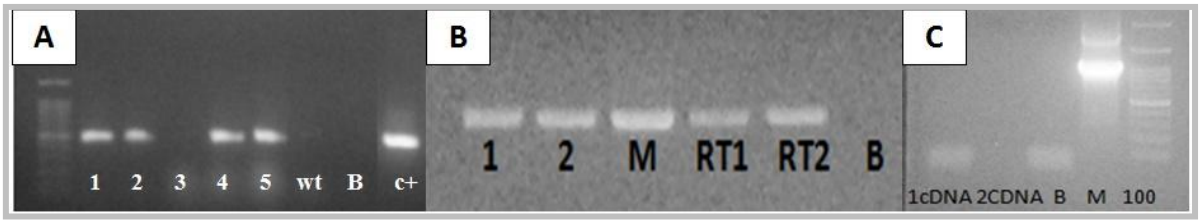

Figure 28: Controls on positive colonies

However all the treatments to the samples we tried in order to analyze the fluorescence signals of Turbo GFP weren't useful to obtain positive results (table 11).

Table 11: fluorescence results on positive colonies after each sample treatment

No.	***Samples treatment***
1	Fluorescence analysis done directly in YPD or RDB → THE MEDIA INTERFERED HAVING AN EMISSION SPECTRUM IN THE SAME REGION OF TURBO-GFP
2	Pellet **resuspended** in 0.7% NaCl → TURBO-GFP RELATED SPECTRA NOT OBSERVED;
3	Pellet **washed** and resuspended in 0.7% NaCl → TURBO-GFP RELATED SPECTRA NOT OBSERVED;
4	Pellet washed, resuspended in 0.7% NaCl and **diluted in sterile water** → TURBO-GFP RELATED SPECTRA NOT OBSERVED;
5	Pellet washed, resuspended in 0.7% NaCl and **supplemented with 1% glucose** → TURBO-GFP RELATED SPECTRA NOT OBSERVED;

The last attempt was to expose the obtained pellets, resuspended as in 3 and 5, to 0.25mM of 17β estradiol but even in this way spectra results weren't seen.

Supposing the problem was in the folding of the chimeric protein it was decided to change the fluorophore with mCherry, an easier to fold fluorescent tag which turns the medium red, thus avoiding the need of molecular techniques to check positive colonies.

4.2.The second attempt

In order to change the fluorophore, the Turbo-GFP sequence was excised from the plasmid of the first attempt digesting with two enzymes:

- MluI, unique restriction site between the GPER and the Turbo-GFP genes;
- HindIII, unique restriction site at the 3' end of the fluorophore.

Unfortunately the two restriction enzymes didn't work well in a double digestion with just a single buffer so it was decided to try two different strategies (results in figure 29):

- single digestion with MluI or HindIII followed by a second digestion reaction with the other enzyme;
- double digestion with Buffer E (Promega) changing the ratios of the two enzymes.

In figure 29 A1 and B1 samples are the single digestions with MluI and HindIII respectively, MluI/HindIII is the double digestion in Buffer E, A2 and B2 are the products of the second digestions done on A1 and B1. As expected the single digestions didn't produce an excision fragment. All the three double digestions instead had the Turbo-GFP excised band.

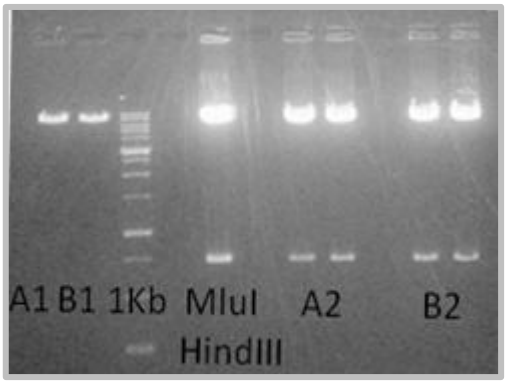

Figure 29: Excision of Turbo-GFP: three strategies of digestion

The sample MluI/HindIII was purified and quantified in comparison with a 1kB marker in an electrophoretic run on agarose 1% gel: estimated 20ng/μL.

A PCR, with two primers designed *ad hoc* to add the restriction sites for MluI and HindIII at 5' and 3' respectively of mCherry was done on the original plasmid containing the mCherry sequence (a gift from professor D'Ovidio's laboratory).
An electrophoretic run with the amplification product was done, also for purification purposes (figure 30).

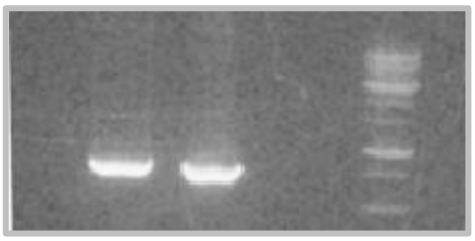

Figure 30: amplification product of PCR (marker 1Kb).

Unfortunately we had a lot of problems in preserving the quantities of DNA during the purification steps so finally we decided to double-digest directly the PCR avoiding a purification step. The digestion product after purification was quantified on gel in around 20ng/µl.

All the ligation reactions tried, with different insert/vector ratios, didn't produce some positively transformed colonies so we thought the problem was in the production of 5' and 3' tails.

A ligation in pGEM Easy vector was then tried: the mCherry gene amplificate obtained was polyadenylated, ligated in the pGEM Easy vector and then transformed in *E.Coli* DH5α competent cells. The plasmidic DNA was extracted from a positive colony, purified and analyzed by double-digestion MluI/HindIII (figure 31). The first line after marker 100bp is a single digestion with MluI product and the next line instead is the double digestion.

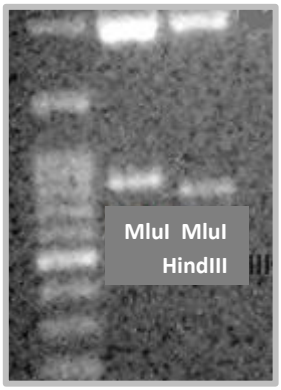

Figure 31: single and double digestion of pGEM Easy vector transformed with mCherry

The electrophoresis shows as the mCherry gene was inserted in the pGEM Easy vector with a MluI/HindIII orientation: a band of around 800bp in the single digestion and a barely shorter one in the single digestion. This means that the digestion with HindIII on the MluI single digestion excided the unwanted fragment HindIII (794)-MluI (857) (figure 32).

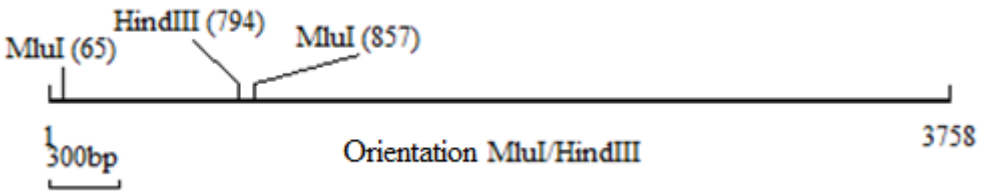

Figure 32: scheme of the insertion orientation of mCherry in pGEM Easy vector

The mCherry gene (with the MluI and HindIII restriction sites) obtained by double-digestion of transformed pGEM Easy vector was ligated in the desired pIB3 (with GPER gene) vector and transformed in *E.Coli* DH5α competent cells but again no positive colonies were found. As probably the GC-richness in 5'end of mCherry sequence was the problem, it was decided to insert the mCherry sequence in the vector containing GPER by a recombination process to avoid the "*cut and paste*" passage.

The mCherry sequence was excised from the original plasmid with a double digestion (figure 33)

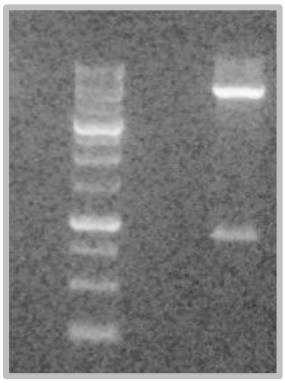

Figure 33: mCherry excision from the original plasmid

The designed GPER_MluI_mCherry_F and pIB3_HindIII_mCherry_R primers were used in a PCR on the mCherry sequence to add the appropriate tails for the recombination process. The recombination product was then checked by digestion with NcoI (figure 34) and by sequencing. In the digestion check three cuts, as expected, are shown and the sequence was completely aligned (fig. S2, in Annexes).

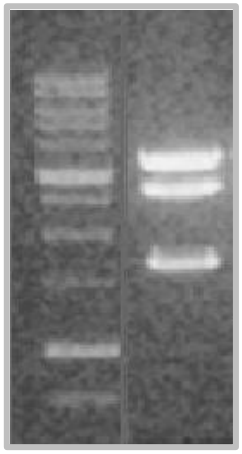

Figure 34: checking digestion with NcoI enzyme

The obtained and checked plasmid was linearized with SalI-HF (Biolabs®) and the reaction was controlled with an electrophoretic run (figure 35, with 5µL of marker 1Kb).

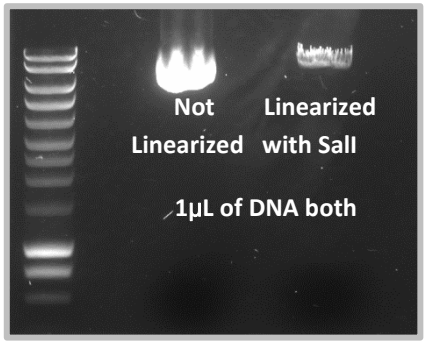

Figure 35: plasmid linearized with SalI

The linearization product was precipitated, with NaAcetate 3M pH 5.2 and EtOH 100% cold, and quantified in 2.2µg/µL (NanoDrop2000c – Thermofisher).

After the transformation of GS115 *Pichia pastoris* competent cells we had some colonies on selective RDB medium and a little part of them were red, as expected. Culturing one red colony and one GS115 colony, after a preinoculum in 5mL/7h and a big growth in 500mL/40h, cultures were as in figure 36. Cellular pellets obtained from these cultures were as in figure 37.

Figure 36: 40h growth, after 7h preinoculum, of transformed red cell and untransformed GS115

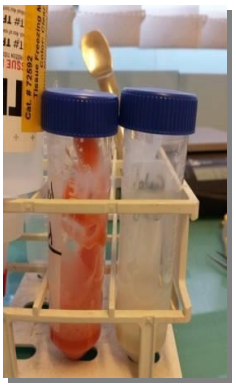

Figure 37: pellet from the cultures of figure 36

The pellets were used to extract the intracellular proteins, without and with a detergent, and fluorescence spectra were done on the extracted samples (figure 38).

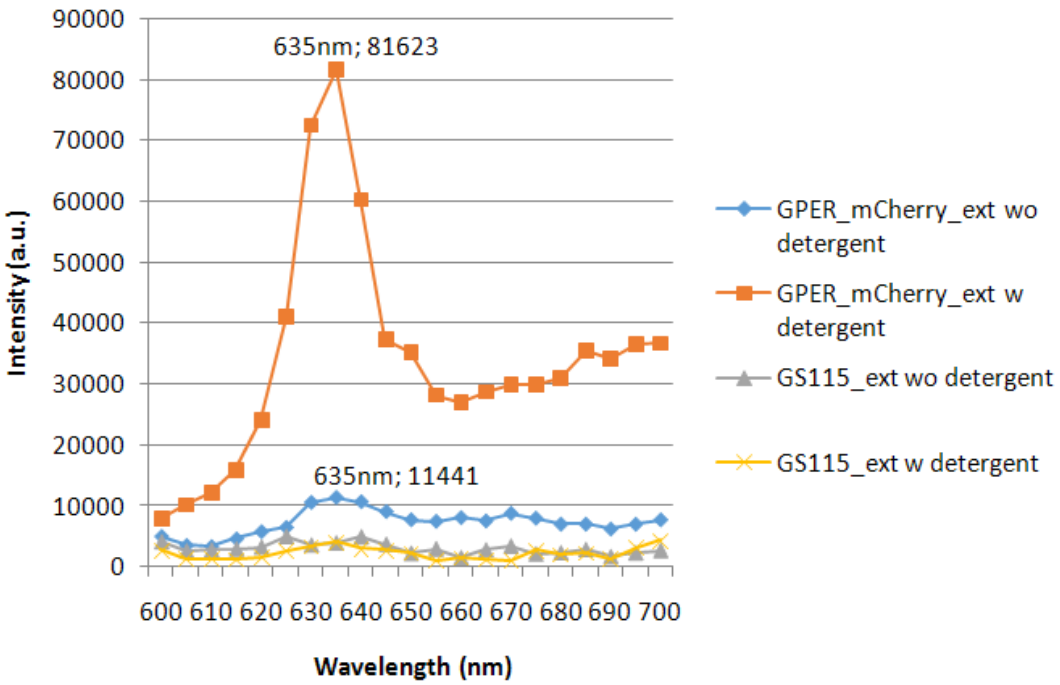

Figure 38: Fluorescence spectra on extraction samples

As we can observe there is a big fluorescence peak in the sample derived from the extraction with a detergent, a small peak in the sample extracted without detergent and both the controls showed no fluorescence. Another interesting evidence is that the maximum of emission of the chimeric protein is different (635 nm) from the expected maximum of the mCherry fluorophore (610 nm).

We analyzed also the endpoint of fluorescence corresponding to 635 nm (figure 39) in the two extracted samples and in the cellular pellets (resuspended in the same quantity of MilliQ water).

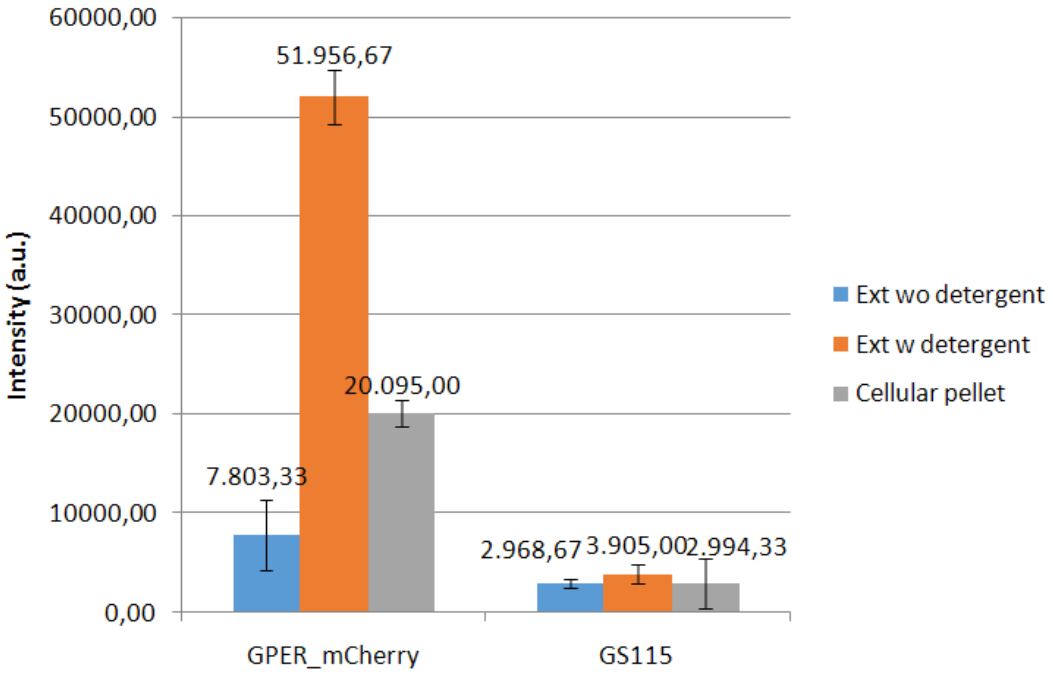

Figure 39: fluorescence endpoint at 635 nm on extracted samples and cellular pellets

As we can observe, the fluorescence of the sample extracted with detergent was 6.7X higher than the one extracted without detergent. This led us think that the chimeric protein could effectively be in the membrane.

To confirm the membrane localization we did several confocal microscopy trials in order to localize the cellular and/or sub-cellular compartments where the GPER-mCherry is in *P. pastoris* cells (column mCherry in fig. 40). We also tagged the cell membrane by WGA-FITC (green, column +/- WGA-FITC in fig. 40) and we overlaid the mCherry and FITC signals (column merge in fig. 40). Results are shown in figure 40:

- line A: untransformed cells without WGA-FITC labeling;
- line B: untransformed cells with WGA-FITC labeling;
- line C: transformed cells without WGA-FITC labeling;
- line D: transformed cells with WGA-FITC labeling

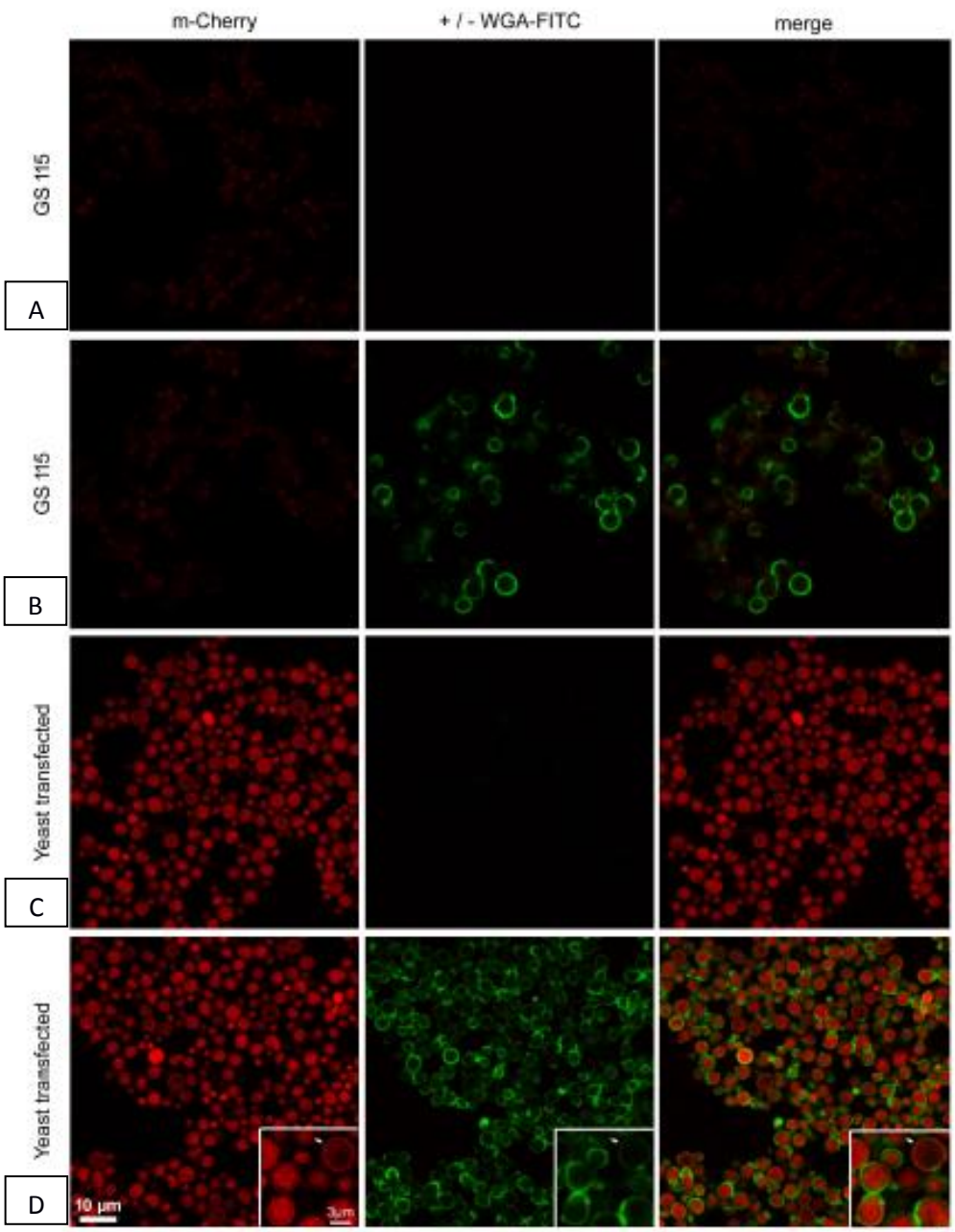

Figure 40: confocal microscopy trials

Basically, we confirmed that the GPER-mCherry is not specifically located at the outer membrane (and/or endoplasmic reticulum) but seems mainly spread all over the cytoplasm (except the nucleus). As we can observe in the panels of figure 40, some cells showed a quite nice membrane labeling whereas others showed mainly a cytoplasm labeling.

These results are in accordance with the controversy about GPER localization found in literature (Prossnitz & Arterburn, 2015) and previously described.

Moreover, as part of the GPER-mCherry is addressed at the outer-membrane, the WGA-FITC labeling seems impossible, that confirms a steric obstruction at the cell surface by the attendance of the GPER-mCherry.

5. Conclusions

In conclusion, during this PhD work, we successfully obtained the yeast strain transformed with the selected receptor tagged by a constitutively expressed fluorophore.

Fluorescent spectral analyses in spiked real matrices to pre-validate the bioprobe will be done by exposing to estrogenic-like EASs the transformed *Pichia pastoris* cells.

As mentioned, a future aim of the project is to use the bioprobe in the analysis of animal metabolism through the time in order to establish the conditions of health, treatments, diet and life's environment in the farm, in an holistic optic, and possibly to use this monitoring system in farm management and HACCP self-monitoring plans.

Chapter II

Untransformed strain: cell-based amperometric sensor for simazine detection

1. Introduction

The biosensoristic device designed in order to detect the triazinic herbicide simazine uses untransformed unicellular yeast cells (*Saccharomyces cerevisiae*) as biomediator and the Clark's type oxygen electrode (oximeter) as transducer. The toxicological endpoint is yeasts' cellular aerobic respiration, linked to mitochondrial activities, which is indirectly measured by the oximeter.

This toxicological endpoint was selected because cellular aerobic respiration was found to be very sensitive to the presence of various toxic chemicals. Thus variations monitoring of dissolved O_2 concentration allows the rapid assessment of toxic substances presence in water (Walmsley R.M & Keenan P, 2000; Dragone et al., 2014; Ribeiro I.C.et al., 2000; Campanella L. et al., 1995 a & b, 1997; Frazzoli et al., 2007).

1.1 Biomediator: *Saccharomyces cerevisiae*

The unicellular yeast *Saccharomyces cerevisiae* is considered a model organism in genetics and molecular biology and in 1996 it was the first eukariotyc organism with fully sequenced genome (Goffeau et al., 1996). *S. cerevisiae* cells (figure 41 A and B –from Grasso G., 2014) are generally elliptical shaped (5 to 10μm the major diameter and 1-7μm the minor) and ~15% of total cellular volume is constituted of cell wall, periplasmic space and membrane: organelles which mainly control the osmotic properties and the cell permeability.

S. cerevisiae, being an unicellular eukaryote organism, has high genetic and proteomic homologies with superior organisms, but, similarly to prokaryote cells, is easy to cultivate in laboratory as it has a short life-cycle and a short cellular duplication time (90-140min at 30°C). Moreover it has complex mitochondria (figure 41 C) with two membranes (internal and external), an own genome and an own protein synthesis machinery.

Finally, *S. cerevisiae* was found to be a good toxicological model in various studies: exposition to diuron –detection till concentrations 4 times below EU legal limits- (Dragone

et al., 2015), mercury nitrate, benzalkonium chloride, and sodium dodecyl sulphate (Campanella et al., 1995 a).

For all the mentioned features, *S. cerevisiae* was selected as a model organism for a respirometric biosensor (yeast-based probe).

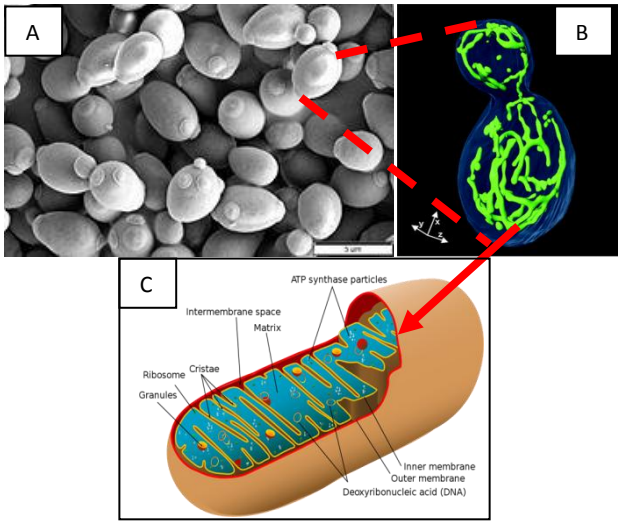

Figure 41: *S. cerevisiae* cells and its tubular mitochondrial network

1.2 Transductor: amperometric oxygen sensors

The transduction of the designed biosensoristic device is constituted by an amperometric sensor. These sensors detect the electric current intensity passing through a reference electrode and a working electrode. Normally, the current intensity passing through the two electrodes immersed in a same solution is constant, but if in this solution a chemical reaction produces/consumes (at the potential applied) electrolyte molecules, a change in current intensity will be registered. This current intensity change (in limit diffusion current conditions) is linearly correlated with changes in chemical species concentrations measured by the sensor.

The amperometric transductor used in this work is the Clark's electrode (figure 42): an oximeter constituted of a working platinum electrode as cathode and a reference Ag/AgCl/Cl^- electrode as anode. Both are immersed in an opportune electrolytic solution (NaCl/NaOH 0.1M) and, during the measure, a ddp of -650mV is maintained between electrodes, to ensure oxygen reduction.

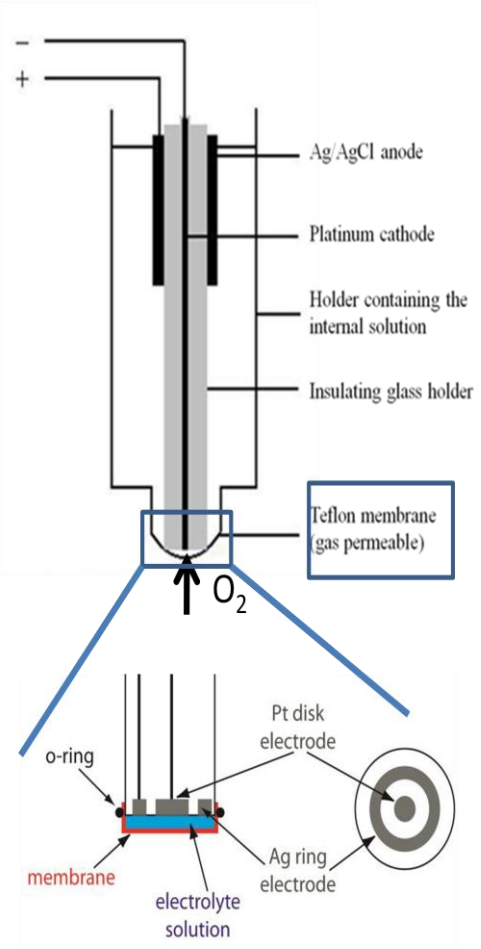

Figure 42: Clark's electrode scheme (from Grasso G., 2014)

In Clark's transductors the interactions between electrodes and outer environment are assured by a thin (~10μm thickness) organic Teflon membrane permeable to O_2. Oxygen diffuses through the membrane and is electrochemically reduced in the cathode, producing a current signal (redox reactions starting at the electrodes are reported in table 12). This signal is then converted in potential difference (ppm) in the analyzer (through a simple calibrated resistance circuit) and correlated to the oxygen concentrations.

Table 12: oxygen reactions occurring in the Clark's type oximeter

Cathode	$O_2 + 2H_2O + 4e^- \rightarrow 4\ OH^-$
Anode:	$Ag + Cl^- \rightarrow AgCl \downarrow + e^-$
Total reaction	$O_2 + 2\ H_2O + 4Ag + 4Cl^- \rightarrow 4AgCl \downarrow + 4\ OH^-$

Oxygen permeable membrane and an opportunely selected fixed potential difference between the electrodes are the features which drastically increase the selectivity of the electrode (Grasso G., 2014) .

1.3 Toxicological endpoint: aerobic respiratory activity

Dissolved oxygen concentration in a solution depends principally on two factors: the atmospheric pressure at the air-solution interface and the solution temperature. However, when a cellular suspension, having an aerobic basal metabolism, is introduced in solution, the oxygen concentration measurable with immersed Clark's type electrodes is the result, in each moment, of two phenomena: atmospheric oxygen solubilization and yeast cells' oxygen consumption by respiratory activity. These dynamics, very sensitive to temperature, are described in the kinetic respirometric curve of figure 43.

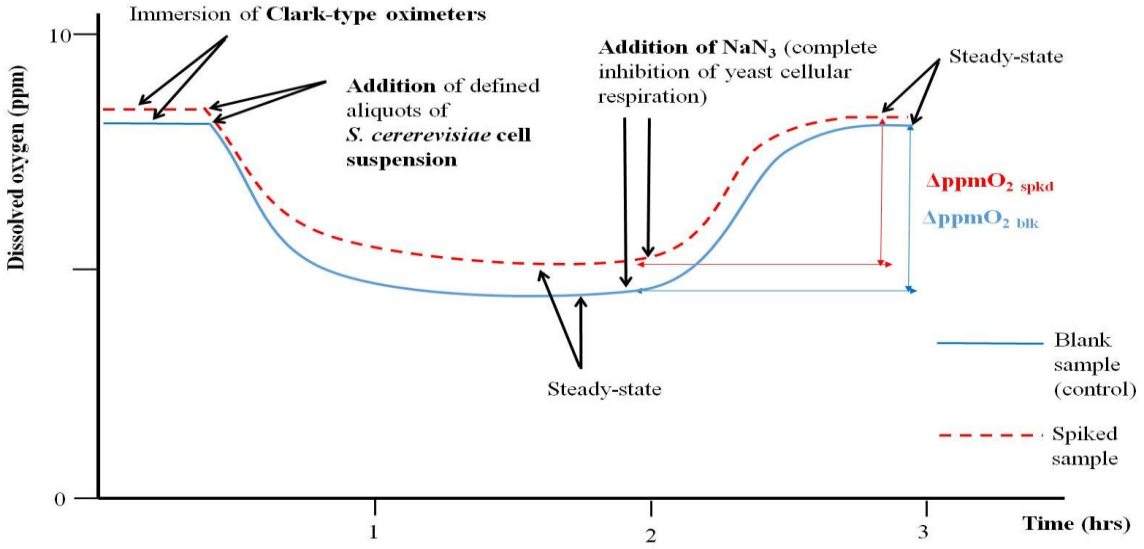

Figure 43: Respirometric curve scheme of blank and exposed samples (from Dragone et al., 2015).

In a respirometric test, when the oxygen diffusion rate from the solution to the cathode equals its solubilization/consumption rate, the current intensity value corresponding to the first steady state (or *plateau*) of a kinetic respirometric curve is determined.

Reached this steady state condition, the addition of sodium azide (NaN_3) in solution completely inhibits the yeast cellular aerobic respiration and thus oxygen rate passing through the Teflon membrane rises and the respirometric curve with it. When the second *plateau* of the kinetic respirometric curve is reached this corresponds to the quantity of dissolved oxygen in a situation of cellular respiration absence.

Differences between the two steady states ($\Delta ppmO_2$, expressed in parts per million, ppm) in spiked and control samples are evaluated (Dragone et al., 2015) and the percentage interference of aerobic respiration ($\rho\%$) is calculated with the following algorithm (1):

$$\rho\% = (1-\frac{\Delta ppmO2spk}{\Delta ppmO2blk})*100 \quad (1)$$

Where:

$\Delta ppmO_2spk$ = variation of the dissolved oxygen concentration (in ppm) values for spiked samples;

$\Delta ppmO_2blk$ = variation of the dissolved oxygen concentration (in ppm) values for control samples.

ρ% values between 0-100% mean that there is an inhibitory interference on cellular respiration in spiked samples; negative values mean that there is an hyperstimulatory interference; ρ% values ~ 0 mean that there is no interference on cellular respiration of spiked samples.

2. Materials and methods

Dried *S. cerevisiae* cells (*Saccharomyces cerevisiae* yeast, Type II) used in the experiments and the simazine ≥ 98% were obtained from Sigma-Aldrich S.r.l. (Milano, Italy). D-(+)-glucose monohydrate for microbiology ≥99.0 % from Fluka Analytical Chemical, Germany); sodium sulphite, boric acid and methanol (assay (GLC) ≥99.9%) from Carlo Erba SRL, Italy; sodium azide ≥99.0% from AMS Biotechnology Ltd, Switzerland. The principal instruments used were: spectrophotometer UV-Vis UNICAM UV2; electrode AMEL model 332/P, O2 electrode; Teflon membranes, YSI model 5775 (Yellow Springs, USA). All the working solutions were prepared diluting the stocks with MilliQ water.

Working conditions for respirometric tests were optimized with various preliminary analyses. A calibration curve between OD_{525}nm and a count in Bürker chamber was used to check that the number of cells was around $2{,}4 \cdot 10^7$ in all samples.

Respirometric tests were designed starting from the method already presented in Frazzoli et al, 2007. All samples were prepared in a final volume of 15mL, continuously stirred at 250 rpm and strictly maintained at 28,0 ± 0.1° C. Two different matrices, agricultural water and raw cow's milk (Pascolini farm, Rome, Italy), were tested (fig. 44):

- Water samples were added only with a final concentration of 0.5M glucose to reach experimental conditions in which the respiratory activity of cells is at the maximum physiological rate in non proliferation conditions;

- Milk samples were added with a 0.16% final concentration of boric acid. This weak acid has the function to control the cellular proliferation of yeast cells, a phenomenon absolutely unwanted in respirometric tests.

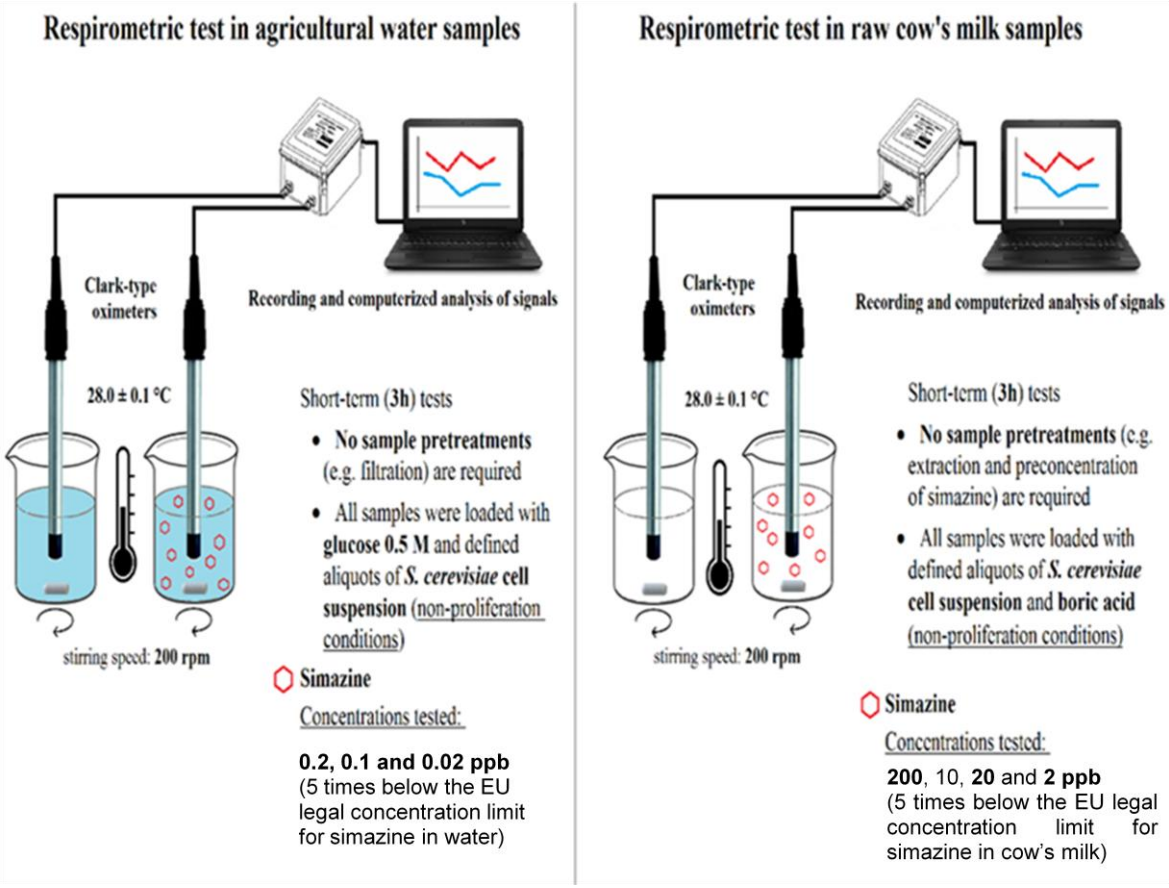

Figure 44: sample preparations for respirometric tests

The concentrations of simazine tested were:

- 0.2, 0.1 (MRL) and 0.02 ppb (5 times below the MRL for simazine in water) for agricultural water samples;
- 200, 20, 10 (MRL) and 2 ppb (5 times below the MRL for simazine in cow's milk) for raw cow's milk samples.

In all the samples *S. cerevisiae* suspension (150 µL of 5 mg/mL) and the needed dilutions of simazine for spiked samples or methanol (always in a concentration<0,1%) for blank samples were added.

Samples were then exposed for 2 hours during which the concentration of oxygen in solution ($[O_2]_{solution}$) was continuously monitored with pre-tared Clark's electrodes. After exposition period, and being sure the first *plateau* was reached, 100µL of 0.2 M NaN_3

solution was added to samples to inhibit yeast cellular respiration and reach the second *plateau* (as previously described in figure 43). Finally, ΔO_2ppmspk and ΔO_2ppmblk were considered and the percentage interferences of aerobic respiration (ρ%) were calculated as previously described.

All tests were repeated for 4 replica samples in 3 different experiments. Relative standards deviation percentages were calculated ($RSD\%_{calculated} \leq 20\%$) for each experiment for repeatability and statistical differences between ΔO_2ppmspk and ΔO_2ppmblk were analyzed with ANOVA Randomized Block Design.

3. Results and discussions

As we can observe from table 13 the differences between ΔO_2ppmspk and ΔO_2ppmblk have statistical significance in agricultural water samples at all the concentrations tested and in raw cow's milk samples at 2ppb and 200ppb.

Table 13: *p-column* values obtained with the statistical analyses done

Agricultural water	
0.02ppb	p<0.01
0.1ppb	P<0.01
2ppb	p<0.01
Raw cow's milk	
2ppb	p<0.01
10ppb	NS
20ppb	NS
200ppb	p<0.01

In agricultural water samples (fig. 45) ρ% values are positive at lower and higher concentrations and negative at 0.1ppb.

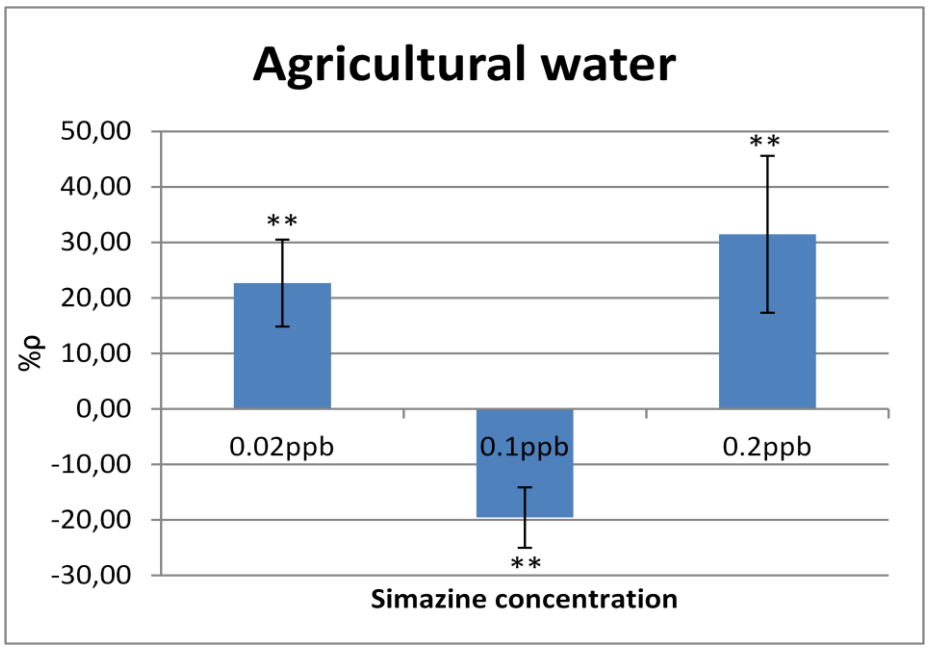

Figure 45: Respirometric results in agricultural water samples

In milk samples (fig. 46) instead we can observe a trend:

- at the lowest concentration tested (2ppb - 5 times lower the EU limit) the %ρ parameter has a positive value;
- at concentrations of 10 and 20ppb it seems we are in an equivalent zero point;
- at the higher concentration tested (200ppb) the %ρ parameter has a negative value.

Even if we didn't obtain statistically significant differences at 10 and 20ppb of simazine, it should be noted that milk is a very complex matrix thus various minor mechanisms (e.g. the simazine can dissolve inside milk's fats) can mask the sensitivity of the biomediator.

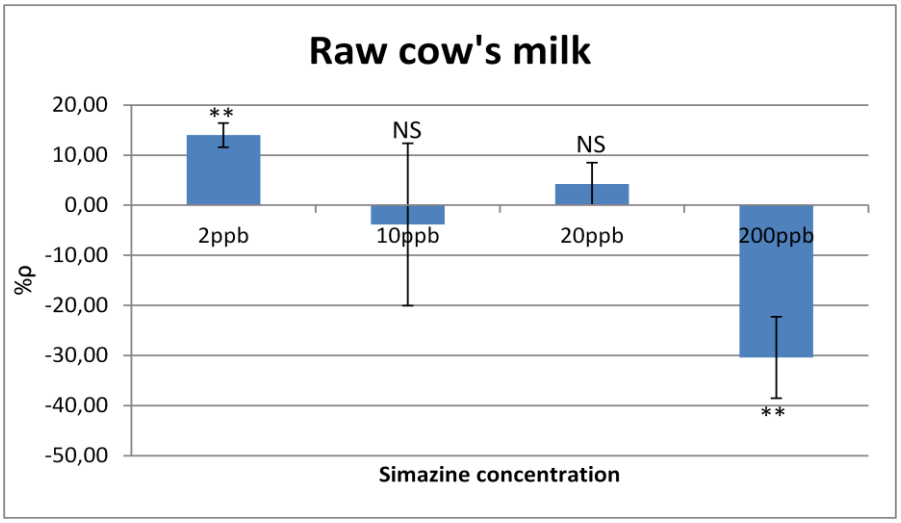

Figure 46: Respirometric results in raw cow's milk samples

The percentage interference of aerobic respiration values obtained could be explained by a combination effect, observed at a fixed point, between three different mechanisms triggered by the presence of simazine, each having its own activation and effect kinetics:

- Simazine can have an uncoupling effect on oxidative phosphorylation (Metcalf et al, 1978) partially inactivating the ATP production thus leading to respiratory hyperstimulation (over the maximum physiological aerobic respiration rate in which cells are in our experimental conditions).
- Simazine however has also a toxicological effect leading to an excess of ROS production. In this condition, natural radical scavengers can't neutralize all of them, resulting in an alteration of cellular redox state, potentially dangerous for cellular structures. Mitochondrial damages led to an inhibition of cellular respiration.
- The third supposed mechanism is represented by cellular detoxification and repairing systems (Dragone et al., 2015), which can bring back the respiratory activity to physiological levels from both the altered states.

Moreover, other minor mechanisms can delay or accelerate the intracellular action of simazine: for example its diffusion inside the cells to the mitochondria.

4. Conclusions

The results we obtained show how this system, evaluating the simazine interference on aerobic catabolism of *S. cerevisiae* yeast (a good toxicological endpoint, as already demonstrated by Frazzoli et al., 2007 and Dragone et al., 2015), is able to detect the simazine herbicide at concentrations 5 times lower than MRL in both agricultural water and milk.

Moreover, as this biosensoristic system doesn't need samples pretreatments, is potentially employable as a field screening method. Moreover thanks to simplicity of execution of tests, this bioprobe lend itself to automation and integration in the patented technological platform BEST (PCT WO/2010/001432): (Bio)Sensors' system in Food Safety as at-line monitoring system for environmental and food surveillance at critical controlpoints.

Chapter III

Untransformed strain: cell-based fluorimetric sensor for diuron detection

1. Introduction

The biosensoristic devices designed in order to detect very low concentrations of the ureic herbicide diuron use untransformed cells of the unicellular green alga *Chlamydomonas reinhardtii* as biomediator, the transduction is fluorimetric and the toxicological endpoint is the interference effect of the herbicide diuron on the chlorophyll a fluorescence.

The fluorescence emission variations of chlorophyll a in samples exposed to different concentrations of diuron were seen in two different ways:

- as single time fluorescence spectra in non dark-adapted samples: the pesticide diuron alters the fluorescence emission at the two chlorophyll maxima, 684 and 735nm;
- as a kinetic curve after dark-adapting for 10 minutes both exposed and control samples (Kautsky effect): the pesticide diuron alters the J step values of the curve.

1.1.Biomediator: *Chlamydomonas reinhardtii*

Unicellular green algae are primary producers at the basis of aquatic food chain and thus bearing high ecological relevance. Their ecological relevance imply that adverse effects on these organisms can negatively influence also higher trophic levels, including zooplankton and fish, thus disturbing the whole ecosystem (Nestler H. et al. 2012). They share many cellular components with the herbicides' target plants and thus, in aquatic ecosystems, algae are probably the first non-targeted organisms who come in contact and interact with these contaminants (González -Barreiro O. et al., 2006). For these features green algae, used as higher plants models, could be really useful biomediators in whole cell-based biosensors for the monitoring of environmental and food samples.

In particular the unicellular green alga *Chlamydomonas reinhardtii* (figure 47, Phylum: Chlorophyta) was used for decades as a model in molecular biology, particularly in the photosynthesis research (Harris E.H., 2001), and recently gained importance also in ecotoxicology where it is used to analyze the effects of stressors, including various herbicides (Fischer B.B. et al., 2010; Jamers A. et al., 2010; Reboud X. et al., 2002).

C. reinhardtti has an average diameter of ~10μm (with significant variation through the cell cycle), multiple mitochondria and a cell wall. It has two anterior flagella for motility and mating, and a chloroplast that houses the photosynthetic apparatus and critical metabolic pathways (Merchant S.S. et al, 2007). *C. reinhardtii* cells is easily grown in defined liquid or agar media at neutral pH, and has no requirements for supplementary vitamins or other co-factors. Moreover it can use acetate as a solely carbon source, with the consequence that growth can occur in the dark (Harris, 2001).

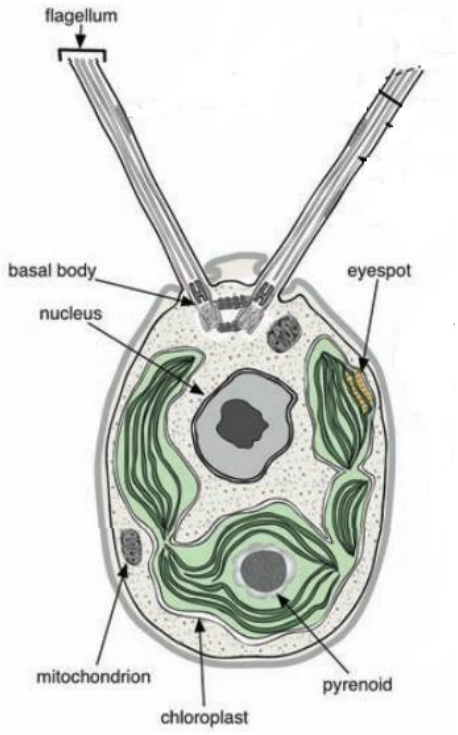

Figure 47: A scheme of a *Chlamydomonas reinhardtii* cell (modified from Merchant S.S. et al, 2007)

For all these mentioned features *C. reinhardtii* was the selected biomediator in the whole cell-based biosensors we designed in this study.

1.2.Toxicological endpoint: chlorophyll fluorescence

Light energy that is absorbed by chlorophyll in the reaction centers of the photosystems can undergo three fates: a) it can be used to drive photosynthesis (photochemistry), b) it can be dissipated as heat or c) it can be re-emitted as red fluorescence. These three processes occur in competition thus any increase in the efficiency of one process will result in a decrease in the yield of the other two. Therefore, chlorophyll fluorescence analyses

can give information about changes in the efficiency of photosynthesis (figure 48) (Misra et al, 2012).

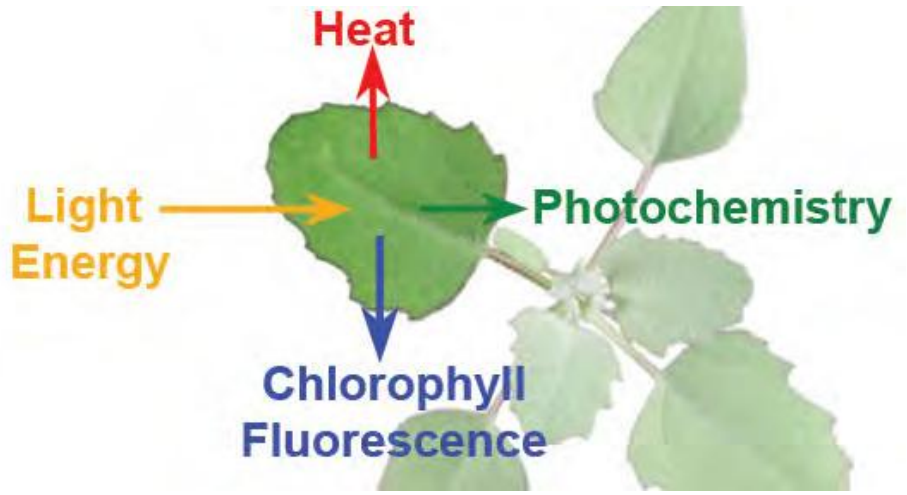

Figure 48: the three fates of absorbed light energy (Misra et al., 2012).

1.3.The F684/F735 chlorophyll fluorescence ratio

Starting with the single time chlorophyll fluorescence spectra, they show two maxima: one in the red region (680-700nm) and the other in the far-red region (730-740nm) (figure 49). The first peak (684nm) is ascribable to the PSII and the second (735nm) to the PSI chlorophyll molecules (Gouveia-Neto, 2011) as the names of the reaction centers, respectively P680 and P700, suggest.

Eullaffroy & Vernet (2003) found F684/735nm ratio as a sensitive tool in water samples to detect trace quantities of photosynthesis-inhibiting herbicides. This study was done on *Scenedesmus obliquus* and a diuron toxicity threshold of 1µg/L (or 1ppb) was found.

However, we observed that, in our experimental conditions of diuron exposition, the two emission peaks rose in comparable ways thus this parameter was unsuitable for our aims.

We found that Fai et al. (2007) had our same problems: variations less significant in F684/F735 ratio than at individual wavelengths. They used the microalga *Selenastrum capricornutum* so they implied this difference to responses peculiarities of different algal species. Moreover, using another technique, the PAM fluorescence, Juneau et al. (2002) showed how *C. reinhardtii* was an organism more sensitive to pollutants than *S. Capricornutum*.

Then, as we were already using *C. reinhardtii*, we decided to analyze our data with the parameter suggested by Fai et al. 2007: the percentage increase (‰ι) of F_{684nm} or F_{735nm}. As we were interested in PSII interference, we putted our focus on ‰ι of F_{684nm}.

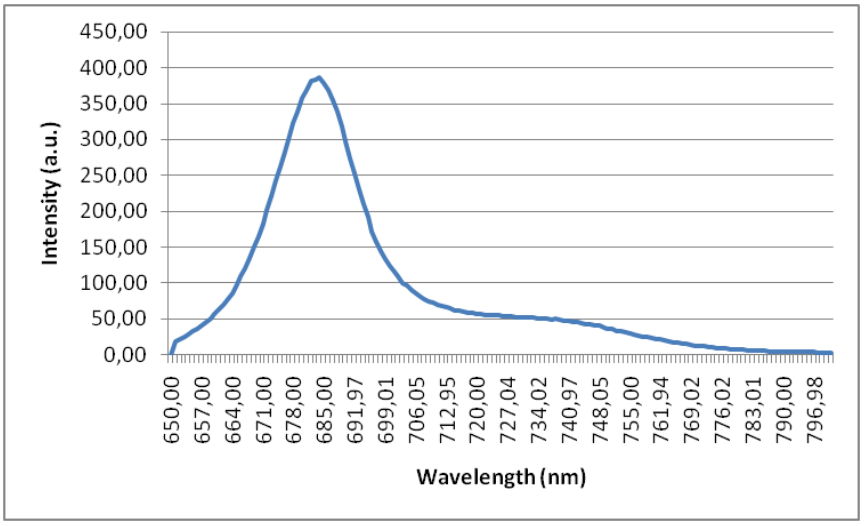

Figure 49: example of a chlorophyll fluorescence spectrum in *C. reinhardtii* (from our data)

1.4.Induction of chlorophyll a fluorescence (or Kautsky effect)

Passing to the Kautsky curve, this is the peculiar fluorescence's kinetic of the chlorophyll a, measurable under continuous light in dark adapted photosynthetic samples after an abrupt switch on of the light. This phenomenon can be described by a curve constituted of two phases: a first exponential (less than a second) and a second one slowly decaying (few minutes). The first phase is called OJIP where O is for origin, the first measured minimal level, J and I are intermediate levels respectively around 2 and 30ms, and P is the peak. The second phase is called PMST where S is for semi-steady state, M is for maximum and T is for terminal state (Stirbet A., 2011) (figure 50).

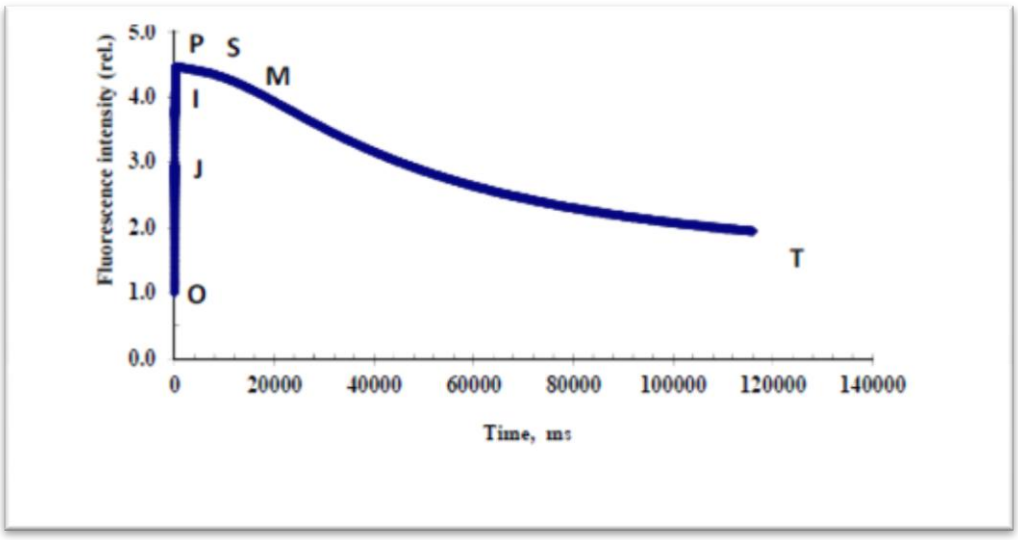

Figure 50: Kautsky curve of a healthy green leaf (Misra et al, 2012)

Changes in OJIP phase values of the Kautsky curve, particularly in the J point, can be correlated with events occurring during the photosynthetic electron transport chain (Stirbet A., 2011) and are an index of the presence of molecules interfering with it, e.g. pesticides inhibiting PSII (figure 51). The SMT phase instead is correlated to various factors like energy transduction, ATP synthesis, CO_2 fixation, state transition, non-photochemical Chl a fluorescence quenching etc. (Misra et al., 2012).

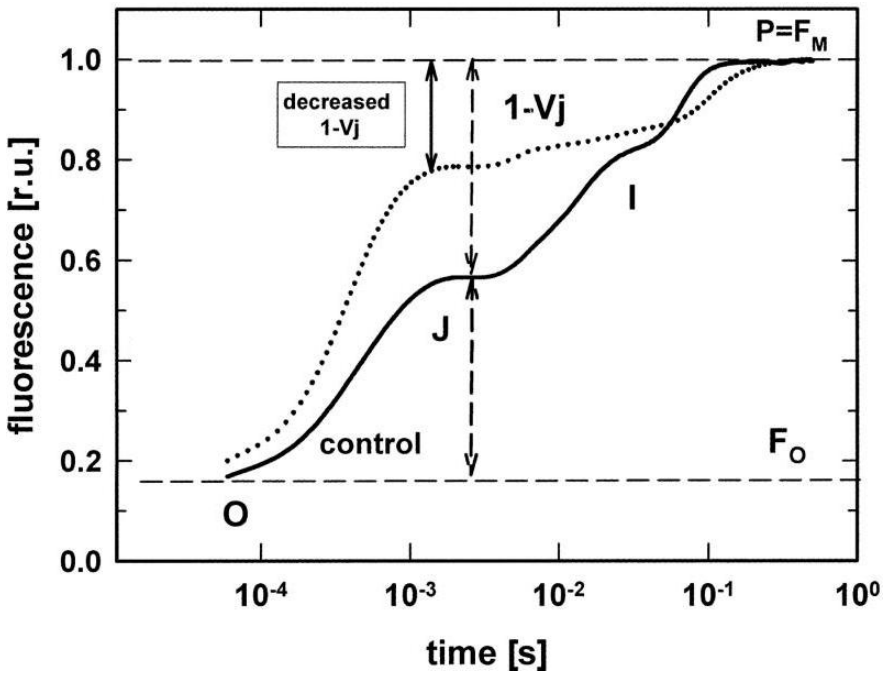

Figure 51: effect of a PSII-inhibiting compound on OJIP phase of the Kautsky curve (Malý J. et al. 2004)

The Kautsky curve can be considered a sensible, non destructive and reliable instrument to rapidly measure the photosynthetic efficiency of PSII. Various works were done on the analysis of the OJIP phase using the wild-type strain of *Chlamydomonas reinhardtii* but also a class of mutants more sensitive to herbicides in order to develop a biosensoristic device able to monitor an herbicide presence (as example Scognamiglio et al., 2009, Bukhov et al., 2004, Giardi et al., 2009). Other techniques and species were also used with the same aim (Ross, 2005, Dragone et al., 2015, Haynes et al., 2000, Touloupakis et al., 2005, Ricart et al., 2009).

However in this study we specifically tested the interference of very low concentrations of diuron with the Kautsky curve in *Chlamydomonas reinhardtii* strain.

2. Materials and methods

Tests were carried out using *Chlamydomonas reinhardtii wild-type C137, mating type +*, (obtained from Chlamycollection, Minnesota), exposed to diuron (or DCMU, CAS number 330-54-1) (obtained from Sigma-Aldrich S.r.l. (Milano, Italy). *Chlamydomonas reinhardtii* suspensions were grown in TAP medium (obtained from Thermo Fisher Scientifics) (fig. 52) for 90hours under the following conditions: constant agitation at 150 rpm; continuous light exposition with light density around 50 µmol m^{-2} s^{-1}; temperature maintained at 23±1°C. Cell density of algae suspension was verified at every experiment measuring OD_{750nm} with spectrophotometer ATI Unicam UV/Vis Spectrophotometer UV2 and dilutions were made to obtain the needed values with TAP medium, measured also as baseline data.

Figure 52: *C. reinhardtii* cultures in TAP medium

Diuron stock solution was prepared dissolving the herbicide in methanol (assay GLC≥99.9%, obtained from Carlo Erba SRL, Italy). Dilutions with water MilliQ were carried out to obtain the working solutions 10X more concentrated that the final tested concentrations. As said before, the MRL for each single chemical (including pesticides) in potable water is 0.1ppb, so three different diuron concentrations were investigated: 2ppb (20 times over the MRL), 0.2ppb (2 times over the MRL) and finally 0.02ppb (four times below the MRL).

2.1. The F684/F735 chlorophyll fluorescence ratio

Preliminary test to optimize the value of OD_{750} and the excitation wavelength were done in algal samples not exposed to diuron . For the first parameter OD_{750nm} values from 0.20 till 0.70 (±0.02) were tested; for the second the excitation length tested were 400 - 489 (Eullaffroy & Vernet 2003) -610 (theoric) and 640 nm. Emission spectra were measured between 650 and 800nm with a scan rate of 600nm/min. Both the slits of excitation and emission were of 10nm.

Following the preliminary results, all tests were done in triplicate using algae cultures diluted to a final OD_{750nm} in a range between 0.18 and 0.22 and using 489nm as excitation length. The used instrument for all the fluorescence spectra was Varian Cary Eclipse Fluorescence Spectrophotometer. Measurements were done after 10 minutes of exposition to diuron or methanol in light and stirring (300 rpm) conditions.

Statistical differences between exposed and control samples were analysed using ANOVA test for Randomised Block Design for all the calculated parameters.

2.2. Induction of chlorophyll a fluorescence (or Kautsky effect)

Multilight instrument from Biosensor SRL (Formello, Italy) was used to perform all the analyses.

Preliminary tests were done in samples exposed to diuron 2ppb to optimize the OD_{750nm}. Values of 0.70 and 1.00 (±0.02) were tested and it was found that data from the first were more reliable thus all the other experiments were done with an OD_{750nm}= 0.70 ± 0.02.

All the samples (exposed with diuron and blank with methanol) were exposed for 10 minutes in light and stirring (200 rpm) conditions before measurements. Samples were then dark-adapted directly in the instrument for 10 minutes before the measures of the

kinetic fluorescence (11 seconds of exposition to light at a density of 127 µmol m^{-2} s^{-1} in 6 different replicates). In figure 53 there is a scheme of the exposition periods used in the kinetic measures.

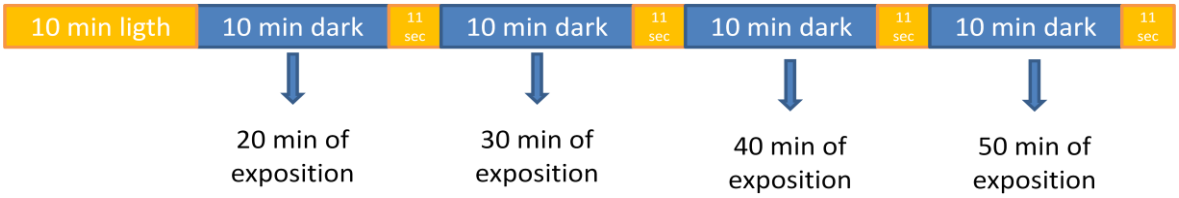

Figure 53: scheme of the exposition periods during each analysis.

Data analyses were done using Excel to calculate, after subtracting the baseline, the Kautsky effect parameters (Strasser R.J. et al, 2000, Appenroth K.J. et al, 2001, Tsimilli-Michael M. & Strasser R.J, 2008)

- Fo (minimum of fluorescence intensity): calculated with data between 0.1 and 0.14ms as the intercept of linear regression (figure 54);
- Fm (maximum of fluorescence intensity): calculated just searching the maximum value obtained (figure 54);
- Fv/Fm (the maximum quantum yield of PSII for primary photochemistry): calculated with the equation $\frac{Fm-Fo}{Fm}$;
- F8ms (fluorescence intensity at 8ms): calculated with data between 7.9 and 8.1ms. Used as the value of fluorescence intensity at J inflection (figure 54). Data at 8ms were chosen, instead of 2ms values, because the variability at this time was lower;
- V8ms (the relative variable fluorescence at the J-step): calculated with the equation $\frac{F8ms-F0}{Fm-F0}$.

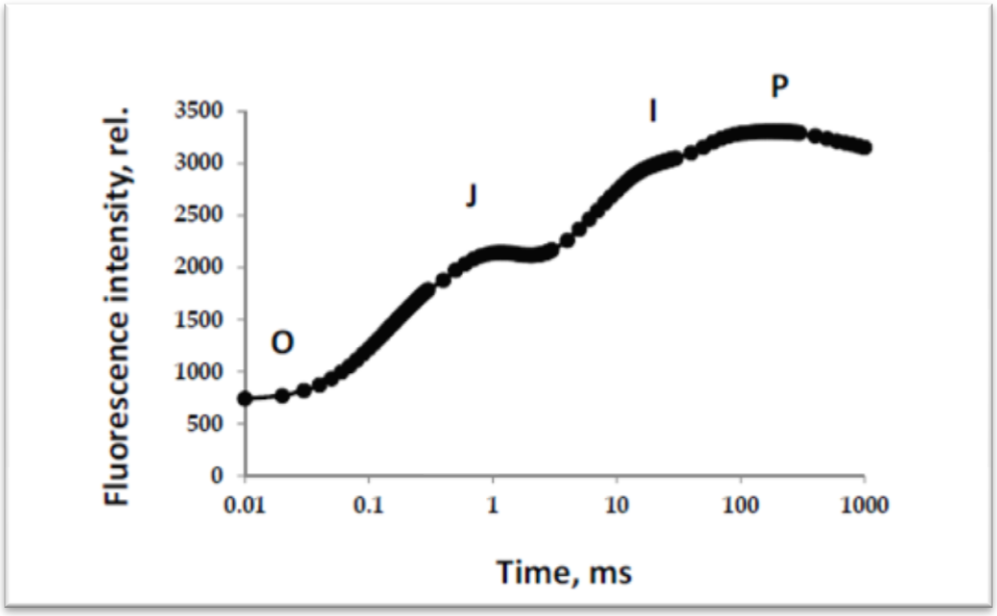

Figure 54: expansion of the exponential 'OJIP' phase of the Kautsky curve (Misra et al, 2012)

We designed and calculated also a normalized effect index (ε) to summarize all the data, calculated as follows (2):

$$\varepsilon = \left(\frac{V8exp - V8blk}{1 - V8blk} * 100 \right) \quad (2)$$

This parameter was calculated with the averages of V8ms values for each concentration.

3. Results and discussion

3.1. The F684 and F735 chlorophyll fluorescence

The F684/F735 ratio values, as in Fai et al (2007), were less indicative than the changes between blank and exposed samples at the individual wavelengths. All data were then analyzed calculating the percentage intensity at 684nm and 735nm variations (increase or inhibition) in samples exposed to diuron (test) relative to the control using in the following equation (3):

$$\% \text{ increase } (\iota) \text{ in F684 } (F684_{test} / F684_{control} - 1) * 100\% \text{ (Fai et al., 2007)} \quad (3)$$

The % of increase trend of the major emission maximum (684nm) at 10 min of exposition to diuron for the three concentrations tested is reported in figure 55.

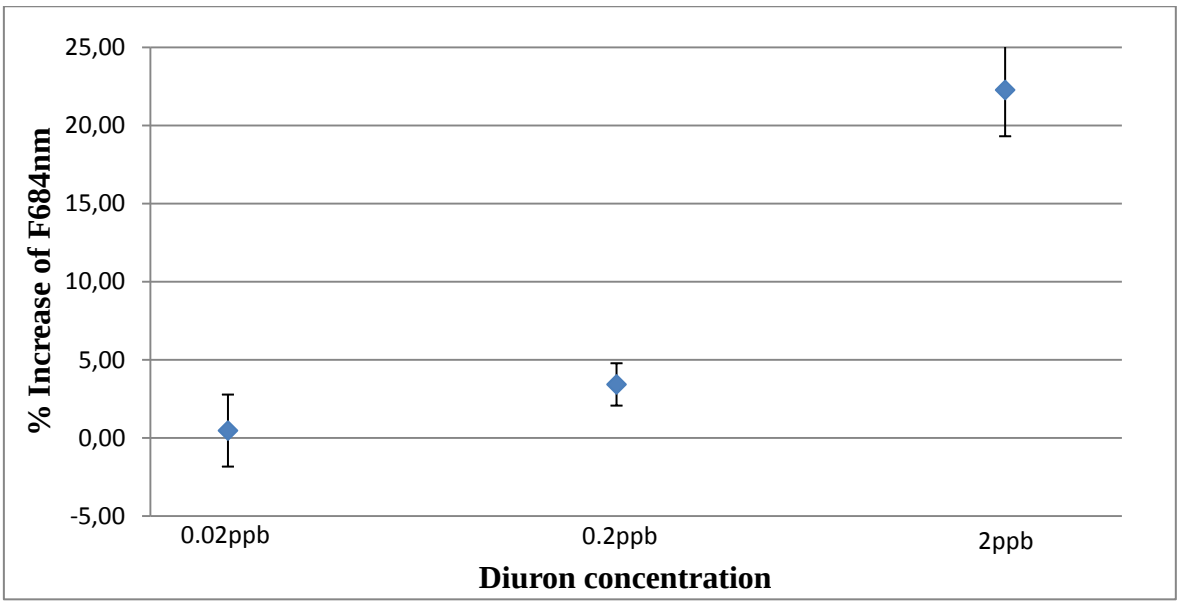

Figure 55: % increase of F684nm after 10 minutes of exposition to the three diuron concentration tested

As we can see, the percentage increase of F684nm is significantly different to zero till 0.2ppb thus this parameter proved to be sensitive and able to detect (without any necessary sample pretreatments) herbicide diuron up to 0.2ppb.

3.2.Induction of chlorophyll a fluorescence (or Kautsky effect)

As variations in the J point of the OJIP curve are particularly interesting because they indicate the presence of molecules interfering with the electron transport chain, our focus was mainly on the last two parameters: fluorescence at 8ms (F8ms) and the relative variable fluorescence at the same time (V8ms)

The results of statistical analyses between blank and exposed samples are summarised in table 14. A statistical significance in these differences was found at all the three concentrations tested for F8ms and at the concentrations of 2ppb and 0.02ppb of diuron for V8ms. Significant differences were not found for V8ms at 0.2ppb. In particular V8ms exposed to 2ppb of diuron data weren't statistically different from the blank data before 30 minutes of total exposition to the herbicide diuron. We can hypothesize that 20 minutes of exposition at this very low concentration were not enough to induce a visible effect.

Table 14: Statistical analyses done on all the tested parameters at the three concentrations tested: 20, 30, 40 and 50 are total (light + dark) minutes of exposition to diuron.

	0.02ppb	0.2ppb	2ppb
Fo	All exp time: NS	All exp time: **	All exp time: NS
Fm	20 min: * 30-50 min: NS	20-30 min: ** 40-50 min: *	All exp time: NS
Fv/Fm	All exp time: NS	20-30 min: NS 40-50 min: *	All exp time: NS
F8ms	20-30 min: ** 40-50 min: * Exp<Blk	All exp time: ** Exp<Blk	All exp time: * Exp>Blk
V8ms	20 min: NS 30-40 min: ** 50 min: * Exp<Blk	All exp time: NS	All exp time: ** Exp>Blk

Legend

NS	Not significant
*	P<0.05
**	P<0.01

Looking at F8ms data we can observe a trend: values of F8ms in samples exposed to 2ppb of diuron are significantly higher than control ones, instead, at a concentration of 0.2ppb and 0.02ppb exposed values are significantly lower than control ones. Analyzing V8ms data we found a comparable trend: at 2ppb of diuron values of exposed samples were significantly ($p<0.01$) higher than the control ones; at 0.2ppb values of exposed samples were not significantly different from control ones; at 0.02ppb values of exposed samples were significantly lower than the control ones, as said, just after 30 minutes of contact of the cells with the herbicide.

The significant decrease in V8ms levels of exposed samples at 0.02ppb of diuron indicate that this very low concentration of herbicide can activate the primary charge separation and the electron transport between the primary (Q_A) and the secondary (Q_B) quinone acceptors (Petit A.N. et al, 2010) by a presumptive hormetic-like effect.

The normalized effect index (ε) trend is shown in figure 56. Analyzing the effect index we can observe an inhibition effect in samples exposed at 2ppb of diuron; a not significant difference between exposed and control samples at 0.2ppb of diuron (we suppose this can be a "zero equivalent point"); a presumptive hormetic-like effect in samples exposed at 0.02ppb of diuron.

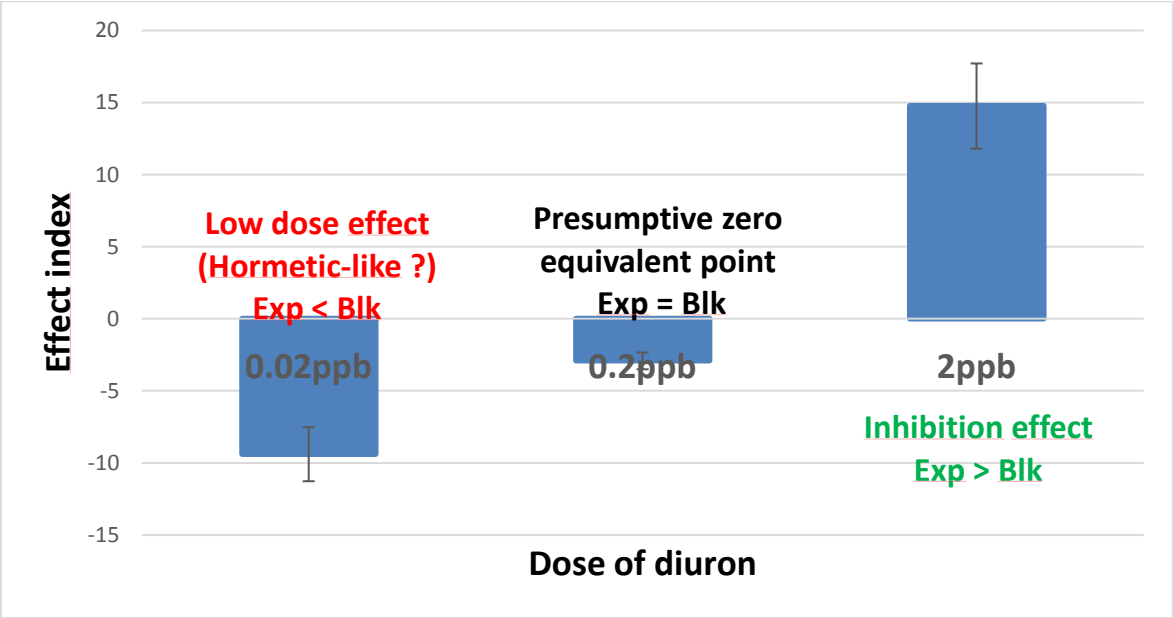

Figure 56: Trend of the effect index (ε) for the three different diuron concentrations tested

4. Conclusions

The results we obtained show how both these systems are able to detect diuron herbicide:

- The percentage increase, ι, of F684nm, in the "*light condition*" we used in our experiments, proved to be able to detect herbicide diuron up to 0.2ppb;
- The Kautsky curve parameters, in the "*dark condition*" we used in our experiments, proved to be able to detect diuron at concentrations 5 times lower than MRL.

OVERALL CONCLUSIONS

EDCs are contaminating compounds whose represent a long-standing concern for International agencies involved in the risk assessment of chemicals, as well as an issue for intense debate among scientists, industries and the public (Mantovani A., 2017).
Moreover Regulation (EC) No 1107/2009 (21th October 2009) of the European Parliament and of the Council states that, in plant protection products (like pesticides), active substances considered to have endocrine disrupting properties that may cause adverse effect in humans or in non-target organisms shall be substituted (see http://eur-lex.europa.eu/LexUriServ/LexUriServ.do?uri=OJ:L:2009:309:0001:0050:EN:PDF). As a consequence, in the future, showing the presence of pesticides with ED properties in environmental media or living organisms might flag illicit agricultural treatments and/or illicit disposal of chemical waste.
In this scenario, monitoring of EDCs in zootechnical environment, as well as in the early stages of the food supply chain (i.e. primary production) are crucial.

This PhD study present three whole cell-based biosensoristic devices for early detection of EDCs acting on estrogenic and androgenic pathways.
The main results obtained are as follows:

- Regarding the transgenic strain cell-based fluorimetric sensor we successfully obtained the yeast strain transformed with the GPER-1 receptor tagged by a constitutively expressed fluorophore, mCherry. Following positive results obtained with *P. pastoris* transformation, performances of the bioprobe will be pre-validated with fluorescence measurements on genetically engineered *P. pastoris* cells exposed to estrogenic-like EASs (both as single chemicals and as mixtures) in spiked real samples;
- Regarding the untransformed strain cell-based amperometric sensor, results shows that the system is able to detect simazine at concentrations 5 times lower than MRL in both agricultural water and milk;
- Finally, regarding the untransformed strain cell-based fluorimetric sensors:
  - Percentage increase results, obtained in *"light condition"*, show that the system is able to detect diuron up to 0.2ppb;
  - Kautsky curve results, obtained in *"dark condition"*, seems to increase sensitivity as diuron can be detected in aqueous solution up to 0.02ppb. Moreover results had

showed a presumptive hormetic-like stimulatory effect on photosynthesis (not previously described in literature) at 0.02ppb.

In conclusion, all the tested whole cells biosensoristic devices proved to be suitable for the prefixed aims. Following specific improved features (e.g. integration, portability, cheapness, and development of efficient high-throughput approaches), such devices could represent a new technological opportunity in future applications in environmental monitoring and surveillance at critical control points throughout the entire agro-food supply chain (in particular in zootechnical environment).

References

Abo-Khatwa, N., & Hollingworth, R. M. (1974). Pesticidal chemicals affecting some energy-linked functions of rat liver mitochondriaIn vitro. Bulletin of environmental contamination and toxicology, 12(4), 446-454;

Alexander, S. P., Benson, H. E., Faccenda, E., Pawson, A. J., Sharman, J. L., McGrath, J. C., ... & Harmar, A. J. (2013). The concise guide to PHARMACOLOGY 2013/14: overview. British journal of pharmacology, 170(8), 1449-1458;

Appenroth, K. J., Stöckel, J., Srivastava, A., & Strasser, R. J. (2001). Multiple effects of chromate on the photosynthetic apparatus of Spirodela polyrhiza as probed by OJIP chlorophyll a fluorescence measurements. Environ. Pollut. 115, 49–64;

Balamurugan, V., Reddy, G. R., & Suryanarayana, V. V. S (2007). *Pichia pastoris*: A notable heterologous expression system for the production of foreign proteins—Vaccines. Indian. J. Biotechnol, 6, 175-186;

Barcelo, D., & Hansen, P. D. (2008). Biosensors for the Environmental Monitoring of Aquatic Systems. Fuel, 5;

Bergman, Å, Heindel, J.J., Jobling, S., Kidd, K.A., Zoeller R.T. (2012). State of the Science of Endocrine Disrupting Chemicals – 2012, ISBN: 978-92-807-3274-0 (UNEP) and 978 92 4 150503 1 (WHO) (NLM classification: WK 102);

Bhasin, S., & Jasuja, R. (2009). Selective androgen receptor modulators (SARMs) as function promoting therapies. Current opinion in clinical nutrition and metabolic care, 12(3), 232;

Bologa, C. G., Revankar, C. M., Young, S. M., Edwards, B. S., Arterburn, J. B., Kiselyov, A. S., ... & Oprea, T. I. (2006). Virtual and biomolecular screening converge on a selective agonist for GPR30. Nat. Chem. Biol., 2, 207–212;

Bovee, T. F., Helsdingen, R. J., Koks, P. D., Kuiper, H. A., Hoogenboom, R. L., & Keijer, J. (2004). Development of a rapid yeast estrogen bioassay, based on the expression of green fluorescent protein. Gene, 325, 187-200;

Bukhov, N. G., Egorova, E. A., Govindachary, S., & Carpentier, R. (2004). Changes in polyphasic chlorophyll a fluorescence induction curve upon inhibition of donor or acceptor side of photosystem II in isolated thylakoids. Biochim. Biophys. Acta, 1657, 121 – 130;

Campanella, L., Favero, G., & Tomassetti, M. (1995, a). Immobilised yeast cells biosensor for total toxicity testing. Science of the total environment, 171(1), 227-234;

Campanella, L., Favero, G., Mastrofini, D., & Tomassetti, M. (1995, b). Respirometric biomonitor for the control of industrial effluent toxicity. In European Symposium on Optics for Environmental and Public Safety (pp. 221-230). International Society for Optics and Photonics;

Campanella, L., Favero, G., Mastrofini, D., & Tomassetti, M. (1997). Further developments in toxicity cell biosensors. *Sensors and Actuators B: Chemical*, *44*(1), 279-285;

Campanella L. (2009). Sensori e Biosensori. Edizioni Compomat. ISBN 978-88-95706-07-8;

Comber, S. D. W. (1999). Abiotic persistence of atrazine and simazine in water. Pest Management Science, 55(7), 696-702;

Commission Decision 04/247/EC: http://eur-lex.europa.eu/legal-content/EN/ALL/?uri=CELEX:32004D0247;

Convent, B. & Briquet, M. (1978). Properties of 3-(3,4-Dichlorophenyl)-1,1-dimethylurea and other inhibitors of the cytochrome bc1 segment of the mitochondrial respiratory chain in *Saccharomyces cerevisiae*. Eur. J. Biochem., 82, 473–481;

Council Directive 98/83/EC: http://eur-lex.europa.eu/legal-content/EN/TXT/?qid=1405609372533&uri=CELEX:31998L0083;

da Silva Simões, M., Bracht, L., Parizotto, A. V., Comar, J. F., Peralta, R. M., & Bracht, A. (2017). The metabolic effects of diuron in the rat liver. Environmental Toxicology and Pharmacology, 54, 53-61;

Dennis, M. K., Field, A. S., Burai, R., Ramesh, C., Petrie, W. K., Bologa, C. G., ... & Hathaway, H. J. (2011). Identification of a GPER/GPR30 antagonist with improved estrogen receptor counterselectivity, J. Steroid Biochem. Mol. Biol., 127, 358–366;

Deroo, B. J., & Korach, K. S. (2006). Estrogen receptors and human disease. J. Clin. Invest., 116(3), 561;

Dragone, R., Frazzoli, C., Grasso, G., & Rossi, G. (2014). Sensor with intact or modified yeast cells as rapid device for toxicological test of chemicals. Journal of Agricultural Chemistry and Environment, 3(02), 35;

Dragone, R., Cheng, R., Grasso, G., & Frazzoli, C. (2015). Diuron in Water: Functional Toxicity and intracellular Detoxification Patterns of Active Concentrations Assayed in Tandem by a Yeast-Based Probe. Int. J. Environ. Res. Public Health, 12, 3731-3740;

Dragone, R., Grasso, G., Muccini, M., & Toffanin, S. (2017). Portable bio/chemosensoristic devices: innovative systems for environmental health and food safety diagnostics. Front Public Health, 5;

Eddleston, M., Karalliedde, L., Buckley, N., Fernando, R., Hutchinson, G., Isbister, G., ... & Sheriff, R. (2002). Pesticide poisoning in the developing world—A minimum pesticides list. Lancet, 360, 1163–1167;

Eldridge, M., Sanseverino, J., de Arãgao Umbuzeiro, G., & Sayler, G. S. (2011). Analysis of environmental samples with yeast-based bioluminescent bioreporters. Environmental Monitoring. InTech;

Estève, K., Poupot, C., Dabert, P., Mietton-Peuchot, M., & Milisic, V. (2009). A *Saccharomyces cerevisiae*-based bioassay for assessing pesticide toxicity. J. Ind. Microbiol. Biotechnol., 36, 1529–1534;

Eullaffroy, P., & Vernet, G. The F684/F735 chlorophyll fluorescence ratio: a potential tool for rapid detection and determination of herbicide phytotoxicity in algae. Water. Res. 37.9 (2003): 1983-1990;

European Food Safety Authority (2010). Scientific report of the Endocrine Active Substances Task Force. EFSA Journal, 8 (11), 1932;

European Food Safety Authority (2011). Reasoned opinion of EFSA: Review of the Existing Maximum Residue Levels (MRLs) for diuron according to article 12 of regulation (EC) No. 396/2005. EFSA J., 9, doi:10.2903/j.efsa.2011.2324;

EFSA PPR Panel (2013). Scientific Opinion on the identification of pesticides to be included in cumulative assessment groups on the basis of their toxicological profile. EFSA Journal 2013;11(7):3293. https://www.efsa.europa.eu/it/efsajournal/pub/3293;

EFSA PPR Panel (2014). Scientific Opinion on good modelling practice in the context of mechanistic effect models for risk assessment of plant protection products. EFSA Journal 2014;12(3):3589. http://www.efsa.europa.eu/it/efsajournal/pub/3589;

EFSA PPR Panel (2016). Guidance on the establishment of the residue definition for dietary risk assessment. EFSA Journal 2016;14(12):4549. https://www.efsa.europa.eu/en/efsajournal/pub/4549;

Eurostat Pesticide sale by major group 2014. http://ec.europa.eu/eurostat/statistics-explained/index.php/Pesticide_sales_statistics;

Fai, P. B., Grant, A., & Reid, B. (2007). Chlorophyll a fluorescence as a biomarker for rapid toxicity assessment. Environ Toxicol Chem, 26(7), 1520-1531;

Filardo, E. J., Quinn, J. A., Bland, K. I., & Frackelton Jr, A. R. (2000). Estrogen-induced activation of Erk-1 and Erk-2 requires the G protein-coupled receptor homolog, GPR30, and occurs via trans-activation of the epidermal growth factor receptor through release of HB-EGF. Mol. Endocrinol., 14, 1649–1660;

Filardo, E. J., Quinn, J. A., Frackelton Jr, A. R., & Bland, K. I. (2002). Estrogen action via the G protein-coupled receptor, GPR30: stimulation of adenylyl cyclase and cAMPmediated attenuation of the epidermal growth factor receptor-to-MAPK signaling axis. Mol. Endocrinol., 16, 70–84;

Filardo, E. J., Graeber, C. T., Quinn, J. A., Resnick, M. B., Giri, D., DeLellis, R. A., ... & Sabo, E. (2006). Distribution of GPR30, a sevenmembrane-spanning estrogen receptor, in primary breast cancer and its association with clinicopathological determinants of tumor progression. Clin. Cancer Res., 12, 6359–6366;

Fischer, B. B., Rüfenacht, K., Dannenhauer, K., Wiesendanger, M., & Eggen, R. I. (2010). Multiple stressor effects of high light irradiance and photosynthetic herbicides on growth and survival of the green alga *Chlamydomonas reinhardtii*. Environ. Toxicol. Chem. 29, 2211–2219;

Frazzoli, C., Dragone, R., Mantovani, A., Massimi, C., & Campanella, L. (2007). Functional toxicity and tolerance patterns of bioavailable Pd (II), Pt (II), and Rh (III) on suspended *Saccharomyces cerevisiae* cells assayed in tandem by a respirometric biosensor. Analytical and bioanalytical chemistry, 389(7-8), 2185-2194;

Gaido, K. W., Leonard, L. S., Lovell, S., Gould, J. C., Babaï, D., Portier, C. J., & McDonnell, D. P. (1997). Evaluation of chemicals with endocrine modulating activity in a yeast-based steroid hormone receptor gene transcription assay. Toxicol. Appl. Pharmacol., 143(1), 205-212;

Giacomazzi, S., & Cochet, N. (2004). Environmental impact of diuron transformation: a review. *Chemosphere*, *56*(11), 1021-1032;

Giardi, M. T., Scognamiglio, V., Rea, G., Rodio, G., Antonacci, A., Lambreva, M., ... & Johanningmeier, U. (2009). Optical biosensors for environmental monitoring based on computational and biotechnological tools for engineering the photosynthetic D1 protein of *Chlamydomonas reinhardtii*. Biosens. Bioelectron., 25, 294–300;

Goffeau, A., Barrell, B. G., Bussey, H., Davis, R. W., Dujon, B., Feldmann, H., & Oliver, S. G. (1996). Life with 6000 genes. Science, 274(5287), 546-567;

González-Barreiro, O., Rioboo, C., Herrero, C., & Cid, A. (2006). Removal of triazine herbicides from freshwater systems using photosynthetic microorganisms. Environ. Pollut. 144, 266–271;

Gouveia-Neto, A. S., da Silva-Jr, E. A., Cunha, P. C., Oliveira-Filho, R. A., Silva, L. M., da Costa, E. B., ... & Willadino, L. G. (2011). Abiotic stress diagnosis via laser induced chlorophyll fluorescence analysis in plants for biofuel. Biofuel Production-Recent Developments and Prospects. InTech;

Grasso G. (2014). Biosonde a cellule per l'identificazione dei pericoli chimico-tossicologici negli alimenti. PhD thesis, University of Molise in collaboration with CNR-ISMN and ISS;

Harris E.H. (2001). *Chlamydomonas* as a model organism. Annu. Rev. Plant Physiol. Plant Mol. Biol. 52, 363–406;

Hase, Y., Tatsuno, M., Nishi, T., Kataoka, K., Kabe, Y., Yamaguchi, Y., ... & Watanabe, H. (2008). Atrazine binds to F 1 F 0-ATP synthase and inhibits mitochondrial function in sperm. Biochemical and biophysical research communications, 366(1), 66-72;

Haynes, D., Ralph, P., Prange, J., & Dennison, B. (2000). The Impact of the Herbicide Diuron on Photosynthesis in Three Species of Tropical Seagrass. Mar. Pollut. Bull. Vol. 41, Nos. 7-12, pp. 288-293;

Heindel, J. J., Vom Saal, F. S., Blumberg, B., Bovolin, P., Calamandrei, G., Ceresini, G., ... & Legler, J. (2015). Parma consensus statement on metabolic disruptors. Environmental Health, 14(1), 54;

Hess, F.D. (2000). Light-dependent herbicides: an overview. Weed Sci. 48, 160–170;

Hiort, O. (2002). Androgens and puberty. Best Practice & Research Clinical Endocrinology & Metabolism, 16(1), 31-41;

http://www.efsa.europa.eu/en/topics/topic/endocrine-active-substances;

http://eur-lex.europa.eu/LexUriServ/LexUriServ.do?uri=OJ:L:2009:309:0001:0050:EN:PDF;

https://pubchem.ncbi.nlm.nih.gov/compound/diuron#section=Safety-and-Hazards;

https://pubchem.ncbi.nlm.nih.gov/compound/simazine#section=Safety-and-Hazards;

Ibarreta, D., Daxenberger, A., & Meyer, H. H. (2001). Possible health impact of phytoestrogens and xenoestrogens in food. APMIS, 109 (3), 161-184;

ISPRA. Rapporto nazionale pesticidi nelle acque. Dati 2013-2014. (2016) http://www.isprambiente.gov.it/it/pubblicazioni/rapporti/rapporto-nazionale-pesticidi-nelle- acque-2013- dati-2013- 2014;

Italian Ministry of Health. Ministero Del Lavoro, Della Salute E Delle Politiche Sociali. Available online: http://www.trovanorme.salute.gov.it/norme/dettaglioAtto?id=29100 (accessed on 26 November 2014);

Jaio, B.W., Yeung, E.K.C., Chan, C.B. & Cheng, C.H.K. (2008). Establishment of a transgenic yeast screening system for estrogenicity and identification of the anti-estrogenic activity of malachite green. J. Cell. Biochem. 105: 1399-1409;

Jamers, A. N., & De Coen, W. (2010). Effect assessment of the herbicide paraquat on a green alga using differential gene expression and biochemical biomarkers. Environ. Toxicol. Chem. 29, 893–901;

Janesick, A. S., & Blumberg, B. (2016). Obesogens: an emerging threat to public health. American journal of obstetrics and gynecology, 214(5), 559-565;

Juneau P, El Berdey A, Popovic R. (2002). PAM fluorometry in the determination of the sensitivity of *Chlorella vulgaris*, *Selenastrum capricornutum*, and *Chlamydomonas reinhardtii* to copper. Arch Environ Contam Toxicol 42:155–164;

Lazár D. (1999). Chlorophyll a fuorescence induction. Biochim. Biophys. Acta, 1412, 1-28;

Latini, G., Knipp, G., Mantovani, A., Marcovecchio, M. L., Chiarelli, F., & Soder, O. (2010). Endocrine disruptors and human health. Mini reviews in medicinal chemistry, 10(9), 846-855;

Leskinen, P., Michelini, E., Picard, D., Karp, M., & Virta, M. (2005). Bioluminescent yeast assays for detecting estrogenic and androgenic activity in different matrices. Chemosphere, 61(2), 259-266;

Liu, X., Zhu, P., Sham, K. W., Yuen, J. M., Xie, C., Zhang, Y., ... & Lin, H. (2009). Identification of a Membrane Estrogen Receptor in Zebrafish with Homology to Mammalian GPER and Its High Expression in Early Germ Cells of the Testis. Biol. Reprod. 80, 1253–1261, DOI: https://doi.org/10.1095/biolreprod.108.070250;

Malý, J., Klem, K., Lukavska, A., & Masojidek, J. (2004). Degradation and Movement in Soil of the Herbicide Isoproturon Analyzed by a Photosystem II–Based Biosensor. J. Environ. Qual., Vol. 34 No. 5, p. 1780-1788;

Mantovani, A., Stazi, A. V., Macri, C., Maranghi, F., & Ricciardi, C. (1999). Problems in testing and risk assessment of endocrine disrupting chemicals with regard to developmental toxicology. Chemosphere, 39(8), 1293-1300;

Mantovani, A. (2006). Risk assessment of endocrine disrupters. Annals of the New York Academy of Sciences, 1076(1), 239-252;

Mantovani, A., Frazzoli, C., & La Rocca, C. (2009). Risk assessment of endocrine-active compounds in feeds. The Veterinary Journal, 182(3), 392-401;

Mantovani, A. (2017). Why research on endocrine disrupting chemicals is still worthwhile. *Annali dell'Istituto Superiore di Sanità*, *53*(1), 1-2;

Maximov, P.Y., Lee, T.M., & Craig, J.V. (2013). The discovery and development of selective estrogen receptor modulators (SERMs) for clinical practice. Curr clin pharmacol, 8(2), 135-155;

McKinlay, R., Plant, J. A., Bell, J. N. B., & Voulvoulis, N. (2008). Endocrine disrupting pesticides: implications for risk assessment. Environment international, 34(2), 168-183;

Merchant, S. S., Prochnik, S. E., Vallon, O., Harris, E. H., Karpowicz, S. J., Witman, G. B., ... & Marshall, W. F. (2007). The *Chlamydomonas* genome reveals the evolution of key animal and plant functions. Science, 318(5848), 245-250;

Metcalf, E. C., & Collin, H. A. (1978). The effect of simazine on the growth and respiration of a cell suspension culture of celery. New Phytologist, 81(2), 243-248;

Miller, C. A., Tan, X., Wilson, M., Bhattacharyya, S., & Ludwig, S. (2010). Single plasmids expressing human steroid hormone receptors and a reporter gene for use in yeast signaling assays. Plasmid 63.2: 73-78;

Misra, A. N., Misra, M., & Singh, R. (2012). Chlorophyll fluorescence in plant biology. In Biophysics. InTech;

Mnif, W., Hassine, A. I. H., Bouaziz, A., Bartegi, A., Thomas, O., & Roig, B. (2011). Effect of endocrine disruptors pesticides: a review. Int. J. Environ. Res. Public Health, 8 (6), 2265-2303;

Nestler, H., Groh, K. J., Schönenberger, R., Behra, R., Schirmer, K., Eggen, R. I., & Suter, M. J. F. (2012). Multiple-endpoint assay provides a detailed mechanistic view of responses to herbicide exposure in *Chlamydomonas reinhardtii*. Aquat. Toxicol. 110– 111, 214–224;

Park, H. & Bae, J. Disturbed relaxin signaling pathway and testicular dysfunction in mouse offspring upon maternal exposure to simazine. *PloS one*, 2012, 7.9: e44856;

Petit, A. N., Eullaffroy, P., Debenest, T., & Gagné, F. (2010). Toxicity of PAMAM dendrimers to *Chlamydomonas reinhardtii*. Aquat. Toxicol., 100, 187–193;

Pinto, P. I., Estêvão, M. D., & Power, D. M. (2014). Effects of estrogens and estrogenic disrupting compounds on fish mineralized tissues. Mar drugs, 12(8), 4474-4494;

Prossnitz, E. R., & Barton, M.. (2014). Estrogen biology: New insights into GPER function and clinical opportunities. Mol. Cell. Endocrinol., 389, 71-83;

Prossnitz, E. R., & Arterburn, J. B. (2015). International Union of Basic and Clinical Pharmacology. XCVII. G Protein–Coupled Estrogen Receptor and Its Pharmacologic Modulators. Pharmacol rev, 67(3), 505-540;

Reboud X. (2002). Response of *Chlamydomonas reinhardtii* to herbicides: negative relationship between toxicity and water solubility across several herbicide families. Bull. Environ. Contam. Toxicol. 69, 554–561;

Regulation (EC) No 396/2005:: http://eur-lex.europa.eu/LexUriServ/LexUriServ.do?uri=OJ:L:2005:070:0001:0016:en:PDF;

Revankar, C. M., Cimino, D. F., Sklar, L. A., Arterburn, J. B., & Prossnitz, E. R. (2005). A transmembrane intracellular estrogen receptor mediates rapid cell signalling. Science 307, 1625–1630;

Ribeiro, I. C., Veríssimo, I., Moniz, L., Cardoso, H., Sousa, M. J., Soares, A. M. V. M., & Leão, C. (2000). Yeasts as a model for assessing the toxicity of the fungicides Penconazol, Cymoxanil and Dichlofluanid. Chemosphere, 41(10), 1637-1642;

Ricart, M., Barceló, D., Geiszinger, A., Guasch, H., de Alda, M. L., Romaní, A. M., ... & Sabater, S, (2009). Effects of low concentrations of the phenylurea herbicide diuron on biofilm algae and bacteria. Chemosphere, Volume 76, Issue 10, 1392–1401;

Ropero, A.B., Alonso-Magdalena, P., Ripoll, C., Fuentes, E., Nadal, A. (2006). Rapid endocrine disruption: Environmental estrogen actions triggered outside the nucleus. J. Steroid Biochem. Mol. Biol., 102, 163–169;

Ross J. (2005). The ecotoxicological effects of Photosystem II herbicides on corals. Mar. Pollut. Bull. 51, 495–506;

Routledge, E.J. & Sumpter J.P. (1996). Estrogenic Activity of Surfactants and Some of Their Degradation Products Assessed Using a Recombinant Yeast Screen. Environ. Toxicol. Chem., 15:241–48;

Roy, J. R., Chakraborty, S., & Chakraborty, T. R. (2009). Estrogen-like endocrine disrupting chemicals affecting puberty in humans –a review. Med. Sci. Monit, 15 (6): RA137-145;

Sanderson, J. T., Letcher, R. J., Heneweer, M., Giesy, J. P., & van den Berg, M. (2001). Effects of chloro-s-triazine herbicides and metabolites on aromatase activity in various human cell lines and on vitellogenin production in male carp hepatocytes. Environmental Health Perspectives, 109(10), 1027;

Sanseverino, J., Gupta, R. K., Layton, A. C., Patterson, S. S., Ripp, S. A., Saidak, L., ... & Sayler, G. S. (2005). Use of *Saccharomyces cerevisiae* BLYES Expressing Bacterial Bioluminescence for Rapid, Sensitive Detection of Estrogenic Compounds. Appl. Environ. Microb., 71 (8), 4455–4460;

Sass, J.B. & Needleman, H.L. (2004). Industry testing of toxic pesticides on human subjects concluded "no effect" despite the evidence. Environ. Health Perspect., 112, 150–151;

Scognamiglio, V., Raffi, D., Lambreva, M., Rea, G., Tibuzzi, A., Pezzotti, G., ... & Giardi, M. T. (2009). *Chlamydomonas reinhardtii* genetic variants as probes for fluorescence sensing system in detection of pollutants. Anal. Bioanal. Chem., 394, 1081–1087;

Sears, I. B., O'Connor, J., Rossanese, O. W., & Glick, B. S. (1998). A Versatile Set of Vectors for Constitutive and Regulated Gene Expression in *Pichia pastoris*. Yeast, 14, 783–790;

Silva, M., & Iyer, P. (2014). Toxicity endpoint selections for a simazine risk assessment. Birth Defects Research Part B: Developmental and Reproductive Toxicology, 101(4), 308-324;

Sridharan, R., Zuber, J., Connelly, S. M., Mathew, E., & Dumont, M. E. (2014). Fluorescent approaches for understanding interactions of ligands with G-protein-coupled receptors. Biochim. Biophys. Acta, 1838, 15–33;

Stirbet, A. (2011). On the relation between the Kautsky effect (chlorophyll a fluorescence induction) and Photosystem II: Basics and applications of the OJIP fluorescence transient. J. Photoch. Photobio. B., 104 236–257;

Strasser, R. J., Srivastava, A., & Tsimilli-Michael, M. (2000). The fluorescence transient as a tool to characterize and screen photosynthetic samples. Probing photosynthesis: mechanisms, regulation and adaptation, 445-483;

Terada, H. (1990). Uncouplers of oxidative phosphorylation. Environmental Health Perspectives, 87, 213;

Thomas, K.V., McHugh, M., Waldock, M., (2002). Antifouling paint booster biocides in the UK coastal waters: inputs, occurrence and environmental fate. Sci. Total Environ. 293, 117–127;

Thomas, P., Pang, Y., Filardo, E. J., & Dong, J. (2005). Identity of an estrogen membrane receptor coupled to a G protein in human breast cancer cells. Endocrinology, 146, 624–632;

Touloupakis, E., Giannoudi, L., Piletsky, S. A., Guzzella, L., Pozzoni, F., & Giardi, M. T. (2005). A multi-biosensor based on immobilized Photosystem II on screen-printed electrodes for the detection of herbicides in river water. Biosens. Bioelectron. 20, 1984–1992;

Trimble, A.J. & Lydy, M. J. (2006).Effects of triazine herbicides on organophosphate insecticide toxicity in *Hyalella azteca*. Archives of environmental contamination and toxicology. 51.1: 29-34;

Tssimilli-Michael, M., & Strasser, R. J. (2008). In vivo assessment of plants' vitality: applications in detecting and evaluating impacts of mycorrhization on host plants. Mycorrhiza: state of the art, genetics and molecular biology, eco-function, biotechnology, eco-physiology, structure and systematics, 3, 679-703;

Walmsley, R. M., & Keenan, P. (2000). The eukaryote alternative: advantages of using yeasts in place of bacteria in microbial biosensor development. Biotechnology and Bioprocess Engineering, 5(6), 387-394;

Wang, C., Liu, Y., & Cao, J. M. (2014). G Protein-Coupled Receptors: Extranuclear Mediators for the Non-Genomic Actions of Steroids. Int. J. Mol. Sci., 15, 15412-15425, doi:10.3390/ijms150915412;

WHO World Health Organization (2014). Food safety. Fact sheet n°399 (http://www.who.int/mediacentre/factsheets/fs399/en/);

Williams, D., Jung, D. W., Khersonsky, S. M., Heidary, N., Chang, Y. T., & Orlow, S. J. (2004). Identification of compounds that bind mitochondrial F1F0 ATPase by screening a triazine library for correction of albinism. Chemistry & biology, 11(9), 1251-1259;

Zorrilla, L. M., Gibson, E. K., & Stoker, T. E. (2010). The effects of simazine, a chlorotriazine herbicide, on pubertal development in the female Wistar rat. Reproductive Toxicology, 29(4), 393-400.

EXTRA ACTIVITIES

(chronological order)

- Detection of RNAs with flow cytometry (webinar – December 16th 2014);
- Gli OGM nella filiera agro-alimentare: una rinuncia ragionata o un'opportunità non colta? (ISS congress - February 10th 2015);
- Internal course of statistical techniques and of the use of the program PAST(PAleontological STatistics);
- Acquired skills in the research and selection of tools and products, contact with representatives and bureaucratic approach to the purchase;
- Photometry made easy! – Obtaining reliable results with nucleic acid measurements (Eppendorf webinar – April 16th 2015);
- Stage in the laboratory of professor Renato D'Ovidio with the aim of preparing the first plasmid attempted (Viterbo – May-June 2015);
- A month stage in the laboratory of professor Luca Sella with the aim of transform in *Pichia pastoris* the first plasmid attempted (Padova – July 2015);
- La buona pratica di misura del pH – GEP (seminario Mettler – 20 Ottobre 2015);
- "Comunicazione della ricerca scientifica: introduzione" mandatory course (Viterbo – December 10th 2015);
- La buona pratica di pipettaggio - GPP™ (Mettler seminar - February 23th 2016);
- Seminari di Statistica Medica per i dottorandi di ricerca (Sapienza university of Rome, June 20th 2016);
- Poster presentation at "Giornata DSCTM" (CNR Workshop, June 22-24th 2016);
- Stage in the laboratory of professor Renato D'Ovidio with the aim of preparing the second plasmid attempted (Viterbo – October 2016);
- Co-author in a poster presented by a colleague at the conference "Environmental risk assessment of pesticides: 25 years of scientific advancements since the adoption of Directive 91/414/EEC" (EFSA, 15-16 November 2016);
- Bachelor's degree candidate tutoring (December 2016);

- Three months stage in the laboratory of professor Thierry Giardina with the aim of transform in *Pichia pastoris* the second plasmid attempted (Marseille – January 26th – April 24th 2017);
- "L'ambiente statistico R: una introduzione all'analisi dei dati ecologici" mandatory course (Viterbo – June 5-9th 2017);
- "Principi di Scrittura Scientifica" mandatory course (Viterbo – July 17-21th 2017);
- Co-author in two posters presented by a colleague at the "12th International Biosensor conference" (CNR Rome, 25-29 September 2017

Acknowledgments (a very long list)

In these three years I grew up so much that now I barely recognize me, so I want to thank everyone who, more or less, has walked through this path with me.

First of all a big thank to Dr. Roberto Dragone for his tutoring and his teaching but maybe more than this because he helped me to grow up and not to give up. A great thank to Dr. Chiara Frazzoli, a big woman always there for me when I needed. I give a big kiss to Lara Blu and Alisa.

I'll give an enormous hug to my colleague and big friend Dr. Gerardo Grasso, who has been so precious for my experience and who helped me to grow up professionally but also personally.

I want to do my best acknowledgments to Prof. Luca Sella (Padova) and to Prof. Thierry Giardina and to Dr. Mickael Lafond (Marseille) for having welcomed me in their labs. They have teached me so much things.

I give a big hug to Prof. Stefania Masci, our course coordinator, who I thank so much for her reproaches.

I acknowledge also the Aix-Marseille University Microscopy Center CP2M and Kevin Poirot for expert guidance and help in confocal imaging.

Thanks to all the people who somehow helped me in my street. It is so easy to forget someone that I hope I didn't: Sabrina, Angelica, Rachel, Elisa, Ludovico, Marina, Roberto and Adriano; Ilaria, Giulia, Silvio, Alessandra, Anna and Francesco; Silvana, Alessandra and Riccardo; Lisa, Sybille and Clarisse. Thank you also to Laura, Sevdiye and Claudia for the time spent together in Padova and to all the other people who somehow changed me and brought me here.

I’m grateful for everything to my best friend Maria, to my family, to Marco and Silvia. I’d like to mention all the table tennis players and umpires which have cleared my head concerns over the weekend but they are so much that I will include all of them in a sole thank to my “faro” Roberto D’Uffizi.

At the end I want to devote this thesis to Lorenzo, my partner, because I love him but mainly because he didn't give up in traveling this tortuous journey with me (TI AMO).

I hope to be able to send to you wherever you are a great thank Prof. Renato D'Ovidio. We miss you!

Grazie!!!!!!!!!!!!!!!!!!!!!!!!!!!!!!!!!!!!

Annexes

Figure S 1: multiple alignment of the maxiprep sequence (first attempt)

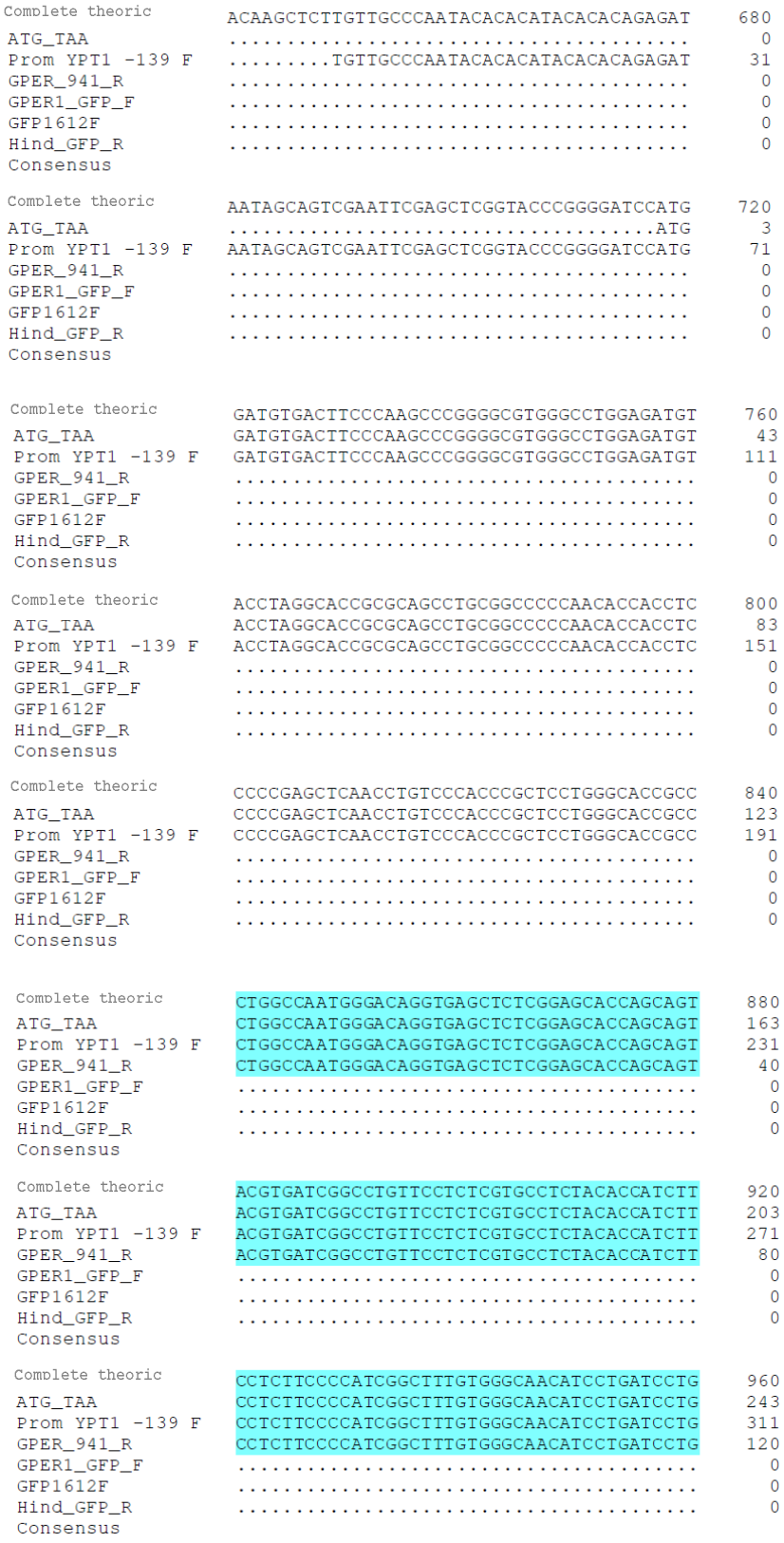

```
Complete theoric      GTGGTGAACATCAGCTTCCGCGAGAAGATGACCATCCCCG   1000
ATG_TAA               GTGGTGAACATCAGCTTCCGCGAGAAGATGACCATCCCCG    283
Prom YPT1 -139 F      GTGGTGAACATCAGCTTCCGCGAGAAGATGACCATCCCCG    351
GPER_941_R            GTGGTGAACATCAGCTTCCGCGAGAAGATGACCATCCCCG    160
GPER1_GFP_F           ........................................      0
GFP1612F              ........................................      0
Hind_GFP_R            ........................................      0
Consensus

Complete theoric      ACCTGTACTTCATCAACCTGGCGGTGGCGGACCTCATCCT   1040
ATG_TAA               ACCTGTACTTCATCAACCTGGCGGTGGCGGACCTCATCCT    323
Prom YPT1 -139 F      ACCTGTACTTCATCAACCTGGCGGTGGCGGACCTCATCCT    391
GPER_941_R            ACCTGTACTTCATCAACCTGGCGGTGGCGGACCTCATCCT    200
GPER1_GFP_F           ........................................      0
GFP1612F              ........................................      0
Hind_GFP_R            ........................................      0
Consensus

Complete theoric      GGTGGCCGACTCCCTCATTGAGGTGTTCAACCTGCACGAG   1080
ATG_TAA               GGTGGCCGACTCCCTCATTGAGGTGTTCAACCTGCACGAG    363
Prom YPT1 -139 F      GGTGGCCGACTCCCTCATTGAGGTGTTCAACCTGCACGAG    431
GPER_941_R            GGTGGCCGACTCCCTCATTGAGGTGTTCAACCTGCACGAG    240
GPER1_GFP_F           ........................................      0
GFP1612F              ........................................      0
Hind_GFP_R            ........................................      0
Consensus

Complete theoric      CGGTACTACGACATCGCCGTCCTGTGCACCTTCATGTCGC   1120
ATG_TAA               CGGTACTACGACATCGCCGTCCTGTGCACCTTCATGTCGC    403
Prom YPT1 -139 F      CGGTACTACGACATCGCCGTCCTGTGCACCTTCATGTCGC    471
GPER_941_R            CGGTACTACGACATCGCCGTCCTGTGCACCTTCATGTCGC    280
GPER1_GFP_F           ........................................      0
GFP1612F              ........................................      0
Hind_GFP_R            ........................................      0
Consensus

Complete theoric      TCTTCCTGCAGGTCAACATGTACAGCAGCGTCTTCTTCCT   1160
ATG_TAA               TCTTCCTGCAGGTCAACATGTACAGCAGCGTCTTCTTCCT    443
Prom YPT1 -139 F      TCTTCCTGCAGGTCAACATGTACAGCAGCGTCTTCTTCCT    511
GPER_941_R            TCTTCCTGCAGGTCAACATGTACAGCAGCGTCTTCTTCCT    320
GPER1_GFP_F           ........................................      0
GFP1612F              ........................................      0
Hind_GFP_R            ........................................      0
Consensus

Complete theoric      CACCTGGATGAGCTTCGACCGCTACATCGCCCTGGCCAGG   1200
ATG_TAA               CACCTGGATGAGCTTCGACCGCTACATCGCCCTGGCCAGG    483
Prom YPT1 -139 F      CACCTGGATGAGCTTCGACCGCTACATCGCCCTGGCCAGG    551
GPER_941_R            CACCTGGATGAGCTTCGACCGCTACATCGCCCTGGCCAGG    360
GPER1_GFP_F           ........................................      0
GFP1612F              ........................................      0
Hind_GFP_R            ........................................      0
Consensus

Complete theoric      GCCATGCGCTGCAGCCTGTTCCGCACCAAGCACCACGCCC   1240
ATG_TAA               GCCATGCGCTGCAGCCTGTTCCGCACCAAGCACCACGCCC    523
Prom YPT1 -139 F      GCCATGCGCTGCAGCCTGTTCCGCACCAAGCACCACGCC.    590
GPER_941_R            GCCATGCGCTGCAGCCTGTTCCGCACCAAGCACCACGCCC    400
GPER1_GFP_F           ........................................      0
GFP1612F              ........................................      0
Hind_GFP_R            ........................................      0
Consensus

Complete theoric      GGCTGAGCTGTGGCCTCATCTGGATGGCATCCGTGTCAGC   1280
ATG_TAA               GGCTGAGCTGTGGCCTCATCTGGATGGCATCCGTGTCAGC    563
Prom YPT1 -139 F      ........................................    590
GPER_941_R            GGCTGAGCTGTGGCCTCATCTGGATGGCATCCGTGTCAGC    440
GPER1_GFP_F           ........................................      0
GFP1612F              ........................................      0
Hind_GFP_R            ........................................      0
Consensus

Complete theoric      CACGCTGGTGCCCTTCACCGCCGTGCACCTGCAGCACACC   1320
ATG_TAA               CACGCTGGTGCCCTTCACCGCCGTGCACCTGCAGCACACC    603
Prom YPT1 -139 F      ........................................    590
GPER_941_R            CACGCTGGTGCCCTTCACCGCCGTGCACCTGCAGCACACC    480
GPER1_GFP_F           ........................................      0
GFP1612F              ........................................      0
Hind_GFP_R            ........................................      0
Consensus
```

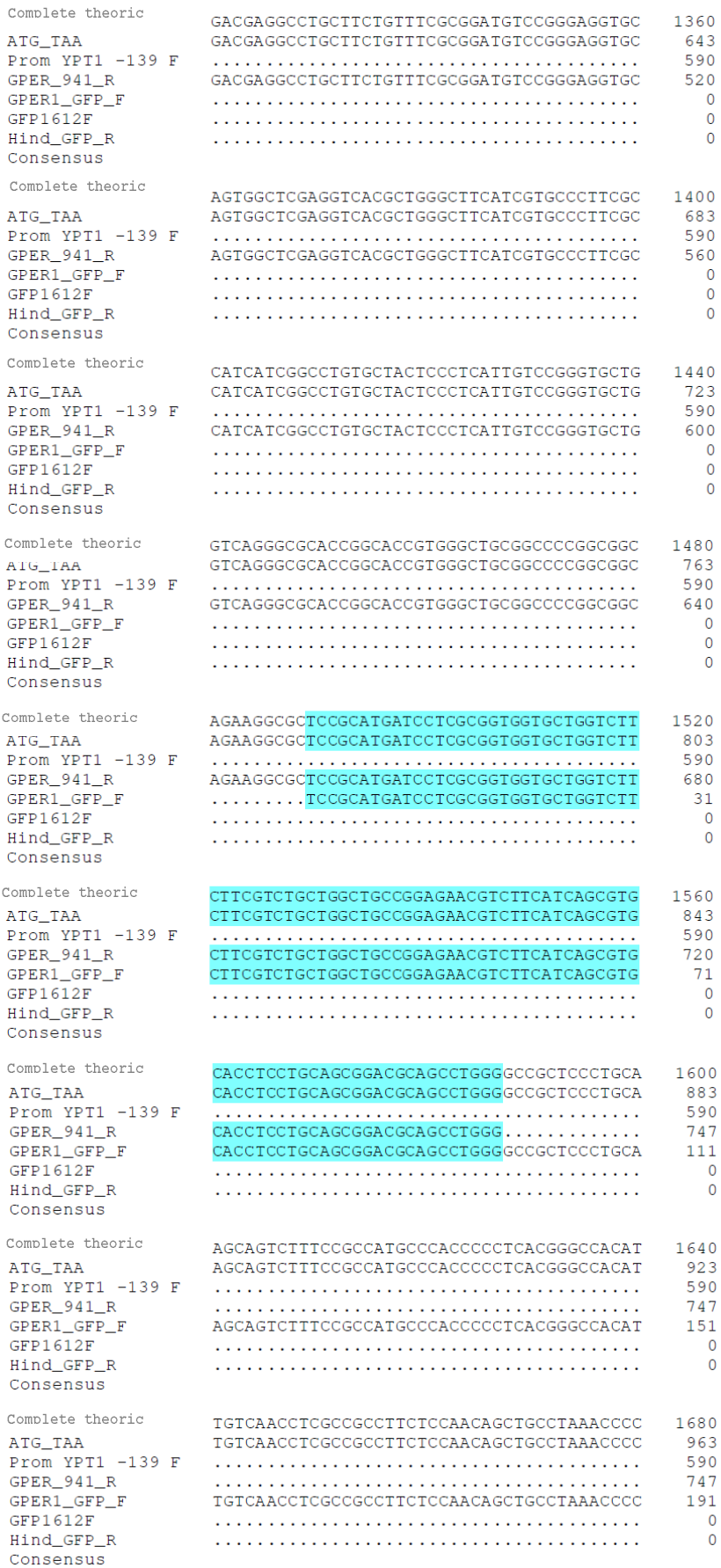
Complete theoric GACGAGGCCTGCTTCTGTTTCGCGGATGTCCGGGAGGTGC 1360
ATG_TAA GACGAGGCCTGCTTCTGTTTCGCGGATGTCCGGGAGGTGC 643
Prom YPT1 -139 F 590
GPER_941_R GACGAGGCCTGCTTCTGTTTCGCGGATGTCCGGGAGGTGC 520
GPER1_GFP_F 0
GFP1612F 0
Hind_GFP_R 0
Consensus
Complete theoric AGTGGCTCGAGGTCACGCTGGGCTTCATCGTGCCCTTCGC 1400
ATG_TAA AGTGGCTCGAGGTCACGCTGGGCTTCATCGTGCCCTTCGC 683
Prom YPT1 -139 F 590
GPER_941_R AGTGGCTCGAGGTCACGCTGGGCTTCATCGTGCCCTTCGC 560
GPER1_GFP_F 0
GFP1612F 0
Hind_GFP_R 0
Consensus
Complete theoric CATCATCGGCCTGTGCTACTCCCTCATTGTCCGGGTGCTG 1440
ATG_TAA CATCATCGGCCTGTGCTACTCCCTCATTGTCCGGGTGCTG 723
Prom YPT1 -139 F 590
GPER_941_R CATCATCGGCCTGTGCTACTCCCTCATTGTCCGGGTGCTG 600
GPER1_GFP_F 0
GFP1612F 0
Hind_GFP_R 0
Consensus
Complete theoric GTCAGGGCGCACCGGCACCGTGGGCTGCGGCCCCGGCGGC 1480
ATG_TAA GTCAGGGCGCACCGGCACCGTGGGCTGCGGCCCCGGCGGC 763
Prom YPT1 -139 F 590
GPER_941_R GTCAGGGCGCACCGGCACCGTGGGCTGCGGCCCCGGCGGC 640
GPER1_GFP_F 0
GFP1612F 0
Hind_GFP_R 0
Consensus
Complete theoric AGAAGGCGCTCCGCATGATCCTCGCGGTGGTGCTGGTCTT 1520
ATG_TAA AGAAGGCGCTCCGCATGATCCTCGCGGTGGTGCTGGTCTT 803
Prom YPT1 -139 F 590
GPER_941_R AGAAGGCGCTCCGCATGATCCTCGCGGTGGTGCTGGTCTT 680
GPER1_GFP_F .....TCCGCATGATCCTCGCGGTGGTGCTGGTCTT 31
GFP1612F 0
Hind_GFP_R 0
Consensus
Complete theoric CTTCGTCTGCTGGCTGCCGGAGAACGTCTTCATCAGCGTG 1560
ATG_TAA CTTCGTCTGCTGGCTGCCGGAGAACGTCTTCATCAGCGTG 843
Prom YPT1 -139 F 590
GPER_941_R CTTCGTCTGCTGGCTGCCGGAGAACGTCTTCATCAGCGTG 720
GPER1_GFP_F CTTCGTCTGCTGGCTGCCGGAGAACGTCTTCATCAGCGTG 71
GFP1612F 0
Hind_GFP_R 0
Consensus
Complete theoric CACCTCCTGCAGCGGACGCAGCCTGGGGCCGCTCCCTGCA 1600
ATG_TAA CACCTCCTGCAGCGGACGCAGCCTGGGGCCGCTCCCTGCA 883
Prom YPT1 -139 F 590
GPER_941_R CACCTCCTGCAGCGGACGCAGCCTGGG..... 747
GPER1_GFP_F CACCTCCTGCAGCGGACGCAGCCTGGGGCCGCTCCCTGCA 111
GFP1612F 0
Hind_GFP_R 0
Consensus
Complete theoric AGCAGTCTTTCCGCCATGCCCACCCCCTCACGGGCCACAT 1640
ATG_TAA AGCAGTCTTTCCGCCATGCCCACCCCCTCACGGGCCACAT 923
Prom YPT1 -139 F 590
GPER_941_R 747
GPER1_GFP_F AGCAGTCTTTCCGCCATGCCCACCCCCTCACGGGCCACAT 151
GFP1612F 0
Hind_GFP_R 0
Consensus
Complete theoric TGTCAACCTCGCCGCCTTCTCCAACAGCTGCCTAAACCCC 1680
ATG_TAA TGTCAACCTCGCCGCCTTCTCCAACAGCTGCCTAAACCCC 963
Prom YPT1 -139 F 590
GPER_941_R 747
GPER1_GFP_F TGTCAACCTCGCCGCCTTCTCCAACAGCTGCCTAAACCCC 191
GFP1612F 0
Hind_GFP_R 0
Consensus

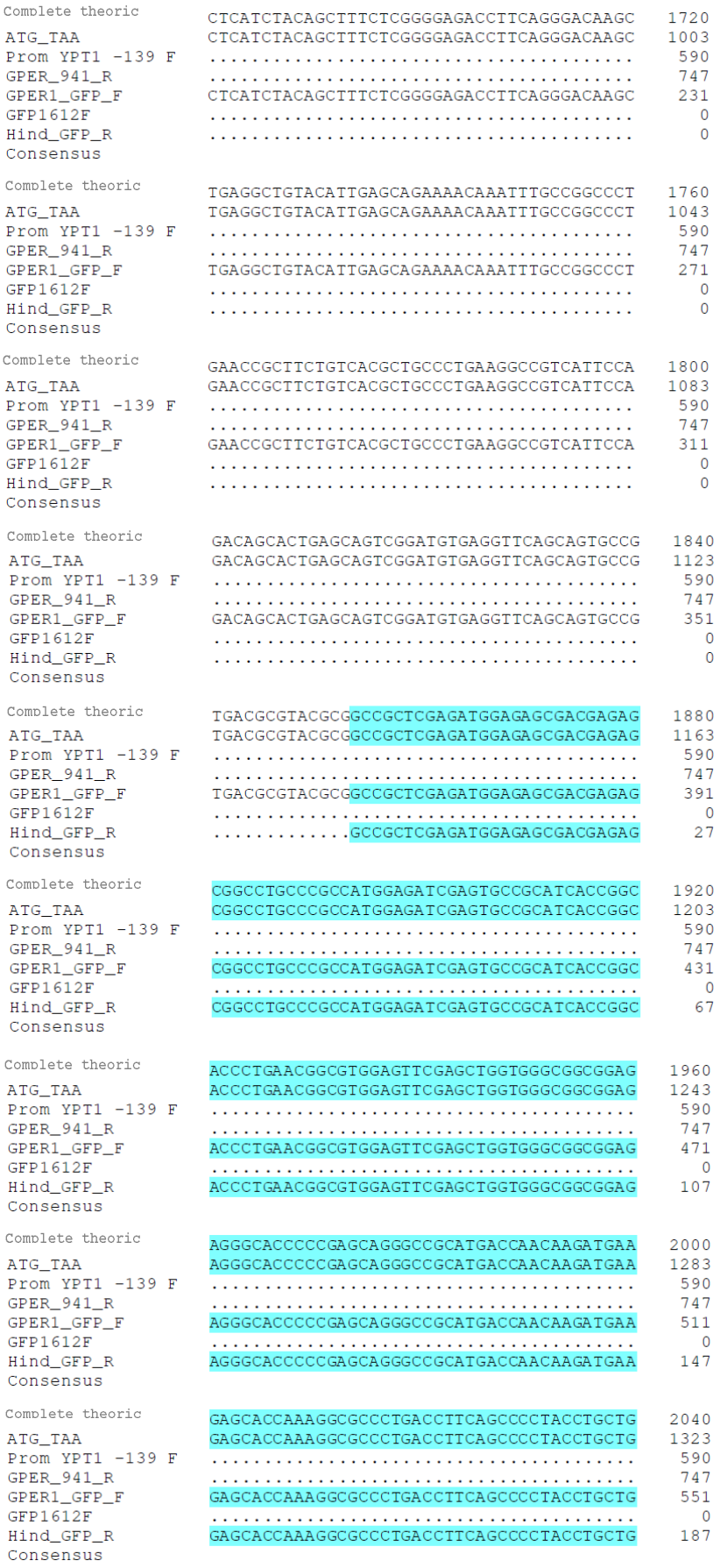
Complete theoric CTCATCTACAGCTTTCTCGGGGAGACCTTCAGGGACAAGC 1720
ATG_TAA CTCATCTACAGCTTTCTCGGGGAGACCTTCAGGGACAAGC 1003
Prom YPT1 -139 F 590
GPER_941_R 747
GPER1_GFP_F CTCATCTACAGCTTTCTCGGGGAGACCTTCAGGGACAAGC 231
GFP1612F 0
Hind_GFP_R 0
Consensus
Complete theoric TGAGGCTGTACATTGAGCAGAAAACAAATTTGCCGGCCCT 1760
ATG_TAA TGAGGCTGTACATTGAGCAGAAAACAAATTTGCCGGCCCT 1043
Prom YPT1 -139 F 590
GPER_941_R 747
GPER1_GFP_F TGAGGCTGTACATTGAGCAGAAAACAAATTTGCCGGCCCT 271
GFP1612F 0
Hind_GFP_R 0
Consensus
Complete theoric GAACCGCTTCTGTCACGCTGCCCTGAAGGCCGTCATTCCA 1800
ATG_TAA GAACCGCTTCTGTCACGCTGCCCTGAAGGCCGTCATTCCA 1083
Prom YPT1 -139 F 590
GPER_941_R 747
GPER1_GFP_F GAACCGCTTCTGTCACGCTGCCCTGAAGGCCGTCATTCCA 311
GFP1612F 0
Hind_GFP_R 0
Consensus
Complete theoric GACAGCACTGAGCAGTCGGATGTGAGGTTCAGCAGTGCCG 1840
ATG_TAA GACAGCACTGAGCAGTCGGATGTGAGGTTCAGCAGTGCCG 1123
Prom YPT1 -139 F 590
GPER_941_R 747
GPER1_GFP_F GACAGCACTGAGCAGTCGGATGTGAGGTTCAGCAGTGCCG 351
GFP1612F 0
Hind_GFP_R 0
Consensus
Complete theoric TGACGCGTACGCGGCCGCTCGAGATGGAGAGCGACGAGAG 1880
ATG_TAA TGACGCGTACGCGGCCGCTCGAGATGGAGAGCGACGAGAG 1163
Prom YPT1 -139 F 590
GPER_941_R 747
GPER1_GFP_F TGACGCGTACGCGGCCGCTCGAGATGGAGAGCGACGAGAG 391
GFP1612F 0
Hind_GFP_R .....GCCGCTCGAGATGGAGAGCGACGAGAG 27
Consensus
Complete theoric CGGCCTGCCCGCCATGGAGATCGAGTGCCGCATCACCGGC 1920
ATG_TAA CGGCCTGCCCGCCATGGAGATCGAGTGCCGCATCACCGGC 1203
Prom YPT1 -139 F 590
GPER_941_R 747
GPER1_GFP_F CGGCCTGCCCGCCATGGAGATCGAGTGCCGCATCACCGGC 431
GFP1612F 0
Hind_GFP_R CGGCCTGCCCGCCATGGAGATCGAGTGCCGCATCACCGGC 67
Consensus
Complete theoric ACCCTGAACGGCGTGGAGTTCGAGCTGGTGGGCGGCGGAG 1960
ATG_TAA ACCCTGAACGGCGTGGAGTTCGAGCTGGTGGGCGGCGGAG 1243
Prom YPT1 -139 F 590
GPER_941_R 747
GPER1_GFP_F ACCCTGAACGGCGTGGAGTTCGAGCTGGTGGGCGGCGGAG 471
GFP1612F 0
Hind_GFP_R ACCCTGAACGGCGTGGAGTTCGAGCTGGTGGGCGGCGGAG 107
Consensus
Complete theoric AGGGCACCCCCGAGCAGGGCCGCATGACCAACAAGATGAA 2000
ATG_TAA AGGGCACCCCCGAGCAGGGCCGCATGACCAACAAGATGAA 1283
Prom YPT1 -139 F 590
GPER_941_R 747
GPER1_GFP_F AGGGCACCCCCGAGCAGGGCCGCATGACCAACAAGATGAA 511
GFP1612F 0
Hind_GFP_R AGGGCACCCCCGAGCAGGGCCGCATGACCAACAAGATGAA 147
Consensus
Complete theoric GAGCACCAAAGGCGCCCTGACCTTCAGCCCCTACCTGCTG 2040
ATG_TAA GAGCACCAAAGGCGCCCTGACCTTCAGCCCCTACCTGCTG 1323
Prom YPT1 -139 F 590
GPER_941_R 747
GPER1_GFP_F GAGCACCAAAGGCGCCCTGACCTTCAGCCCCTACCTGCTG 551
GFP1612F 0
Hind_GFP_R GAGCACCAAAGGCGCCCTGACCTTCAGCCCCTACCTGCTG 187
Consensus

```
Complete theoric      AGCCACGTGATGGGCTACGGCTTCTACCACTTCGGCACCT   2080
ATG_TAA               AGCCACGTGATGGGCTACGGCTTCTACCACTTCGGCACCT   1363
Prom YPT1 -139 F      ........................................    590
GPER_941_R            ........................................    747
GPER1_GFP_F           AGCCACGTGATGGGCTACGGCTTCTACCACTTCGGCACCT   591
GFP1612F              ........................................      0
Hind_GFP_R            AGCCACGTGATGGGCTACGGCTTCTACCACTTCGGCACCT   227
Consensus

Complete theoric      ACCCCAGCGGCTACGAGAACCCCTTCCTGCACGCCATCAA   2120
ATG_TAA               ACCCCAGCGGCTACGAGAACCCCTTCCTGCACGCCATCAA   1403
Prom YPT1 -139 F      ........................................    590
GPER_941_R            ........................................    747
GPER1_GFP_F           ACCCCAGCGGCTACGAGAACCCCTTCCTGCACGCCATCAA   631
GFP1612F              ........................................      0
Hind_GFP_R            ACCCCAGCGGCTACGAGAACCCCTTCCTGCACGCCATCAA   267
Consensus

Complete theoric      CAACGGCGGCTACACCAACACCCGCATCGAGAAGTACGAG   2160
ATG_TAA               CAACGGCGGCTACACCAACACCCGCATCGAGAAGTACGAG   1443
Prom YPT1 -139 F      ........................................    590
GPER_941_R            ........................................    747
GPER1_GFP_F           CAACGGCGGCTACACCAACACCCGCATCGAGAAGTACGAG   671
GFP1612F              ........................................      0
Hind_GFP_R            CAACGGCGGCTACACCAACACCCGCATCGAGAAGTACGAG   307
Consensus

Complete theoric      GACGGCGGCGTGCTGCACGTGAGCTTCAGCTACCGCTACG   2200
ATG_TAA               GACGGCGGCGTGCTGCACGTGAGCTTCAGCTACCGCTACG   1483
Prom YPT1 -139 F      ........................................    590
GPER_941_R            ........................................    747
GPER1_GFP_F           GACGGCGGCGTGCTGCACG.....................    690
GFP1612F              ........................................      0
Hind_GFP_R            GACGGCGGCGTGCTGCACGTGAGCTTCAGCTACCGCTACG   347
Consensus

Complete theoric      AGGCCGGCCGCGTGATCGGCGACTTCAAGGTGATGGGCAC   2240
ATG_TAA               AGGCCGGCCGCGTGATCGGCGACTTCAAGGTGATGGGCAC   1523
Prom YPT1 -139 F      ........................................    590
GPER_941_R            ........................................    747
GPER1_GFP_F           ........................................    690
GFP1612F              ........................................      0
Hind_GFP_R            AGGCCGGCCGCGTGATCGGCGACTTCAAGGTGATGGGCAC   387
Consensus

Complete theoric      CGGCTTCCCCGAGGACAGCGTGATCTTCACCGACAAGATC   2280
ATG_TAA               CGGCTTCCCCGAGGACAGCGTGATCTTCACCGACAAGATC   1563
Prom YPT1 -139 F      ........................................    590
GPER_941_R            ........................................    747
GPER1_GFP_F           ........................................    690
GFP1612F              ........................................      0
Hind_GFP_R            CGGCTTCCCCGAGGACAGCGTGATCTTCACCGACAAGATC   427
Consensus

Complete theoric      ATCCGCAGCAACGCCACCGTGGAGCACCTGCACCCCATGG   2320
ATG_TAA               ATCCGCAGCAACGCCACCGTGGAGCACCTGCACCCCATGG   1603
Prom YPT1 -139 F      ........................................    590
GPER_941_R            ........................................    747
GPER1_GFP_F           ........................................    690
GFP1612F              ........................................      0
Hind_GFP_R            ATCCGCAGCAACGCCACCGTGGAGCACCTGCACCCCATGG   467
Consensus

Complete theoric      GCGATAACGATCTGGATGGCAGCTTCACCCGCACCTTCAG   2360
ATG_TAA               GCGATAACGATCTGGATGGCAGCTTCACCCGCACCTTCAG   1643
Prom YPT1 -139 F      ........................................    590
GPER_941_R            ........................................    747
GPER1_GFP_F           ........................................    690
GFP1612F              ........................................      0
Hind_GFP_R            GCGATAACGATCTGGATGGCAGCTTCACCCGCACCTTCAG   507
Consensus

Complete theoric      CCTGCGCGACGGCGGCTACTACAGCTCCGTGGTGGACAGC   2400
ATG_TAA               CCTGCGCGACGGCGGCTACTACAGCTCCGTGGTGGACAGC   1683
Prom YPT1 -139 F      ........................................    590
GPER_941_R            ........................................    747
GPER1_GFP_F           ........................................    690
GFP1612F              ........................................      0
Hind_GFP_R            CCTGCGCGACGGCGGCTACTACAGCTCCGTGGTGGACAGC   547
Consensus
```

Figure S 2: multiple alignment of the maxiprep sequence (second attempt)

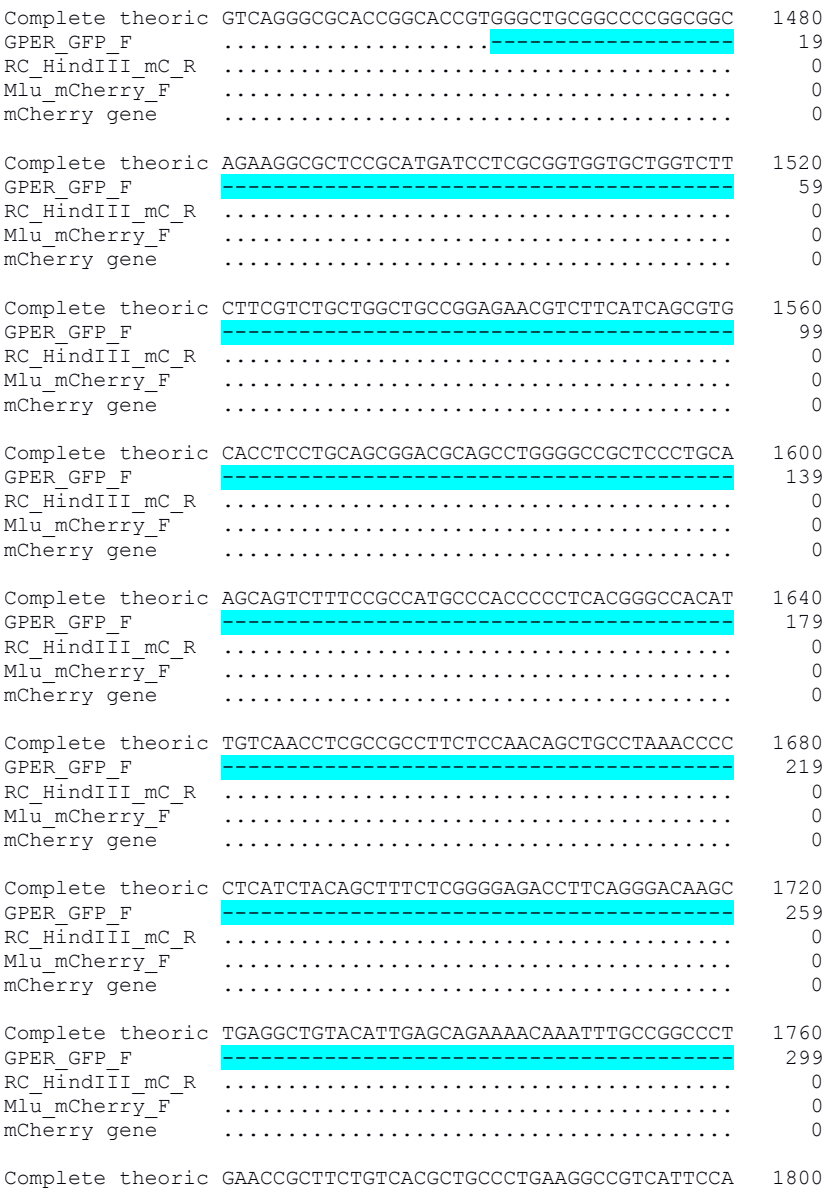

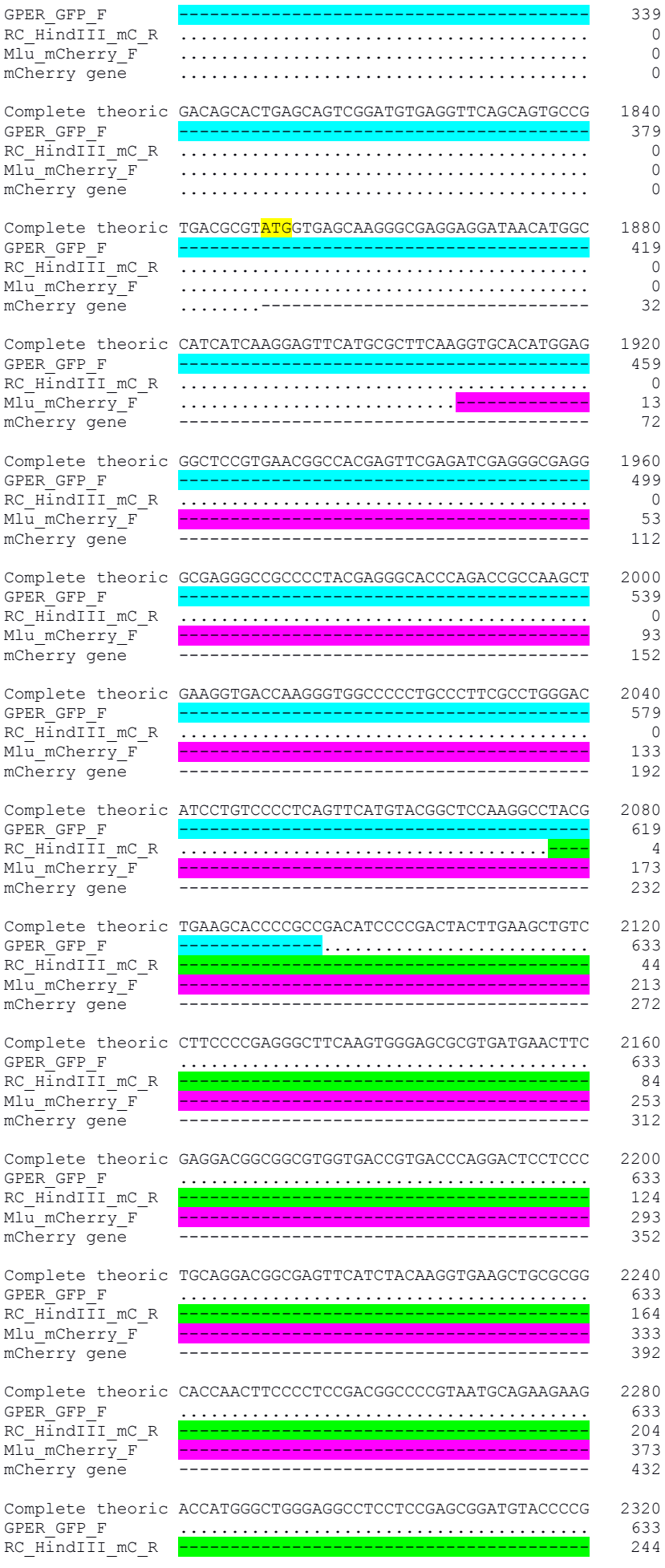
GPER_GFP_F ---------- 339
RC_HindIII_mC_R 0
Mlu_mCherry_F 0
mCherry gene 0
Complete theoric GACAGCACTGAGCAGTCGGATGTGAGGTTCAGCAGTGCCG 1840
GPER_GFP_F ---------- 379
RC_HindIII_mC_R 0
Mlu_mCherry_F 0
mCherry gene 0
Complete theoric TGACGCGTATGGTGAGCAAGGGCGAGGAGGATAACATGGC 1880
GPER_GFP_F ---------- 419
RC_HindIII_mC_R 0
Mlu_mCherry_F 0
mCherry gene ....---------- 32
Complete theoric CATCATCAAGGAGTTCATGCGCTTCAAGGTGCACATGGAG 1920
GPER_GFP_F ---------- 459
RC_HindIII_mC_R 0
Mlu_mCherry_F ....---------- 13
mCherry gene ---------- 72
Complete theoric GGCTCCGTGAACGGCCACGAGTTCGAGATCGAGGGCGAGG 1960
GPER_GFP_F ---------- 499
RC_HindIII_mC_R 0
Mlu_mCherry_F ---------- 53
mCherry gene ---------- 112
Complete theoric GCGAGGGCCGCCCCTACGAGGGCACCCAGACCGCCAAGCT 2000
GPER_GFP_F ---------- 539
RC_HindIII_mC_R 0
Mlu_mCherry_F ---------- 93
mCherry gene ---------- 152
Complete theoric GAAGGTGACCAAGGGTGGCCCCCTGCCCTTCGCCTGGGAC 2040
GPER_GFP_F ---------- 579
RC_HindIII_mC_R 0
Mlu_mCherry_F ---------- 133
mCherry gene ---------- 192
Complete theoric ATCCTGTCCCCTCAGTTCATGTACGGCTCCAAGGCCTACG 2080
GPER_GFP_F ---------- 619
RC_HindIII_mC_R ....---- 4
Mlu_mCherry_F ---------- 173
mCherry gene ---------- 232
Complete theoric TGAAGCACCCCGCCGACATCCCCGACTACTTGAAGCTGTC 2120
GPER_GFP_F ----------.......... 633
RC_HindIII_mC_R ---------- 44
Mlu_mCherry_F ---------- 213
mCherry gene ---------- 272
Complete theoric CTTCCCCGAGGGCTTCAAGTGGGAGCGCGTGATGAACTTC 2160
GPER_GFP_F 633
RC_HindIII_mC_R ---------- 84
Mlu_mCherry_F ---------- 253
mCherry gene ---------- 312
Complete theoric GAGGACGGCGGCGTGGTGACCGTGACCCAGGACTCCTCCC 2200
GPER_GFP_F 633
RC_HindIII_mC_R ---------- 124
Mlu_mCherry_F ---------- 293
mCherry gene ---------- 352
Complete theoric TGCAGGACGGCGAGTTCATCTACAAGGTGAAGCTGCGCGG 2240
GPER_GFP_F 633
RC_HindIII_mC_R ---------- 164
Mlu_mCherry_F ---------- 333
mCherry gene ---------- 392
Complete theoric CACCAACTTCCCCTCCGACGGCCCCGTAATGCAGAAGAAG 2280
GPER_GFP_F 633
RC_HindIII_mC_R ---------- 204
Mlu_mCherry_F ---------- 373
mCherry gene ---------- 432
Complete theoric ACCATGGGCTGGGAGGCCTCCTCCGAGCGGATGTACCCCG 2320
GPER_GFP_F 633
RC_HindIII_mC_R ---------- 244

```
Mlu_mCherry_F    ----------------------------------------    413
mCherry gene     ----------------------------------------    472

Complete theoric AGGACGGCGCCCTGAAGGGCGAGATCAAGCAGAGGCTGAA   2360
GPER_GFP_F       ........................................    633
RC_HindIII_mC_R  ----------------------------------------    284
Mlu_mCherry_F    ----------------------------------------    453
mCherry gene     ----------------------------------------    512

Complete theoric GCTGAAGGACGGCGGCCACTACGACGCTGAGGTCAAGACC   2400
GPER_GFP_F       ........................................    633
RC_HindIII_mC_R  ----------------------------------------    324
Mlu_mCherry_F    ----------------------------------------    493
mCherry gene     ----------------------------------------    552

Complete theoric ACCTACAAGGCCAAGAAGCCCGTGCAGCTGCCCGGCGCCT   2440
GPER_GFP_F       ........................................    633
RC_HindIII_mC_R  ----------------------------------------    364
Mlu_mCherry_F    ----------------------------------------    533
mCherry gene     ----------------------------------------    592

Complete theoric ACAACGTCAACATCAAGTTGGACATCACCTCCCACAACGA   2480
GPER_GFP_F       ........................................    633
RC_HindIII_mC_R  ----------------------------------------    404
Mlu_mCherry_F    ----------------------------------------    573
mCherry gene     ----------------------------------------    632

Complete theoric GGACTACACCATCGTGGAACAGTACGAACGCGCCGAGGGC   2520
GPER_GFP_F       ........................................    633
RC_HindIII_mC_R  ----------..........                        418
Mlu_mCherry_F    ----------------------------------------    613
mCherry gene     ----------------------------------------    672

Complete theoric CGCCACTCCACCGGCGGCATGGACGAGCTGTACAAGGGAG   2560
GPER_GFP_F       ........................................    633
RC_HindIII_mC_R  ........................................    418
Mlu_mCherry_F    ----------------------------------------    653
mCherry gene     ----------------------------------------    712

Complete theoric GTGGTTCCTAGAAGCTTCTTAGACATGACTGTTCCTCAGT   2600
GPER_GFP_F       ........................................    633
RC_HindIII_mC_R  ........................................    418
Mlu_mCherry_F    ----------------------------------------    693
mCherry gene     ----------..............................    723

Complete theoric TCAAGTTGGGCACTTACGAGAAGACCGGTCTTGCTAGATT   2640
GPER_GFP_F       ........................................    633
RC_HindIII_mC_R  .........................................    418
Mlu_mCherry_F    ---------.................................    702
mCherry gene     ........................................    723
```